LA--11952

DE91 007165

MCNP $S(\alpha,\beta)$ Detector Scheme

John S. Hendricks
Richard E. Prael

MASTER

DISTRIBUTION OF THIS DOCUMENT IS UNLIMITED

Los Alamos
Los Alamos National Laboratory
Los Alamos, New Mexico 87545

MCNP $S(\alpha,\beta)$ DETECTOR SCHEME

by

John S. Hendricks and Richard E. Prael

ABSTRACT

An approximate method to allow $S(\alpha,\beta)$ thermal collision contributions to point detectors and DXTRAN by Prael has been implemented in MCNP4. The method is described and test results are presented, including some results that indicate inadequacies in the NJOY processing of the nuclear data.

I. INTRODUCTION

A new approximate method to allow $S(\alpha,\beta)$ thermal collision contributions to point detectors and DXTRAN by Richard E. Prael has been implemented in MCNP[1,2] version 4.

The $S(\alpha,\beta)$ scattering model[3,4,5] is a complete ENDF/B[6] representation of thermal neutron scattering by molecules and crystalline solids which is important in the energy range 4 eV down to 10^{-5} eV. A point detector[1,3,7] is a deterministic estimate of the flux at a point in space that is made from source and collision events throughout a Monte Carlo random walk. DXTRAN[1,7] is an MCNP variance reduction option that uses point estimates similar to point detectors to put particles in small regions of space (DXTRAN spheres) where their random walk can be continued.

Until now it has been impossible to use point detectors and DXTRAN in conjunction with $S(\alpha,\beta)$ scattering because the calculation of a necessary point detector/DXTRAN quantity, $p(\mu)$, is impossible. The quantity $p(\mu)$ is the value of the probability density function for scattering from the incident random walk particle direction at a polar angle $\mu = cos\theta$ exactly toward the point detector or sampled point on the DXTRAN sphere. The reason this calculation is not possible is that the $S(\alpha,\beta)$ scattering data is represented as discrete polar angles, μ, at each collision, and the probability of any of these angles pointing toward a point detector or DXTRAN point is infinitesimally small. An exact $S(\alpha,\beta)$ - point detector/DXTRAN scheme may be possible in which at each collision the particle is backed up along its random walk trajectory to a point where scattering exactly in the direction of the detector/DXTRAN point is possible. Then particle weights could be appropriately adjusted, but this would be horrendously complicated, particularly if the trajectory crossed any geometric boundaries in between. Prael's approximate method uses another approach in which the discrete angles are represented approximately by histogram functions following certain rules to preserve selected properties. Calculation of the $p(\mu)$ values from a histogram distribution rather than from a discrete distribution is then relatively straightforward.

Forty-nine calculations requiring over 40 hours of Cray XMP-48 computer time have been run to test Prael's approximate scheme. These indicate that the method is working as intended but that the approximation is sometimes quite poor. Additionally, these calculations indicate that the discrepancies between detector tallies using the approximate scheme and tallies using the "exact" random walk are often caused by inadequacies of the data representation used in the random walk! In particular, *the representation of the scattering distributions by the NJOY*[8,9] *code as a few discrete lines (typically seven) is poor for distributions which are continuous, particularly isotropic distributions.*

First, Prael's approximate method will be described, including its implementation into MCNP4. Then the test problems and results will be described and interpreted.

II. PRAEL'S METHOD

The approximate method of Richard E. Prael for estimating the contributions to detectors or DXTRAN from discrete angle scattering will now be described. First we review $S(\alpha,\beta)$ thermal scattering, borrowed largely from the MCNP manual[1] Chapter 2; then we examine the pertinent aspects of point detectors and DXTRAN. Prael's method is pictorially illustrated, and finally his FORTRAN algorithm and its MCNP4 counterpart are presented.

A. S(α,β) Theoretical Background

The $S(\alpha,\beta)$ thermal scattering model is a complete representation of thermal neutron scattering by molecules and crystalline solids including Bragg scattering. Two processes are allowed: (1) inelastic scattering with cross section σ_{in} and a coupled energy-angle representation derived from an ENDF/B $S(\alpha,\beta)$ scattering law, and (2) elastic scattering with no change in the outgoing neutron energy for solids with cross section σ_{el} and an angular treatment derived from lattice parameters. The elastic scattering treatment is chosen with probability $\sigma_{el}/(\sigma_{el}+\sigma_{in})$. This thermal scattering treatment also allows the representation of scattering by multiatomic molecules (for example, BeO).

For the inelastic treatment, the distribution of secondary energies is represented by a set of equally probable final energies (typically 16 or 32) for each member of a grid of initial energies from an upper limit of typically 4 eV down to 10^{-5} eV along with a set of angular data for each initial and final energy. The selection of a final energy E', given an initial energy E, may be characterized by sampling from the distribution

$$p(E' \mid E_i < E < E_{i+1}) = \frac{1}{N}\sum_{i=1}^{N}\delta\left[E' - \rho E_{i,j} - (1-\rho)E_{i+1,j}\right] \quad ,$$

where E_i and E_{i+1} are adjacent elements on the initial energy grid,

$$\rho = \frac{E_{i+1} - E}{E_{i+1} - E_i} \quad ,$$

N is the number of equally probable final energies, and $E_{i,j}$ is the j^{th} discrete final energy for incident energy E_i.

There are three allowed schemes for the selection of a scattering cosine following selection of a final energy and final energy index j. In each case, the $(i,j)^{th}$ set of angular data is associated with the energy transition $E = E_i \rightarrow E' = E_{i,j}$.

1. The data consist of equiprobable histogram cosine bins. For $k = 1, \ldots, \nu$ cosine bin boundaries and a random number ξ, index k is selected by $k = \xi\nu$ and μ is obtained by the relation

$$\mu = \mu_k + (\xi - k/\nu)(\mu_{k+1} - \mu_k)$$

   In practice, no data for this scattering representation is processed by the NJOY code and therefore it is unused in MCNP.

2. The data consist of sets of equally probable discrete cosines $\mu_{i,j,k}$ for $k = 1, \ldots, \nu$ with ν typically 4 or 8. An index k is selected with probability $1/\nu$, and μ is obtained by the relation

$$\mu = \rho\mu_{i,j,k} + (1-\rho)\mu_{i+1,j,k} \quad .$$

3. The data consist of bin boundaries of equally probable cosine bins. In this case, random linear interpolation is used to select one set or the other, with ρ being the probability of selecting the set corresponding to incident energy E_i. The subsequent procedure consists of sampling for one of the equally probable bins and then choosing μ uniformly in the bin.

For elastic scattering, the above second and third angular representations are allowed for data derived by an incoherent approximation. In this case, one set of angular data appears for each incident energy and is used with the interpolation procedures on incident energy described above.

For elastic scattering, when the data have been derived in the coherent approximation, a completely different representation occurs. In this case, the data actually stored are the set of parameters D_k, where

$$\sigma_{el} = D_k/E \quad \text{for } E_{Bk} \leq E < E_{Bk+1}$$
$$\sigma_{el} = 0 \quad \text{for } E < E_{B1}$$

and E_{Bk} are Bragg energies derived from the lattice parameters. For incident energy E such that $E_{Bk} \leq E \leq E_{Bk+1}$,

$$P_i = D_i/D_k \text{ for } i = 1, \ldots, k$$

represents a discrete cumulative probability distribution that is sampled to obtain index i, representing scattering from the i^{th} Bragg edge. The scattering cosine is then obtained from the relationship

$$\mu = 1 - 2E_{Bi}/E \quad .$$

B. Detector/DXTRAN Theoretical Background

The contribution or tally, T, to a point detector, or ring detector, or the sampled point on a DXTRAN sphere from each source or collision event is:

$$T = (Wp(\mu)e^{-\lambda})/(2\pi R^2) \quad ,$$

where

W = particle weight of random walk particle from source or entering collision;

λ = $\int_0^R \sigma_t(s)ds$ = total number of mean free paths integrated over the trajectory from the source or collision point to the detector or DXTRAN point;

$e^{-\lambda}$ = attenuation term; for transmission from source or collision point to detector or DXTRAN point;

R = distance from source or collision point to detector or DXTRAN point;

$p(\mu)$ = value of probability density function at μ, the cosine of the polar angle between the particle trajectory and the direction to the detector.

The probability density function, $p(\mu)$, is such that

$$P(\mu) = \int_{-1}^{\mu} p(\mu) d\mu$$

where $P(\mu)$ is the probability of scattering between -1 and μ. Note that $p(\mu)$ must be normalized such that

$$\int_{-1}^{1} p(\mu) d\mu = 1 \quad .$$

Whereas $p(\mu)$ is not a probability it can have any values greater than zero, including values greater than one. $P(\mu)$ is a probability and therefore,

$$0 \le P(\mu) \le 1$$

As an example, consider the cosine distribution $p(\mu) = \mu$ illustrated in Fig. 1. Actually, $p(\mu) = .5(\mu + 1)$. If μ_0 is the cosine of the polar angle between a collision point and a detector point, then $p(\mu)$ in the point detector expression is simply

$$p(\mu) = p(\mu_0) = .5(\mu_0 + 1)$$

In this case with a cosine distribution scattering law, the detector contributions are straightforward. However, consider the case encountered with $S(\alpha, \beta)$ thermal scattering data, where the angular distributions are discrete as in Fig. 2. This is a cosine distribution approximated by eight discrete lines. If μ_0 is again the cosine of the polar angle between the collision point and the detector point, then $p(\mu_0) = 0$ unless μ_0 is one of the discrete scattering angles, in which case $p(\mu_0) = \infty$. The probability of the scattering angle between the collision and detector being exactly the same as one of the discrete scattering angles is zero. Thus, contributions to detectors and DXTRAN from $S(\alpha, \beta)$ thermal collisions have hitherto been impossible.

C. Prael's Histogram Method

Richard E. Prael has devised an approximate method for getting contributions from $S(\alpha, \beta)$ thermal collisions to detectors or DXTRAN points by representing the discrete scattering angles as histograms rather than lines. The histograms are chosen by the following rules:

- The midpoint of the histogram must be centered at the location of the line to preserve the mean;
- Histograms may not overlap;

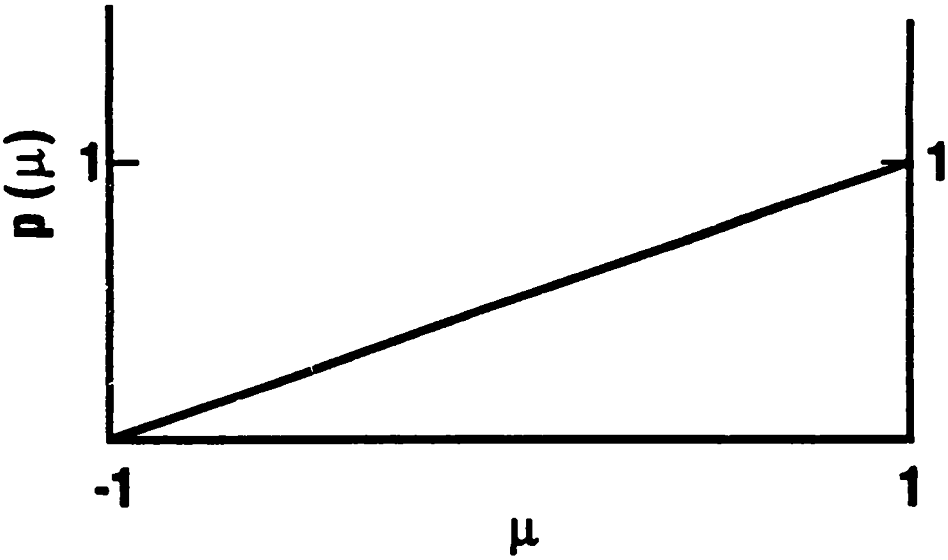

Fig. 1. Cosine scattering distribution.

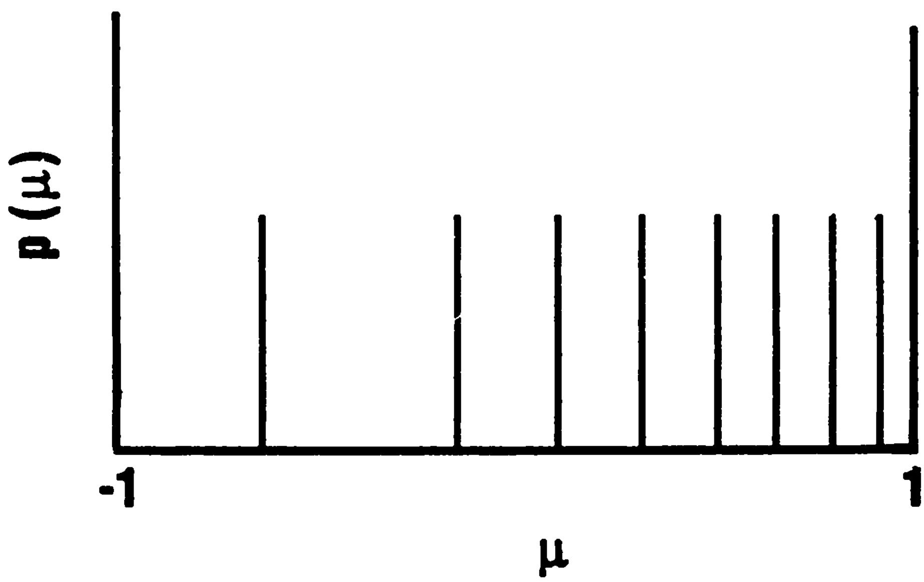

Fig. 2. Discrete representation of cosine scattering distribution.

- Histograms may not exceed the cosine boundaries -1 and +1;
- For coherent elastic scattering, the width of the histogram cannot exceed $\delta\mu \leq .1$.

For incoherent elastic scattering and inelastic scattering, the histogram width is governed only by the first three criteria because line spectra are sometimes a poor representation of the true physical situation. In particular, the NJOY processed $S(\alpha, \beta)$ angular distribution data frequently represents isotropic or near-isotropic scattering as seven equiprobable lines. By letting the histogram width expand without the fourth constraint, the histogram approximation is a more accurate representation of the physics than is the discrete data used in the random walk as illustrated in Fig. 3. This figure shows how Prael's approximate histogram method would represent the discrete distribution of Fig. 2. Clearly this approximation, Fig. 3, is a better approximation to the cosine distribution of Fig. 1 than is the line distribution of Fig. 2.

For a line cosine distribution of $\mu_1, \mu_2, \ldots, \mu_\nu$ and a polar angle cosine, μ_0, between the random walk particle trajectory and the detector or DXTRAN point, there are five cases for deciding whether or not μ_0 is within a histogram and contributes to a detector tally or DXTRAN sphere or not.

1. Case 1: $\mu_2 < \mu_0 < \mu_{\nu-1}$

This case is illustrated in Fig. 4a. The half-width of the histograms at $\mu = a_0$ and $\mu = b_0$ are:

$$\Delta_a = \frac{1}{2} min(b_0 - a_0, a_0 - a_1)$$

$$\Delta_b = \frac{1}{2} min(b_1 - b_0, b_0 - a_0) \quad .$$

If $a_0 \leq \mu_0 < a_0 + \Delta_a$, then μ_0 is in the histogram at $\mu = a_0$ and

$$p(\mu_0) = 1/(\nu 2\Delta_a) \quad .$$

If $b_0 - \Delta_b < \mu_0 \leq b_0$, then μ_0 is in the histogram at $\mu = b_0$ and

$$p(\mu_0) = 1/(\nu 2\Delta_b) \quad .$$

If $a_0 + \Delta_a < \mu_0 \leq b_0 - \Delta_b$, then μ_0 is in neither histogram and

$$p(\mu_0) = 0 \quad .$$

— that is, there is no contribution to the detector or DXTRAN.

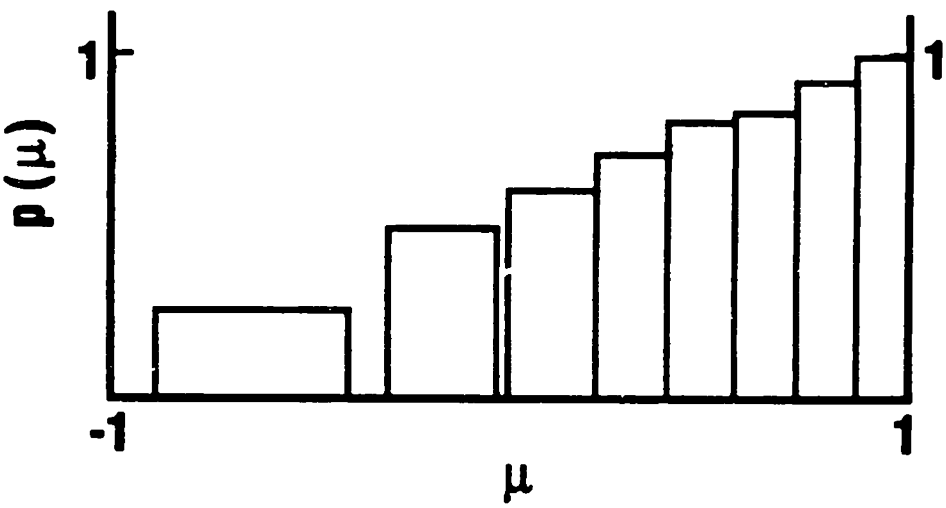

Fig. 3. Histogram approximation of cosine scattering distribution.

2. Case 2: $-1 < \mu_0 < \mu_1$

This case is illustrated in Fig. 4b. The half-width of the histograms at $\mu = b_C = \mu_1$ is:

$$\Delta_b = \frac{1}{2} min(b_1 - b_0, b_0 - (-1)) \quad .$$

If $b_0 - \Delta_b < \mu_0 \leq b_0$, then μ_0 is in the histogram at $\mu = b_0$ and

$$p(\mu_0) = 1/(\nu 2\Delta_b) \quad .$$

If $-1 \leq \mu_0 \leq b_0 - \Delta_b$, then μ_0 is not in histogram and

$$p(\mu_0) = 0 \quad .$$

3. Case 3: $\mu_1 < \mu_0 < \mu_2$

This case is illustrated in Fig. 4c. The half-width of the histograms at $\mu = a_0$ and $\mu = b_0$ are:

$$\Delta_a = \frac{1}{2} min(b_0 - a_0, a_0 - (-1)) \quad , \quad \text{and}$$

$$\Delta_b = \frac{1}{2} min(b_1 - b_0, b_0 - a_0) \quad .$$

If $a_0 \leq \mu_0 < a_0 + \Delta_a$, then μ_0 is in the histogram at $\mu = a_0$ and

$$p(\mu_0) = 1/(\nu 2\Delta_a) \quad .$$

If $b_0 - \Delta_b < \mu_0 \leq b_0$, then μ_0 is in the histogram at $\mu = b_0$ and

$$p(\mu_0) = 1/(\nu 2\Delta_b) \quad .$$

If $a_0 + \Delta_a < \mu_0 \leq b_0 - \Delta_b$, then μ_0 is in neither histogram and

$$p(\mu_0) = 0 \quad .$$

4. Case 4: $\mu_{\nu-1} < \mu_0 < \mu_\nu$

This case is illustrated in Fig. 4d. The half-width of the histograms at $\mu = a_0$ and $\mu = b_0$ are:

$$\Delta_a = \frac{1}{2} min(b_0 - a_0, a_0 - a_1) \quad ,$$

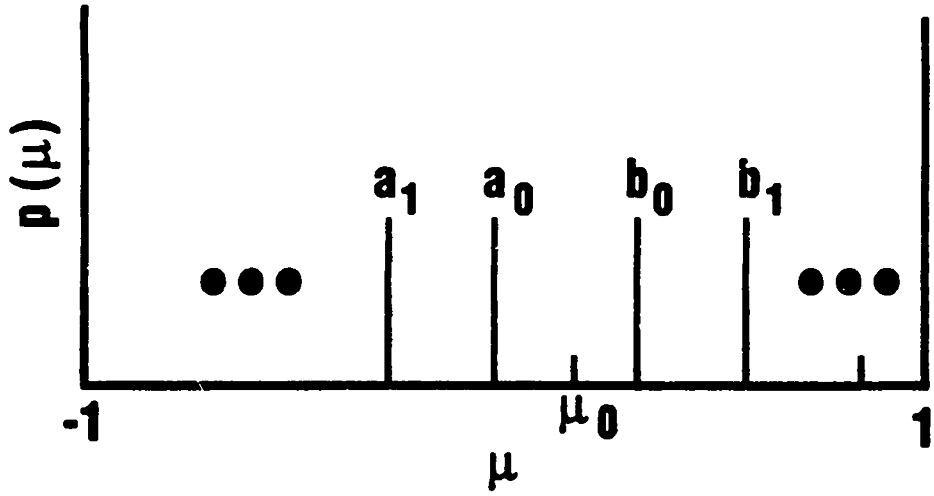

Fig. 4a. Case 1, $\mu_2 < \mu_0 < \mu_{\nu-1}$

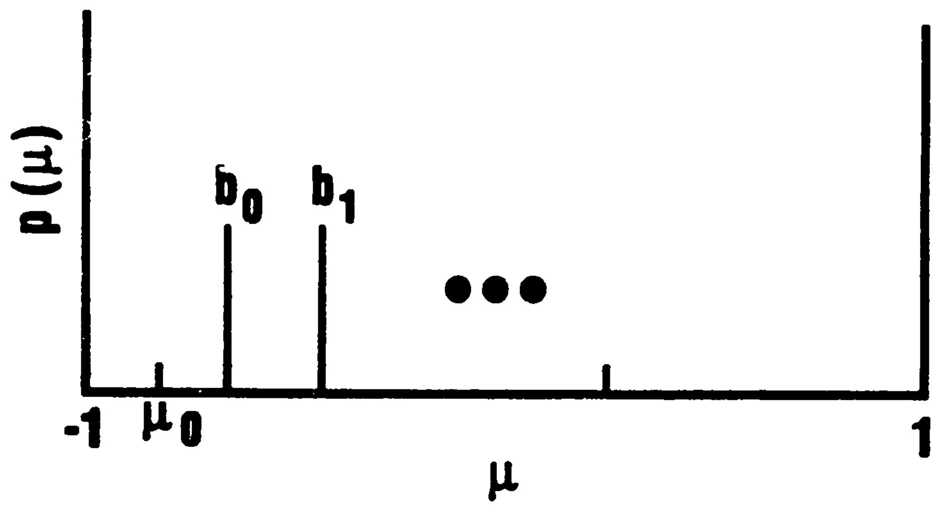

Fig. 4b. Case 2, $-1 < \mu_0 < \mu_1$

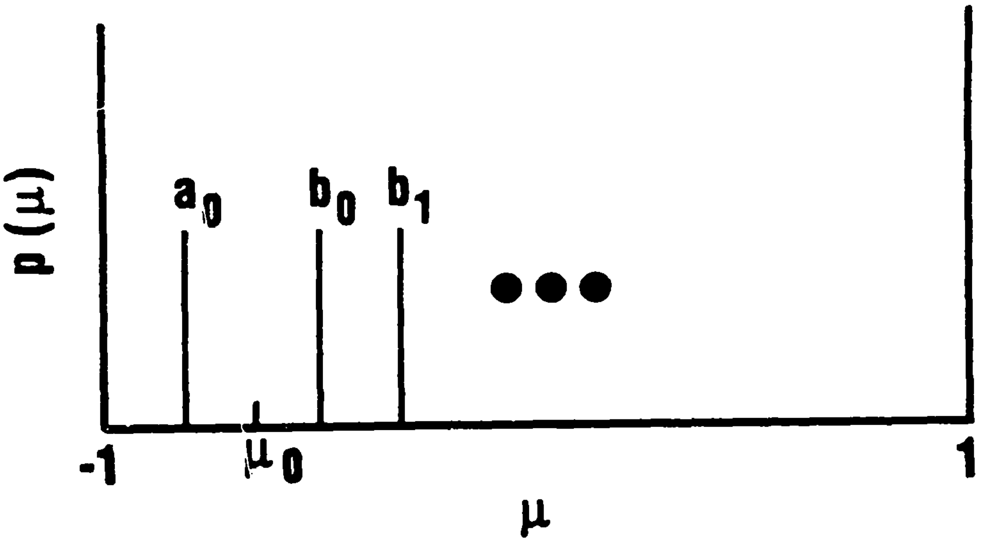

Fig. 4c. Case 3, $\mu_1 < \mu_0 < \mu_2$

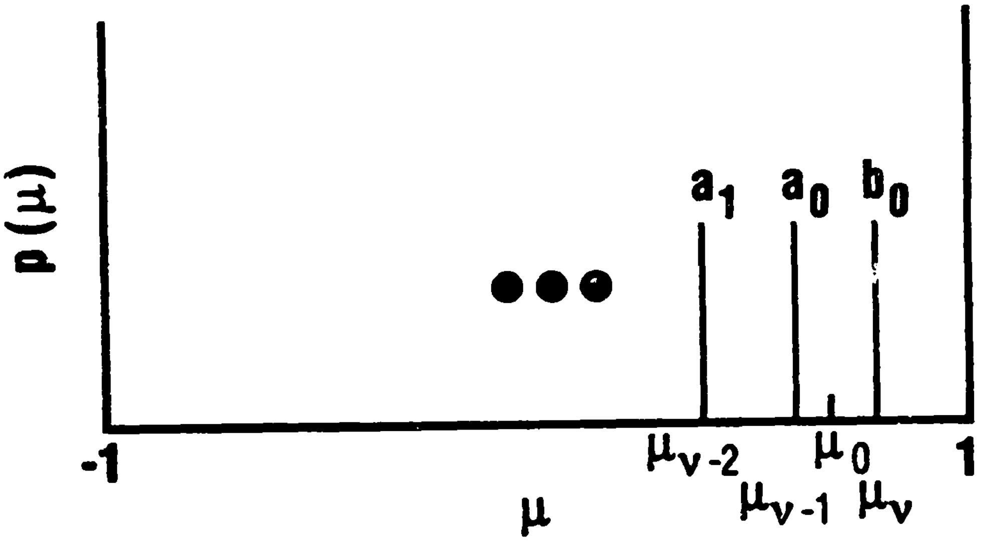

Fig. 4d. Case 4, $\mu_{\nu-1} < \mu_0 < \mu_\nu$

and

$$\Delta_b = \frac{1}{2} min(1 - b_0, b_0 - a_0) \quad .$$

If $a_0 \le \mu_0 < a_0 + \Delta_a$, then μ_0 is in the histogram at $\mu = a_0$ and

$$p(\mu_0) = 1/(\nu 2\Delta_a) \quad .$$

If $b_0 - \Delta_b < \mu_0 \le b_0$, then μ_0 is in the histogram at $\mu = b_0$ and

$$p(\mu_0) = 1/(\nu 2\Delta_b) \quad .$$

If $a_0 + \Delta_a < \mu_0 \le b_0 - \Delta_b$, then μ_0 is in neither histogram and

$$p(\mu_0) = 0 \quad .$$

5. Case 5: $\mu_\nu < \mu_0 < 1$

This case is illustrated in Fig. 4e. The half-width of the histogram at $\mu = a_0$ is:

$$\Delta_a = \frac{1}{2} min(1 - a_0, a_0 - a_1) \quad .$$

If $a_0 \le \mu_0 < a_0 + \Delta_a$, then μ_0 is in the histogram at $\mu = a_0$ and

$$p(\mu_0) = 1/(\nu 2\Delta_a) \quad .$$

If $a_0 + \Delta_a < \mu_0 \le 1$, then μ_0 is outside the histogram and

$$p(\mu_0) = 0 \quad .$$

a. Coherent Elastic Scattering: In the case of coherent elastic scattering the treatment is similar, but the μ values are obtained from the Bragg energies, E_{Bi}, and incident (precollision) neutron energy, E,

$$\mu = 1 - 2E_{Bi}/E \quad .$$

Whereas the tabulated Bragg energies are increasing,

$$E_{Bi} < E_{Bi+1} \quad ,$$

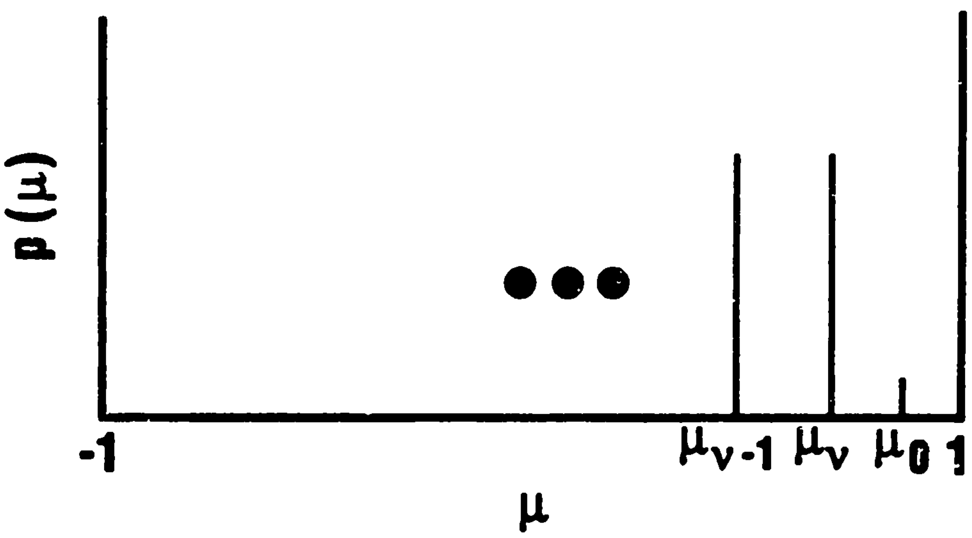

Fig. 4e. Case 5, $\mu_\nu < \mu_0 < 1$

the scattering angles are decreasing,

$$\mu_{i+1} = 1 - E_{Bi+1}/E < 1 - E_{Bi}/E = \mu_i \quad .$$

Also, since the scattering angles are sampled from a cumulative probability distribution with cumulative probabilities $D_1, D_2, \ldots, D_k, \ldots D_\nu$ the values of $p(\mu_0)$ are either zero, or

$$p(\mu_0) = (D_k - D_{k-1})/(2D_\nu \Delta_a) \quad ,$$

or

$$p(\mu_0) = (D_{k+1} - D_k)/(2D_\nu \Delta_b) \quad .$$

D. Prael's Algorithm

Prael's algorithm to implement the above approximate method is shown in Table I, which is a listing of his patch to MCNP3B. The five separate cases described above are consolidated by setting default values of a_1, a_0, b_0, b_1. Table II shows the MCNP4 version of the same patch, converted to compatibility with the pre-public (LANL floor version) of MCNP4 and also converted to Tom Godfrey's MCNP programming style. Further modifications include reducing the number of divides by multiplying by energy, ERG. Both versions of the patch can be made to give identical answers even though they apply to radically different versions of MCNP. All the testing reported herein was done with the MCNP4 version.

III. Test Problems and Results

Forty-nine calculations requiring over 40 hours of Cray XMP-48 computer time have been run to test Prael's approximate scheme. These indicate that the method is working as intended. Additionally, these calculations indicate that the discrepancies between detector tallies using the approximate scheme and tallies using the "exact" random walk are often caused by inadequacies of the data representation used in the random walk. In particular, *the representation of the scattering distributions by the NJOY code as a few discrete lines (typically seven) is poor for distributions which are continuous, particularly isotropic distributions.*

The test calculations can be divided into two families: thick sphere problems and single collision problems. These two families of problems will now be described along with a discussion of the associated results.

TABLE I

S(α,β) PATCH FOR MCNP 3B

```
*ID 2HM3B
*/ START PATCH TO PERMIT S(A,B) WITH DETECTORS AND DXTRAN
*D TD3B.5,9
C        RETURN IF KCODE PROBLEM IS NOT SETTLED.
      IF(KZKF.NE.0)RETURN
*I SB.9
      IXCOS=0
*I SB.34
      NTYN=1
*I SB.41
      NTYN=2
*I SB.82
      IXCOS=-KX
*I SB.87
      IXCOS=KX
*I SB.94
      IC=IC-1
*D CT3B.2
      GO TO(30,40,50,130,160,210,410,250,390,399)IPSC-2
*I CT3A.249
C
C >>>>>  IPSC=9 -- NEUTRON FROM S(A,B) COLLISION
  410 CONTINUE
      CS=UOLD*UUU+VOLD*VVV+WOLD*WWW
      IF (NTYN.EQ.1) THEN
        IF (IXCOS) 420,400,500
      ELSEIF (NTYN.EQ.2) THEN
        IF (IXCOS) 420,550,500
      ELSE
        GO TO 400
      ENDIF
C
C >>>>>  EQUALLY-PROBABLE ANGLE BINS.
  420 CONTINUE
      J=-IXCOS
      LL=NXS(3,IET)
      DO 430 I=1,LL
      IF (CS.LE.YSS(I-IXCOS)) GO TO 440
  430 CONTINUE
      I=LL
  440 CONTINUE
      J=I-IXCOS
      PR=1.0/LL
      DNOM=1.0/(YSS(J-1)-YSS(J))
      GO TO 600
C
C >>>>>  EQUALLY-PROBABLE DISCRETE ANGLES.
  500 CONTINUE
      IF (NTYN.EQ.1) THEN
        RI=RTCR(1,IET)
        LL=NXS(3,IET)
        NI=NXS(4,IET)*(LL+2)
      ELSE
        RI=RTCR(4,IET)
        LL=NXS(6,IET)
        NI=LL+1
      ENDIF
      LLO=IXCOS
      LHI=LLO+LL
      A0=-10.
      A1=-10.
      B1=10.
      B0=10.
      IC=LLO-1
      IB=LHI+1
  510 IF(IB-IC.EQ.1)GO TO 530
      IH=(IC+IB)/2
      IF(CS.LT.(YSS(IH)+RI*(YSS(IH+NI)-YSS(IH))))GO TO 520
      IC=IH
      GO TO 510
  520 IB=IH
      GO TO 510
  530 CONTINUE
      IF (IC.GT.LLO) A1=YSS(IC-1)+RI*(YSS(IC-1+NI)-YSS(IC-1))
      IF (IC.GE.LLO) A0=YSS(IC)+RI*(YSS(IC+NI)-YSS(IC))
      IF (IB.LE.LHI) B0=YSS(IB)+RI*(YSS(IB+NI)-YSS(IB))
      IF (IB.LT.LHI) B1=YSS(IB+1)+RI*(YSS(IB+1+NI)-YSS(IB+1))
      A=A0+MIN(0.5*(B0-A0),0.5*(A0-A1),1.-A0,A0+1.)
      B=B0-MIN(0.5*(B0-A0),0.5*(B1-B0),1.-B0,B0+1.)
      IF (CS.LE.A) THEN
```

TABLE I (cont)

S(α,β) PATCH FOR MCNP 3B

```
          DNOM=0.5/(A-AO)
        ELSEIF (CS.GE.B) THEN
          DNOM=0.5/(BO-B)
        ELSE
          GO TO 400
        ENDIF
        PR=1.0/(LL+1)
        GO TO 600
C
C >>>>>  EXACT TREATMENT OF COHERENT ELASTIC SCATTERING
  550 CONTINUE
      LLO=JXS(5,IET)
      LHI=JXS(5,IET)+KTCR(2,IET)-1
      AO=-10.0
      A1=-10.0
      BO=10.0
      B1=10.0
      IC=LLO-1
      IB=LHI+1
  560 IF(IB-IC.EQ.1) GO TO 580
      IM=(IC+IB)/2
      IF(CS.GT.(1.-2.*YSS(IM-INT(YSS(JXS(4,IET))))/ERG))GO TO 570
      IC=IM
      GO TO 560
  570 IB=IM
      GO TO 560
  580 CONTINUE
      IF (IC.GT.LLO)  B1=1.-2.*YSS(IC-1-INT(YSS(JXS(4,IET))))/ERG
      IF (IC.GE.LLO) BO=1.-2.*YSS(IC-INT(YSS(JXS(4,IET))))/ERG
      IF (IB.LE.LHI) AO=1.-2.*YSS(IB-INT(YSS(JXS(4,IET))))/ERG
      IF (IB.LT.LHI) A1=1.-2.*YSS(IB+1-INT(YSS(JXS(4,IET))))/ERG
      TMPLIM=0.05
      B=BO-MIN(0.5*(BO-AO),0.5*(B1-BO),1.-BO,BO+1.,TMPLIM)
      A=AO+MIN(0.5*(BO-AO),0.5*(AO-A1),1.-AO,AO+1.,TMPLIM)
      IF (CS.LT.A) THEN
        DNOM=0.5/(A-AO)
        DPA=YSS(IB)
        IF (IB.GT.LLO) DPA=DPA-YSS(IB-1)
        PR=DPA/YSS(LHI)
      ELSEIF (CS.GT.B) THEN
        DNOM=0.5/(BO-B)
        DPB=YSS(IC)
        IF (IC.GT.LLO) DPB=DPB-YSS(IC-1)
        PR=DPB/YSS(LHI)
      ELSE
        GO TO 400
      ENDIF
  600 PSC=PR*DNOM
      RETURN
*D DX3A.1
*D ST3A.24
*D ST.150
*/ END PATCH TO PERMIT S(A,B) WITH DETECTORS AND DXTRAN
```

TABLE II

S(α, β) PATCH FOR MCNP 4

```
*IDENT SABFIX <<<<< S(ALPHA,BETA) DXTRAN AND DETECTORS >>>>> 6/12/90
*/
*/ ------------------------------------------------------------ STUFF
*D,ST.187 LINE 9822
*D,ST.190 LINE 9825 ELIMINATE CALL SABERR
*/
*/ ------------------------------------------------------------ SABERR
*D,SJ.1,SJ.30 LINES 10163 - 10192 ELIMINATE ROUTINE SABERR
*/
*/ ------------------------------------------------------------ DXTRAN
*D,DX.6 LINE 18338 IF(IPSC.EQ.9)
*D,DX.69,DX.74 LINES 18401 - 18406
  110 L=ICL+MXA*(NDX(1)*(IPT-1)-1)
      DO 140 IX=1,NDX(IPT)
      IF(IDX.NE.IX)NZIYTC(1,IX,IPT)=NZIYTC(1,IX,IPT)+1
*/
*/ ------------------------------------------------------------ SABCOL
*I,SB.7 LINE 20739 AFTER LINE 20739
      NTYN=0
      IXCOS=0
*I,SB.32 LINE 20764 BEFORE GO TO(
      NTYN=1
*I,SB.39 LINE 20771 BEFORE GO TO(
      NTYN=2
*I,SB.46 LINE 20778 BEFORE GO TO 130
      IXCOS=-KX
*I,SB.51 LINE 20783 BEFORE GO TO 130
      IXCOS=KX
*/
*/ ------------------------------------------------------------ TALLYD
*D,TD.7 LINE 23296
C         RETURN IF KCODE PROBLEM IS NOT SETTLED.
*D,TD.9 LINE 23298 IF(IPSC.EQ.9)
*D,TD.352,TD.357 LINES 23641 - 23646 IPSC=9 CASE
*/
*/ ------------------------------------------------------------ CALCPS
*D,CT.9 LINE 23738
      GO TO(10,20,30,120,150,200,251,260,400,440,460)IPSC-2
*I,CT.150 LINE 23879 BEFORE IPSC=10 BLOCK
C
C >>>>>  IPSC=9 -- NEUTRON FROM S(A,B) COLLISION.
  251 CS=UOLD*UUU+VOLD*VVV+WOLD*WWW
      IF(IXCOS.EQ.0.AND.NTYN.EQ.2)GO TO 550
      IF(IXCOS.GT.0)GO TO 255
      IF(IXCOS.EQ.0)GO TO 460
C
C         EQUALLY-PROBABLE ANGLE BINS.  IXCOS < 0
      LL=NXS(LNXS+3*NTYN,IET)
      IF(CS.LT.XSS(-IXCOS).OR.CS.GT.XSS(LL-IXCOS))GO TO 460
      DO 253 I=1,LL
  253 IF(CS.LE.XSS(I-IXCOS))GO TO 254
  254 PSC=1./(LL*(XSS(I-IXCOS-1)-XSS(I-IXCOS)))
      RETURN
C
C         EQUALLY-PROBABLE DISCRETE ANGLES.  IXCOS > 0
  255 IF(NTYN.NE.1)GO TO 490
      RI=RTC(KRTC+1,IET)
      LL=NXS(LNXS+3,IET)
      NI=NXS(LNXS+4,IET)*(LL+2)
      GO TO 500
  490 RI=RTC(KRTC+4,IET)
      LL=NXS(LNXS+6,IET)
      NI=LL+1
  500 PSC=0.
      A1=-10.
      A0=-10.
      B0=10.
      B1=10.
      IC=IXCOS-1
      IB=IXCOS+LL+1
  510 IF(IB-IC.EQ.1)GO TO 530
      IH=(IC+IB)/2
      IF(CS.LT.(XSS(IH)+RI*(XSS(IH+NI)-XSS(IH))))GO TO 520
      IC=IH
      GO TO 510
  520 IB=IH
      GO TO 510
  530 IF(IC.GT.IXCOS)A1=XSS(IC-1)+RI*(XSS(IC-1+NI)-XSS(IC-1))
      IF(IC.GE.IXCOS)A0=XSS(IC)+RI*(XSS(IC+NI)-XSS(IC))
      IF(IB.LE.IXCOS+LL)B0=XSS(IB)+RI*(XSS(IB+NI)-XSS(IB))
```

TABLE II (cont)

S(α,β) PATCH FOR MCNP 4

```
      IF(IB.LT.IXCOS+LL)B1=XSS(IB+1)+RI*(XSS(IB+1+NI)-XSS(IB+1))
      DA=MIN(.5*(BO-AO),.5*(AO-A1),1.-AO,AO+1.)
      DB=MIN(.5*(BO-AO),.5*(B1-BO),1.-BO,BO+1.)
      IF(CS.LT.AO+DA)PSC=.5/((LL+1)*DA)
      IF(CS.GT.BO-DB)PSC=.5/((LL+1)*DB)
      RETURN
C
C        EXACT TREATMENT OF COHERENT ELASTIC SCATTERING. IXCOS=O, NTYN=2
  550 NC=INT(XSS(JXS(LJXS+4,IET)))
      LO=JXS(LJXS+5,IET)-NC
      IC=LO-1
      IB=LO+KTC(KKTC+2,IET)
      LH=IB-1
      A1=-10.*ERG
      AO=-10.*ERG
      BO=10.*ERG
      B1=10.*ERG
  560 IF(IB-IC.EQ.1)GO TO 580
      IH=(IC+IB)/2
      IF(CS*ERG.GT.ERG-2.*XSS(IH))GO TO 570
      IC=IH
      GO TO 560
  570 IB=IH
      GO TO 560
  580 IF(IB.LT.LH)A1=ERG-2.*XSS(IB+1)
      IF(IB.LE.LH)AO=ERG-2.*XSS(IB)
      IF(IC.GE.LO)BO=ERG-2.*XSS(IC)
      IF(IC.GT.LO)B1=ERG-2.*XSS(IC-1)
      DA=MIN(.5*(BO-AO),.5*(AO-A1),ERG-AO,AO+ERG,.05*ERG)
      DB=MIN(.5*(BO-AO),.5*(B1-BO),ERG-BO,BO+ERG,.05*ERG)
      IF(CS*ERG.LT.AO+DA)GO TO 590
      IF(CS*ERG.LT.BO-DB)GO TO 460
      DX=XSS(IC+NC)
      IF(IC.GT.LO)DX=DX-XSS(IC+NC-1)
      PSC=.5*ERG*DX/(XSS(LH+NC)*DB)
      RETURN
  590 DX=XSS(IB+NC)
      IF(IB.GT.LO)DX=DX-XSS(IB+NC-1)
      PSC=.5*ERG*DX/(XSS(LH+NC)*DA)
      RETURN
*/ REORDER LABELS IN ROUTINE DXTRAN.
*/ REORDER LABELS IN ROUTINE TALLYD.
*/ REORDER LABELS IN ROUTINE CALCPS.
```

A. Thick Sphere Problems

The thick sphere test problem is simply a 12 cm sphere composed of the following materials:

Material	MCNP $S(\alpha,\beta)$ designator	Isotopic composition
Light water	LWTR	H_2O
Polyethylene	POLY	CH_2
H in ZrH_x	H/ZR	ZrH
Benzene	BENZ	CH_2
Heavy Water	HWTR	D_2O
Beryllium metal	BE	Be
Beryllium oxide	BEO	BeO
Graphite	GRPH	C
Zr in ZrH_x	ZR/H	ZrH

Nine problems were run in this family of problems, each for 100,000 histories or 30 minutes Cray XMP48 time, whichever was less. The only difference between the problems was the substitution of different materials. In each case there was a monoenergetic 10 keV point source at the center of the sphere and there were surface, point, and ring detector flux tallies on the outside of the sphere to tally escaping neutrons in a fine energy group structure from .0001 eV to 20 keV. Room temperature (300°K) $S(\alpha,\beta)$ thermal data sets were used everywhere, and a free gas thermal treatment was used for non-$S(\alpha,\beta)$ collisions, also at room temperature (.02584 eV). An unambiguous description of this family of test problems is the MCNP input file which is presented in Table III for the BeO case.

The purpose of the thick sphere problem was to compare surface tallies of the random walk thermalization to both point and ring detector tallies of the same problem. Results are presented in Figs. 5-13. Agreement between the random walk surface tally (solid lines), and the point and ring detector estimates (dashed lines) is excellent.

B. Single Collision Problems

The single collision family of problems consists of 40 problems using the following materials:

TABLE III

LARGE THICK SPHERE PROBLEM INPUT FILE

```
LARGE BEO SPHERE
1       1 0.1 -1
2       0 1 -2
3       0 2

1       SO 12.
2       SO 16.

M1      4009 1 8016 1
MT1     BEO.01
PHYS:N  100
TMP1   2.584-8  0 0
THTME   1.0E+123
SDEF ERG=.00001
IMP:N    1 1 0
F2:N    2
FC2     LARGE BEO SPHERE
SD2     3217.
F5:N     0 0 16. 0
F15Z:N  0. 16. 0
EO      1.-10 3.16-10 1.-9 3.16-9 1.-8 3.16-8 1.-7 3.16-7 1.-6
        2.-6 3.-6 4.-6 5.-6 6.-6 7.-6 8.-6 9.-6 9.999-6 1.0001-5 2.-5
NPS     100000
PRDMP 2J 1
PRINT
```

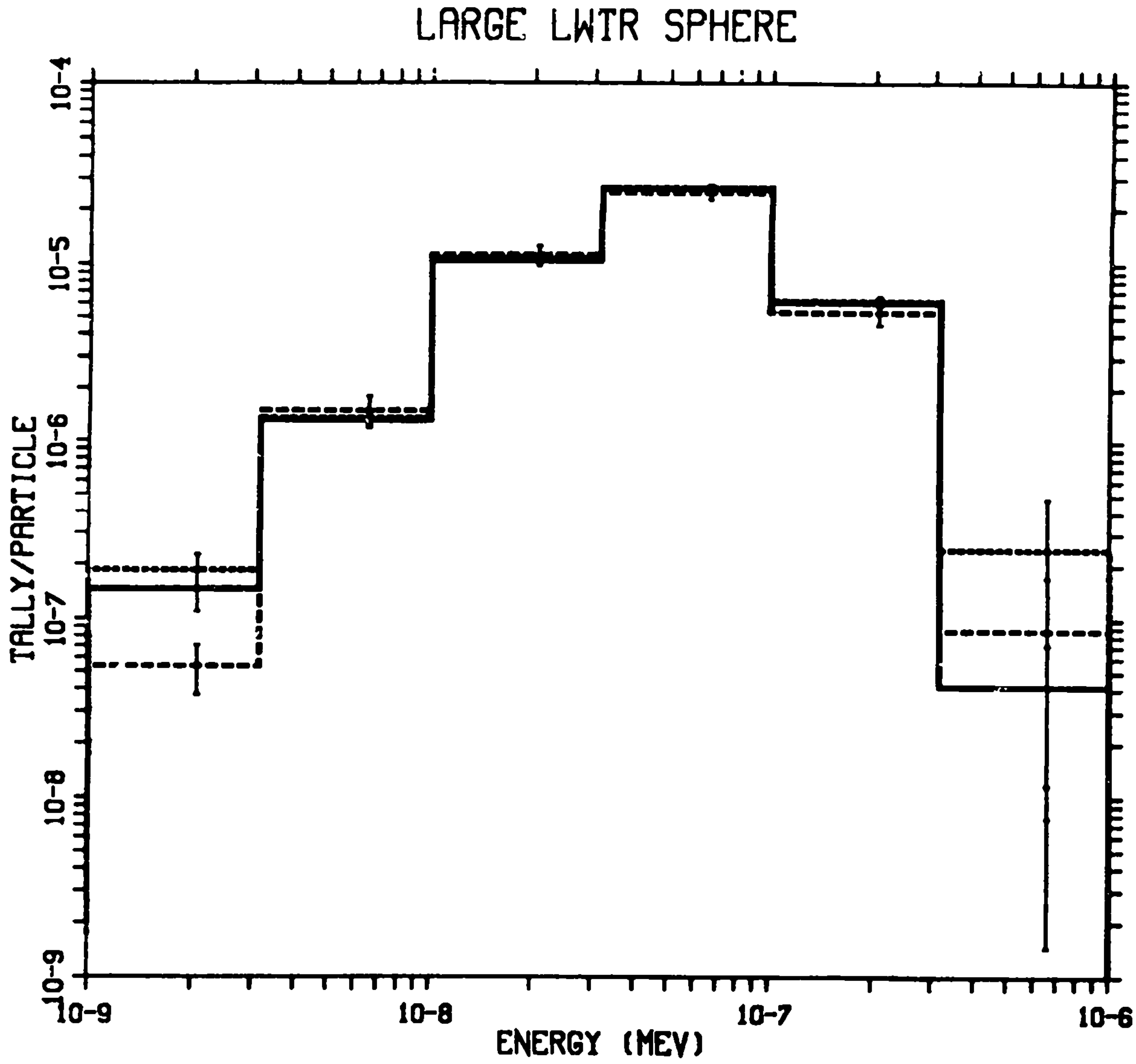
LARGE LWTR SPHERE
TALLY/PARTICLE
10-4
10-5
10-6
10-7
10-8
10-9
10-9
10-8
10-7
10-6
ENERGY (MEV)

Fig. 5.

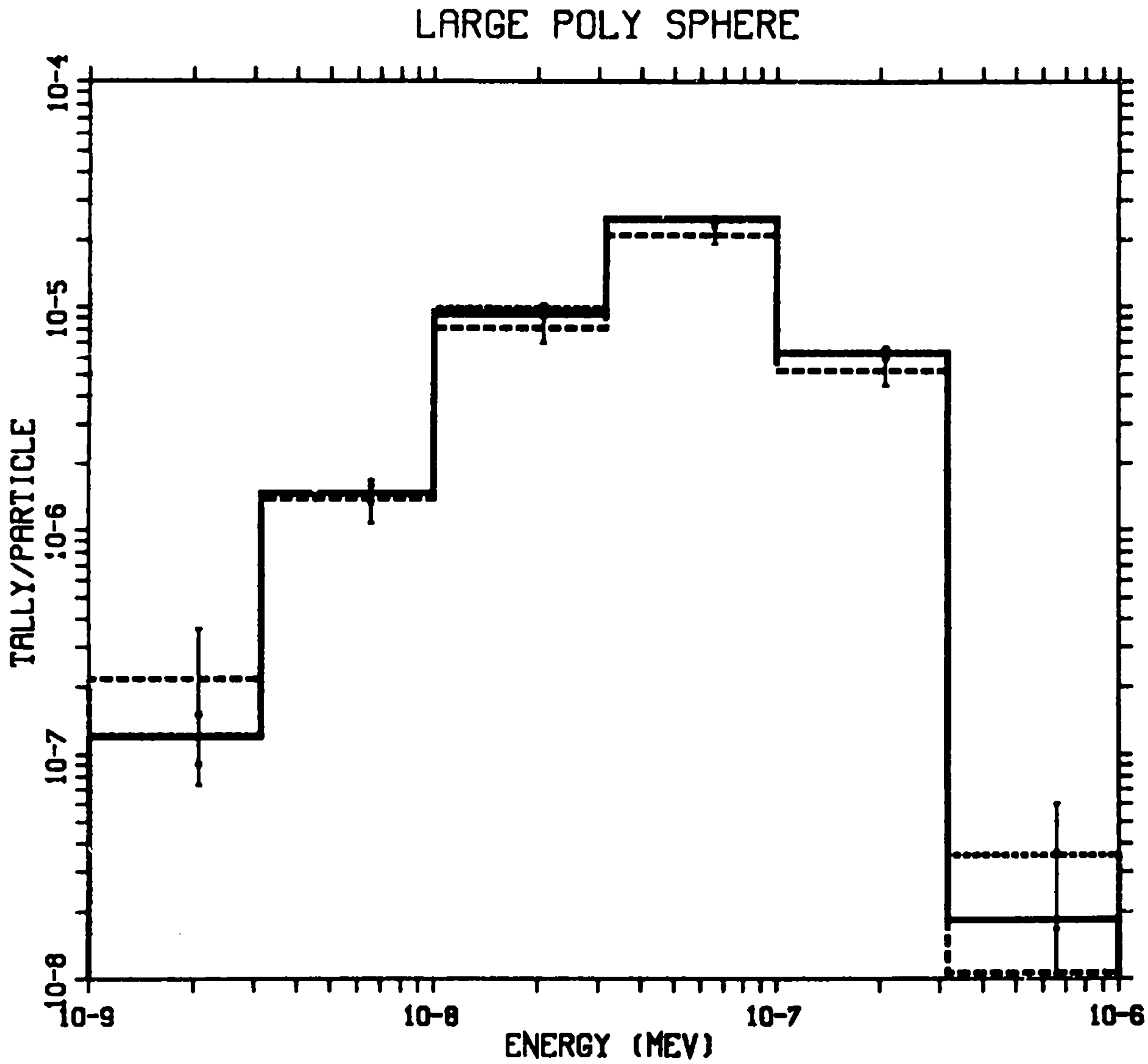
LARGE POLY SPHERE
10-4
10-5
10-6
10-7
10-8
TALLY/PARTICLE
10-9
10-8
10-7
10-6
ENERGY (MEV)

Fig. 6.

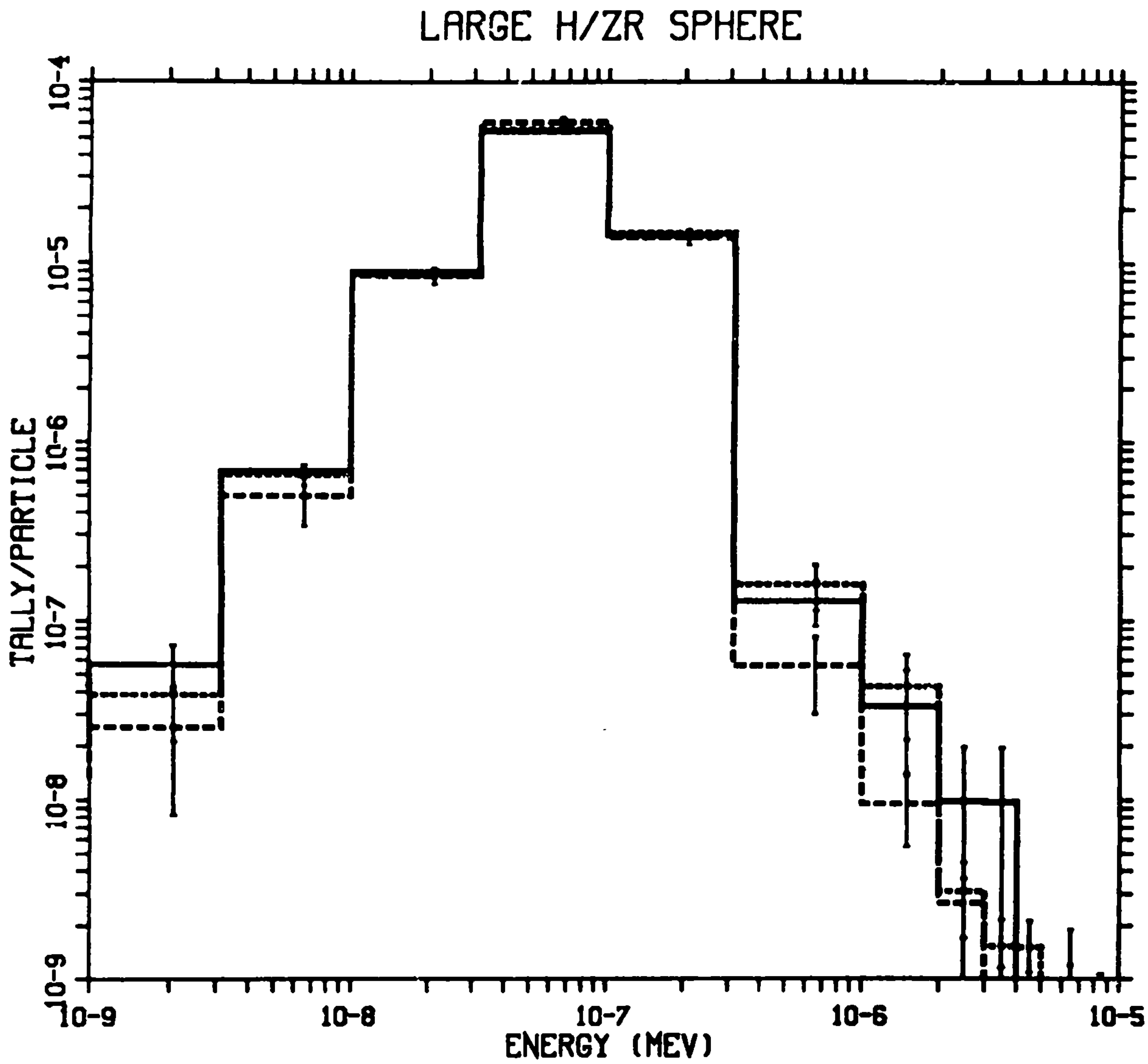
LARGE H/ZR SPHERE
TALLY/PARTICLE
10-4
10-5
10-6
10-7
10-8
10-9
10-9
10-8
10-7
10-6
10-5
ENERGY (MEV)

Fig. 7.

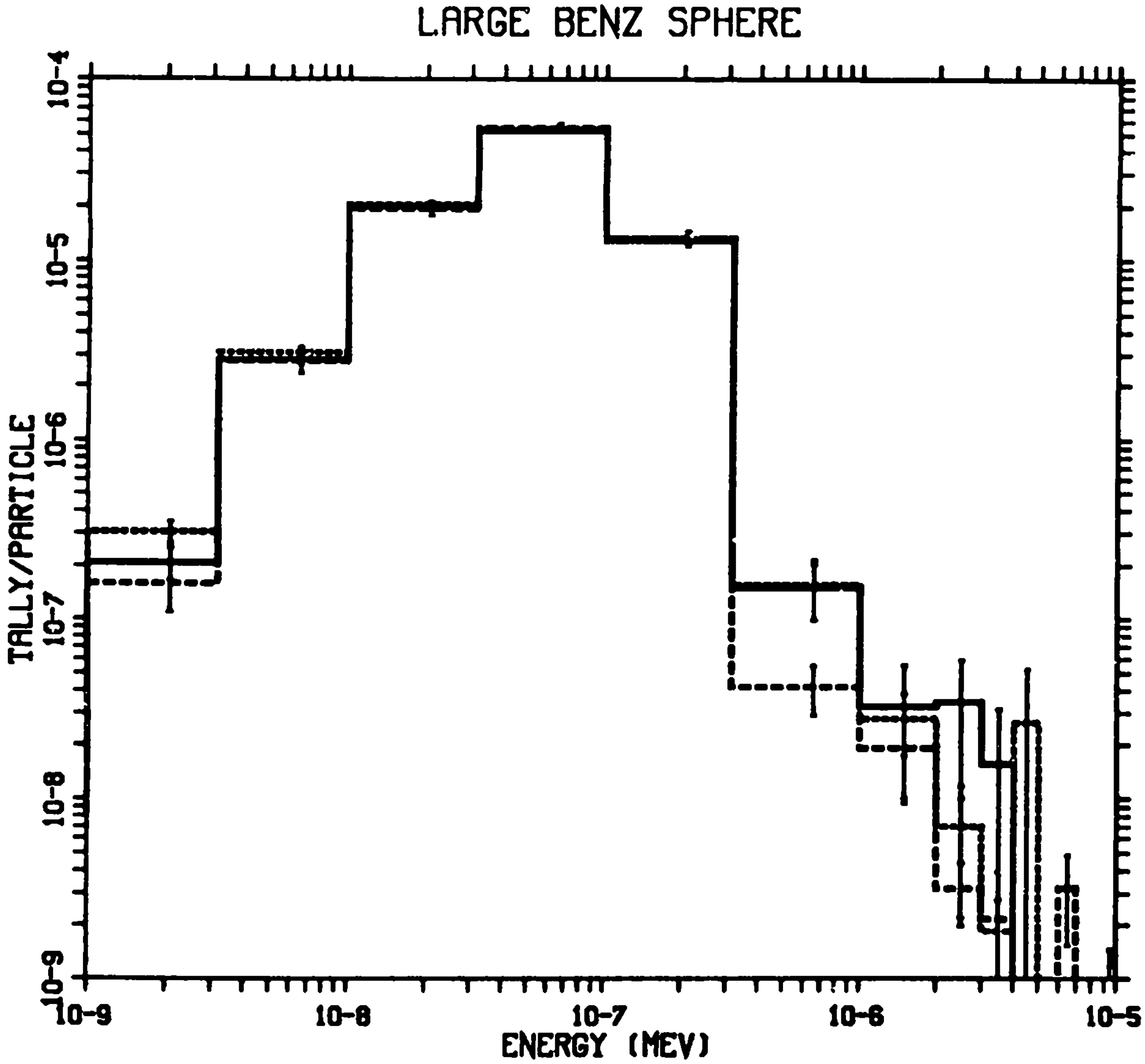

LARGE BENZ SPHERE
TALLY/PARTICLE
10-4
10-5
10-6
10-7
10-8
10-9
10-9
10-8
10-7
10-6
10-5
ENERGY (MEV)

Fig. 8.

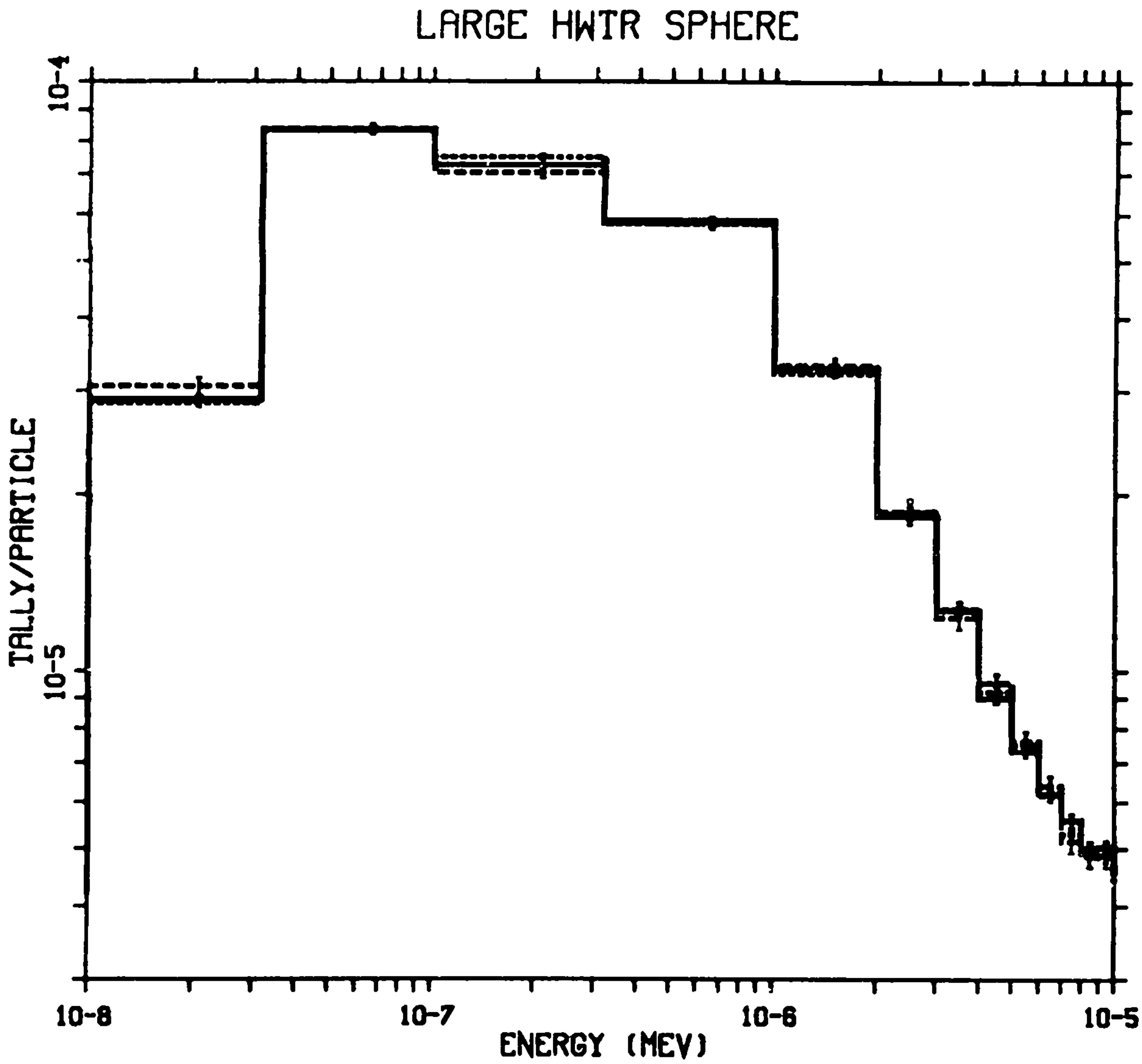
LARGE HWTR SPHERE
10-4
10-5
TALLY/PARTICLE
10-8
10-7
10-6
10-5
ENERGY (MEV)

Fig. 9.

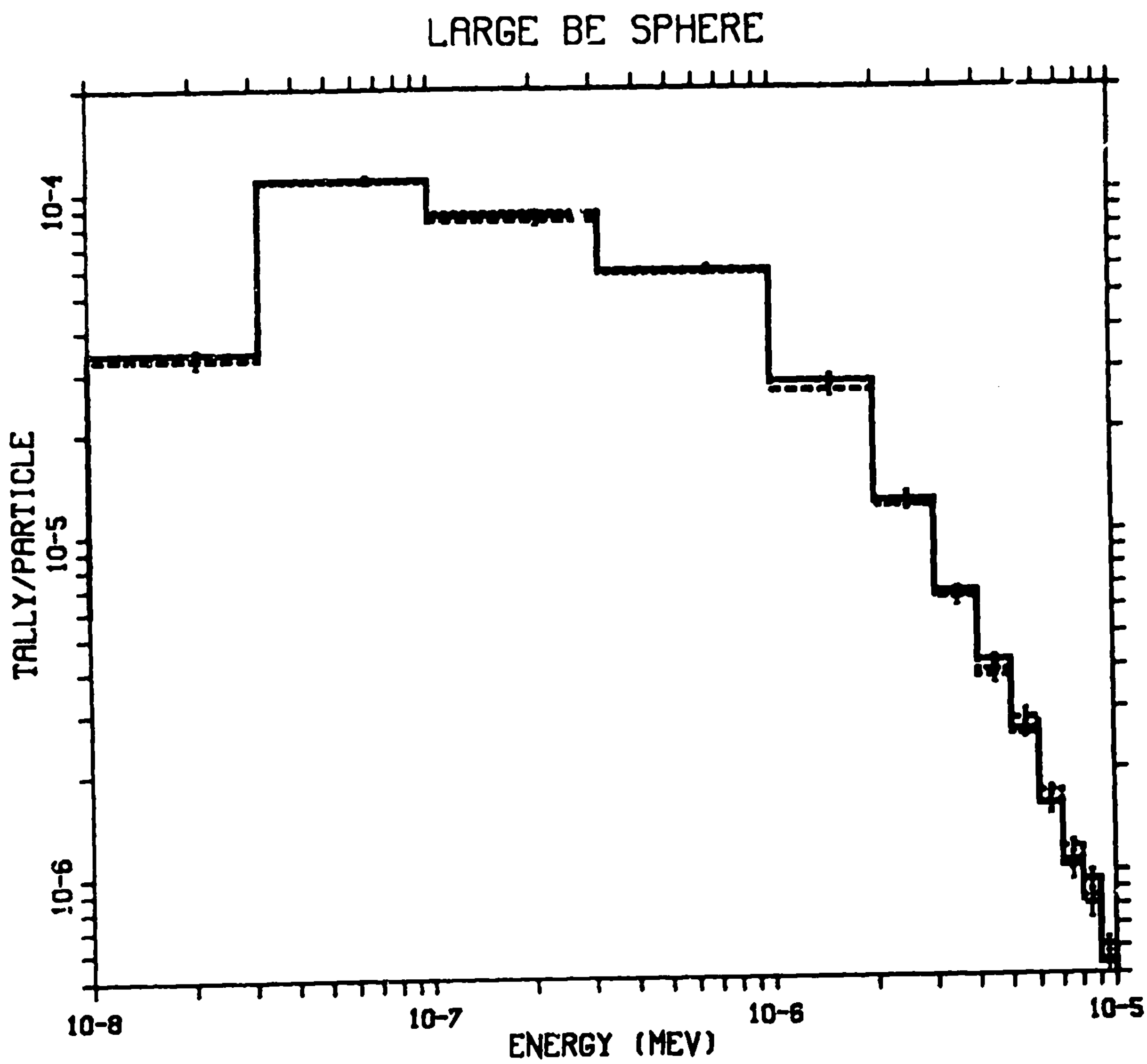
LARGE BE SPHERE
TALLY/PARTICLE
10-4
10-5
10-6
10-8
10-7
10-6
10-5
ENERGY (MEV)

Fig. 10.

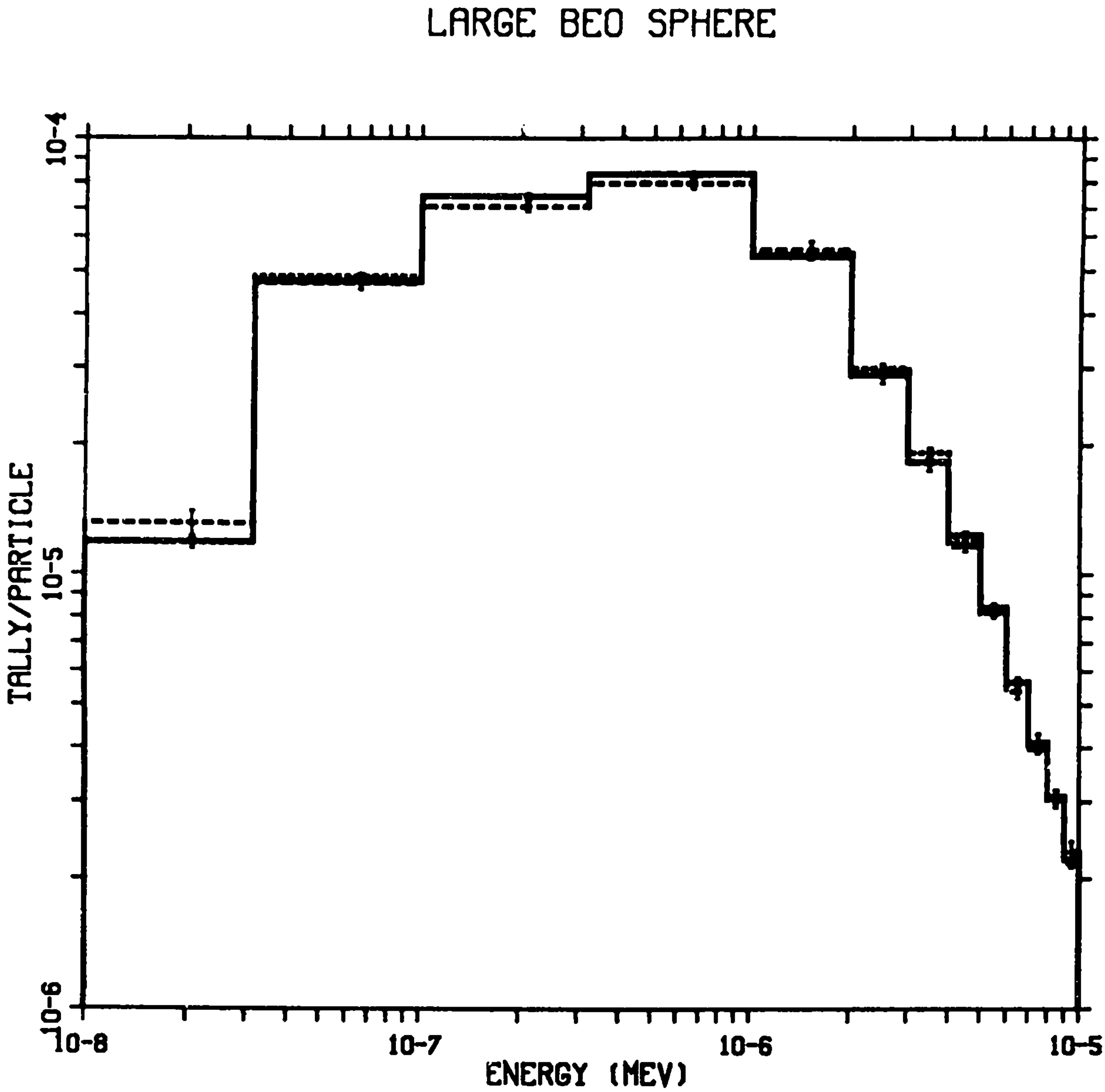
LARGE BEO SPHERE
TALLY/PARTICLE
10-4
10-5
10-6
10-8
10-7
10-6
10-5
ENERGY (MEV)

Fig. 11.

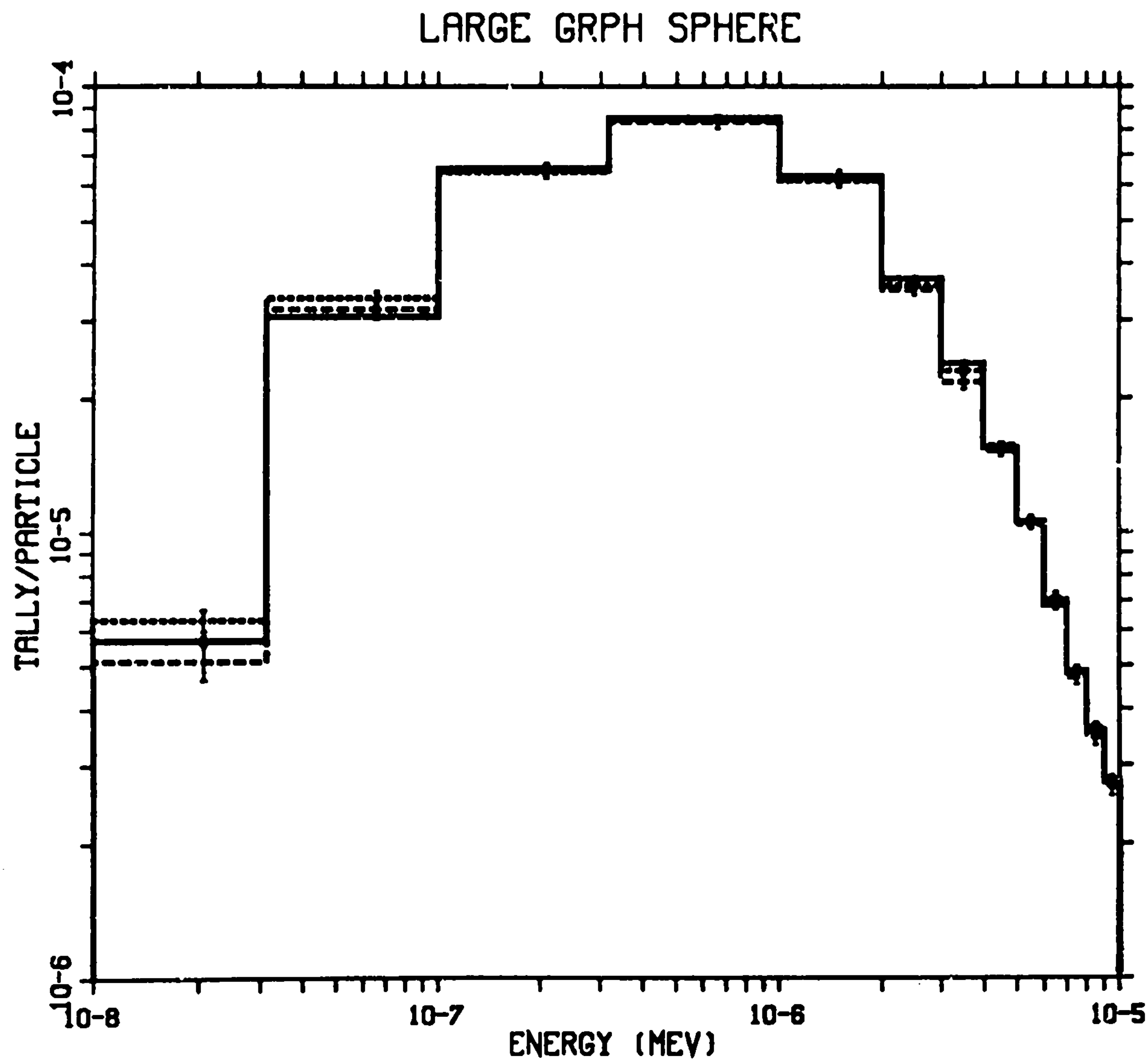
LARGE GRPH SPHERE
TALLY/PARTICLE
10-4
10-5
10-6
10-8
10-7
10-6
10-5
ENERGY (MEV)

Fig. 12.

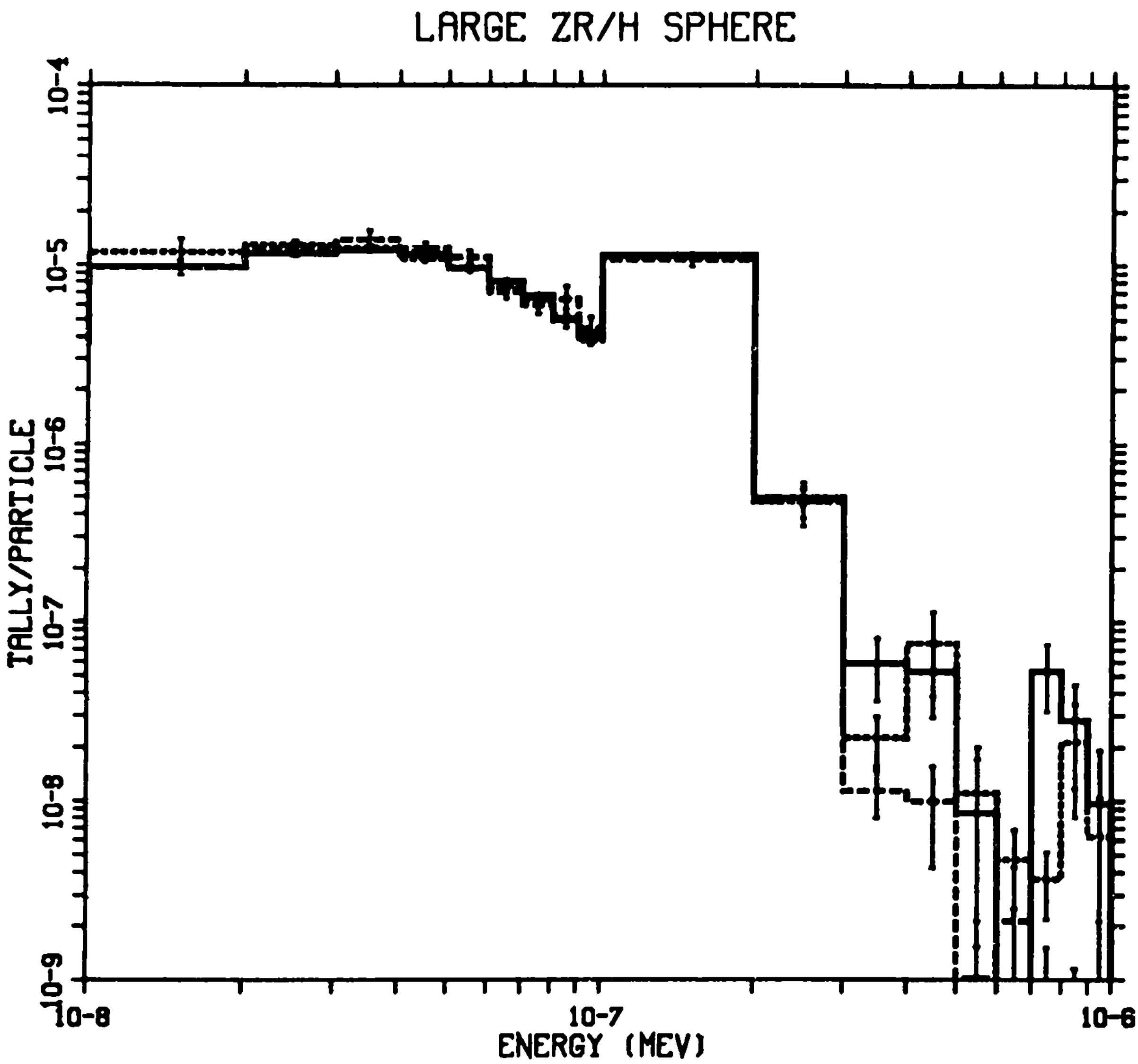
LARGE ZR/H SPHERE
TALLY/PARTICLE
10-4
10-5
10-6
10-7
10-8
10-9
10-8
10-7
10-6
ENERGY (MEV)

Fig. 13.

Material	MCNP $S(\alpha,\beta)$ designator	Isotopic composition
Light water	LWTR	H_2O
Polyethylene	POLY	CH_2
H in ZrH_x	H/ZR	ZrH
Benzene	BENZ	CH_2
Heavy Water	HWTR	D_2O
Beryllium metal	BE	Be
Beryllium oxide	BEO	BeO
Graphite	GRPH	C
Zr in ZrH_x	ZR/H	ZrH
Zr in ZrH_x	ZR/H	ZrH_2

For each of these materials problems were run at the source energies of 1 eV, .1 eV, .01 eV, and .001 eV. The neutron sources were all monodirectional line sources aimed at a tiny sphere where exactly one collision was forced. Scattering from this collision was then tallied in 20 equispaced angular cosine bins relative to the incident particle direction in a current tally on a spherical surface far away from the collision. The current tally was converted to a flux tally by dividing by surface areas and is plotted in the histogram plots in Figs. 14a - 53a. These are compared to point detector tallies plotted in Figs. 14b - 53b. An unambiguous description of the problem is the MCNP input file for one of this family of problems which is presented in Table IV.

In many cases, the results indicate excellent agreement between the approximate detector scheme and the random walk. The low values for the detectors at $\mu = -1$ and $\mu = 1$ (detectors 1 and 20) come from placing the detectors inadvertently on histogram edges and are to be ignored.

As an example of good agreement between the approximate detector method and the random walk, consider the case of BeO at .01 eV (Figs. 40a and 40b). The Bragg edges are all predicted quite well. Another example of good agreement is the forward-peaked angular distribution of light water at 1 eV (Figs. 14a and 14b).

In some cases, however, the detector-calculated fluxes differ greatly from those of the random walk. Consider the case of hydrogen in zirconium hydride (H/Zr) with a .001 eV source. The random walk results (Fig. 25a) look like a picket fence ranging over two orders of magnitude of flux; the detector approximation (Fig. 25b), on the other hand, is flat. This is an isotropic distribution, and the flux at each angle should therefore be uniform as in the detector result. The picket fence result of the random walk is caused by the representation of this isotropic distribution as a set of a few discrete lines by the NJOY nuclear data processing code. This representation of the data is clearly inadequate for these problems with a high

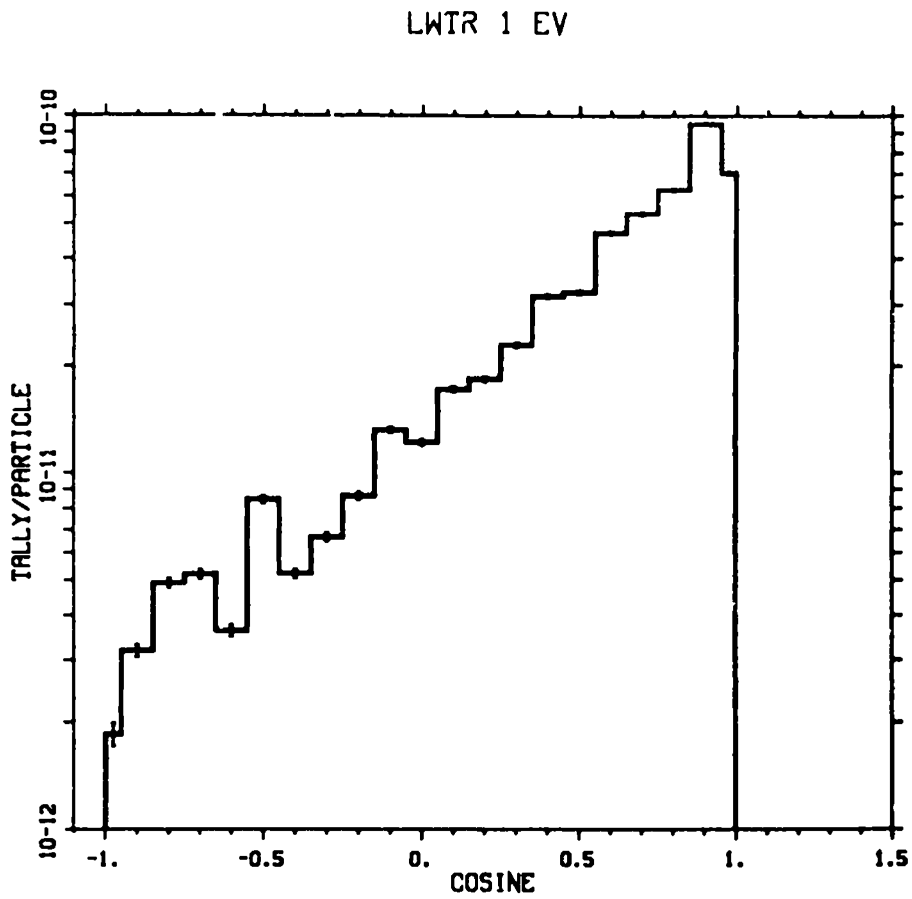

Fig. 14a.

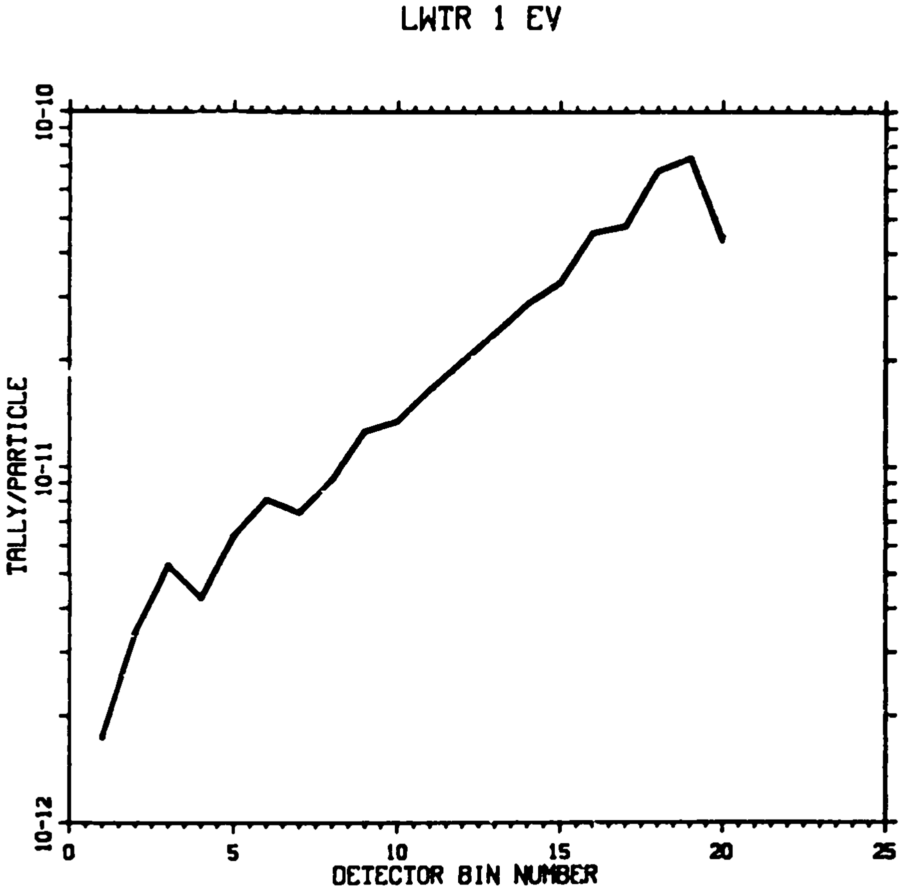

Fig. 14b.

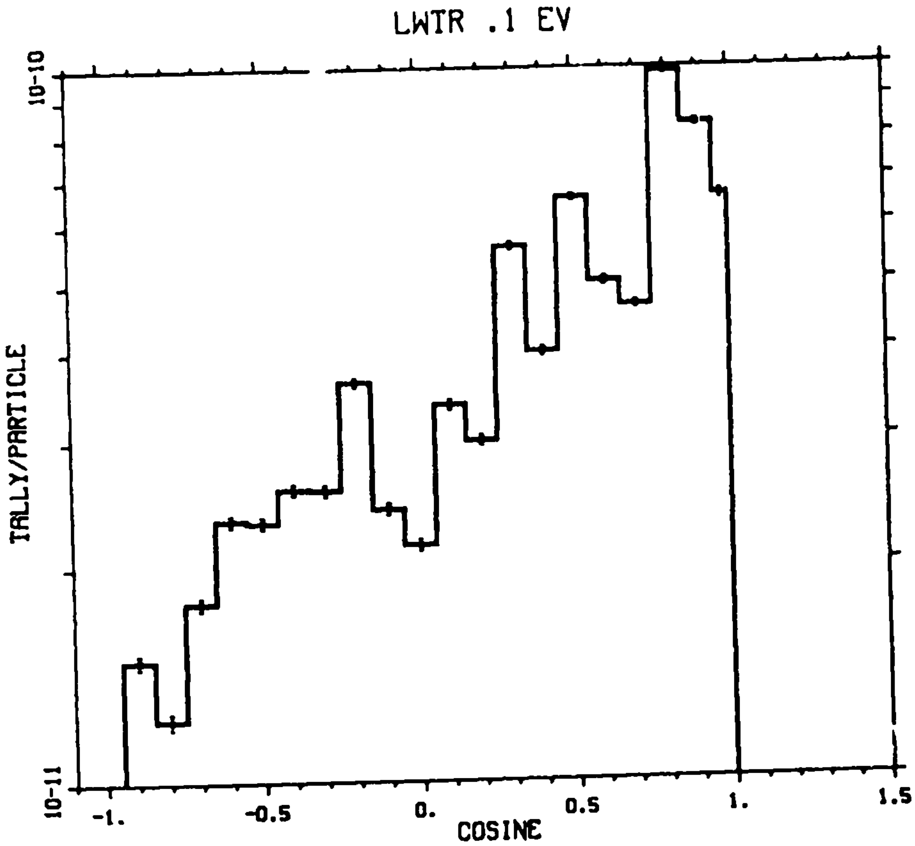

Fig. 15a.

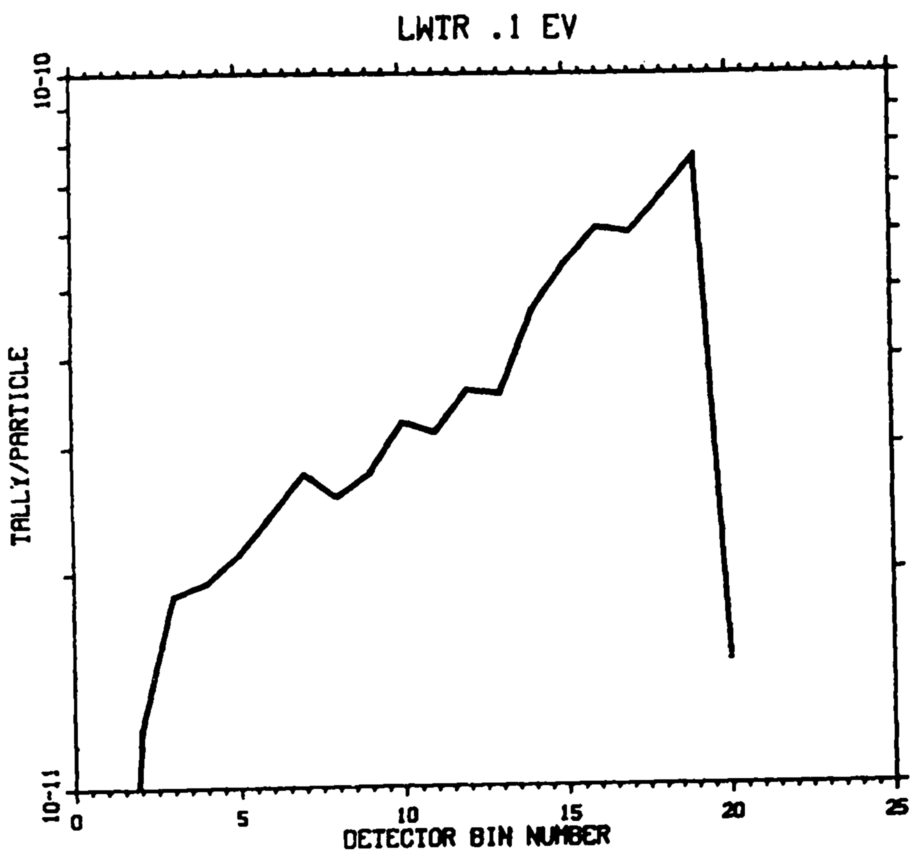

Fig. 15b.

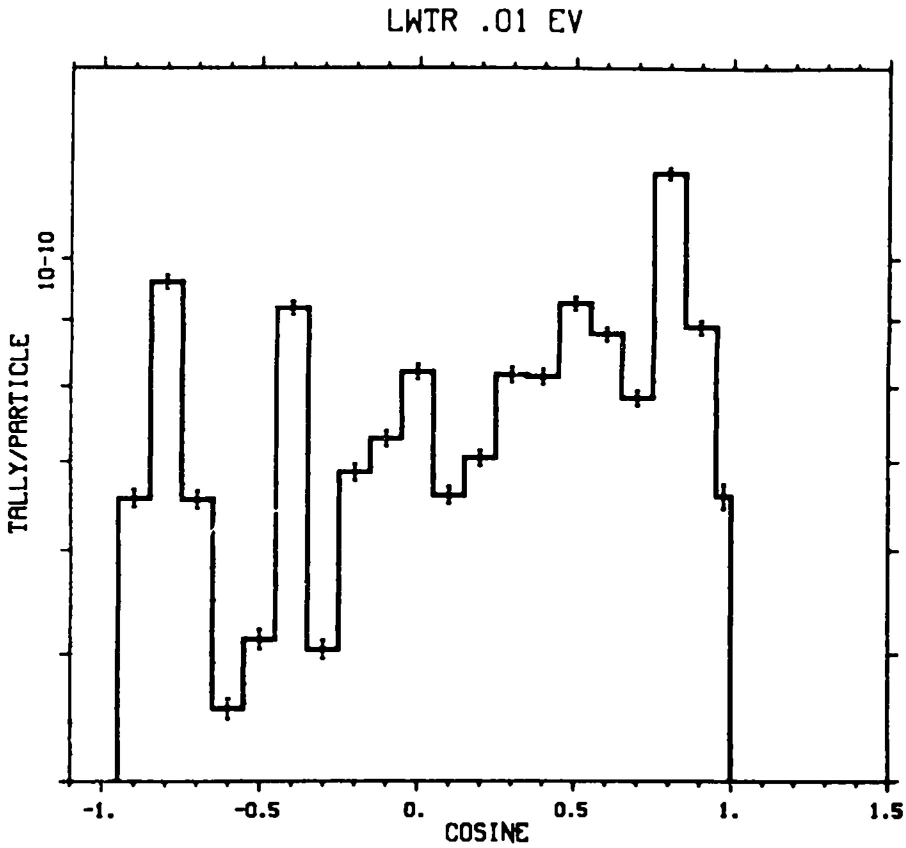

Fig. 16a.

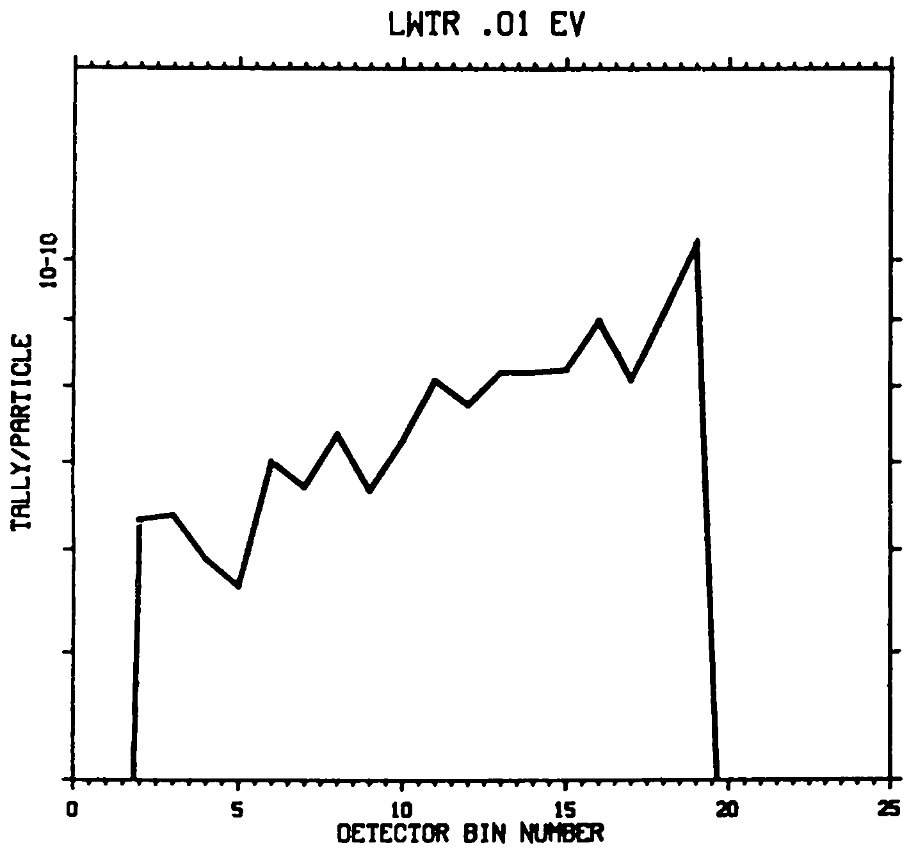

Fig. 16b.

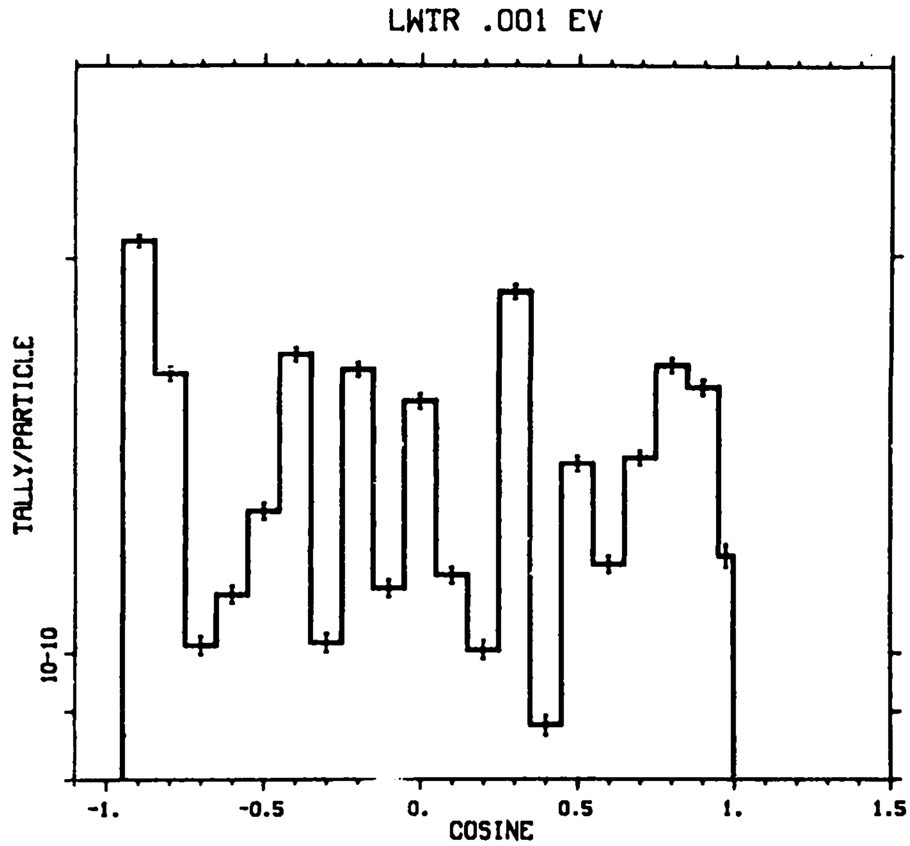

Fig. 17a.

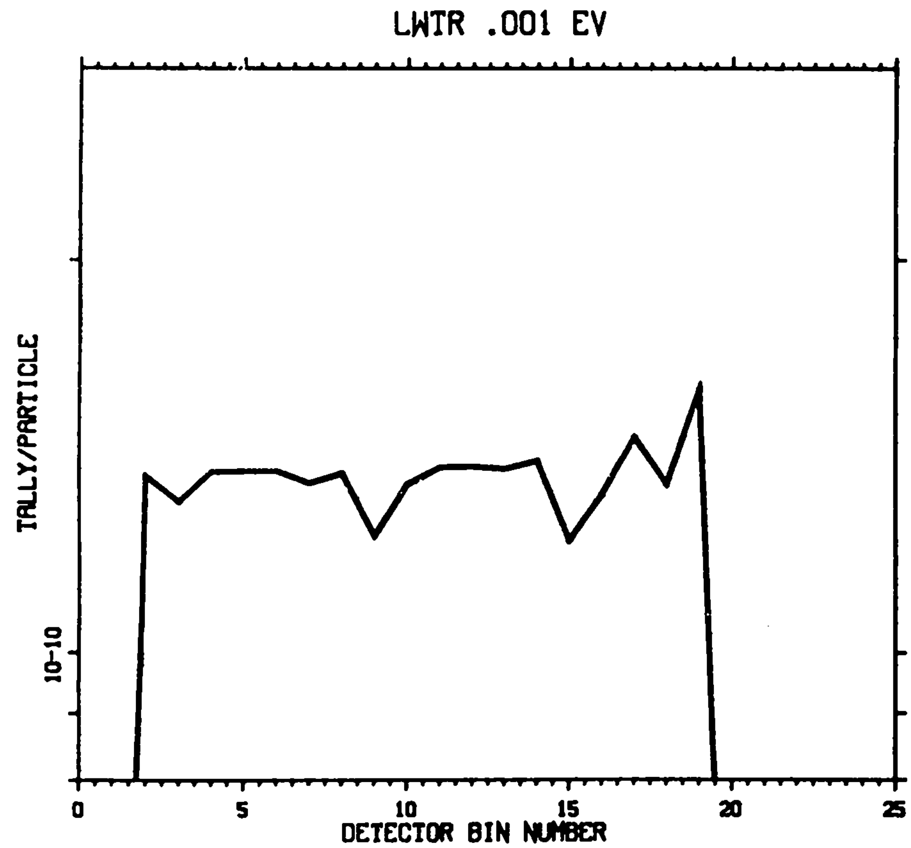

Fig. 17b.

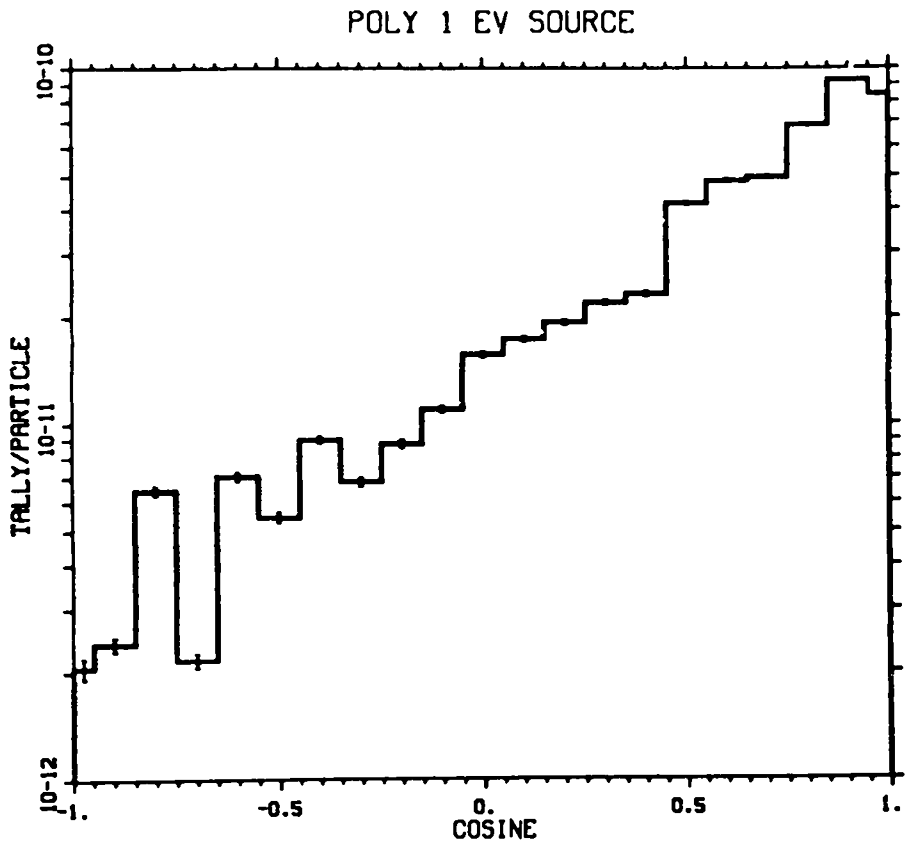

Fig. 18a.

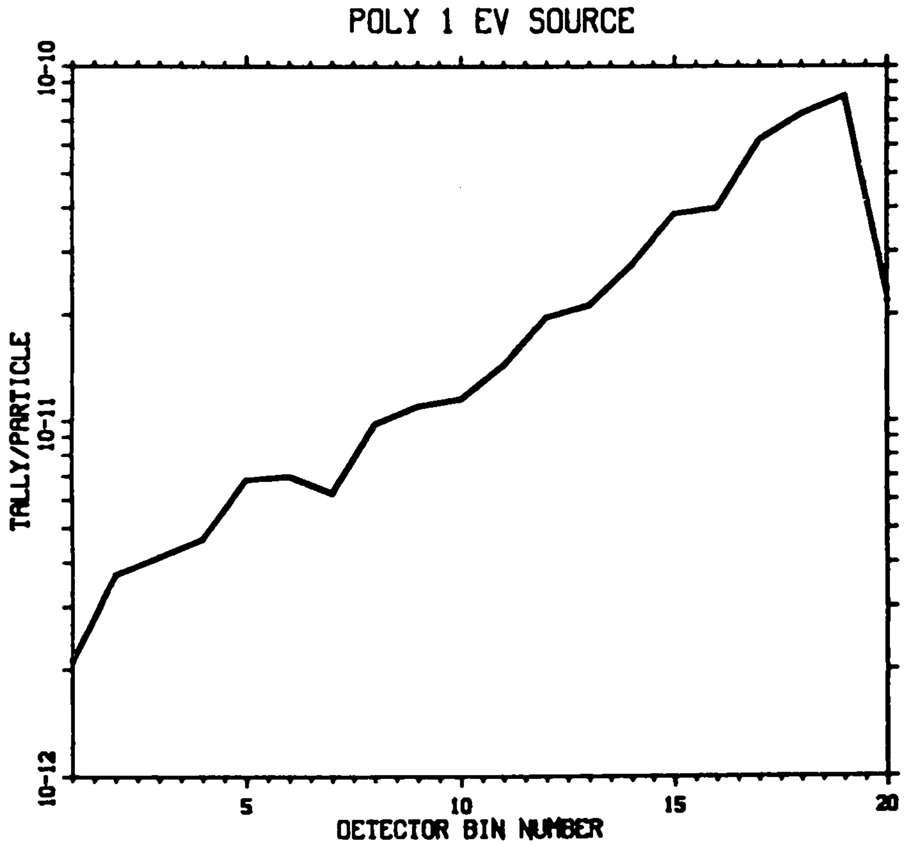

Fig. 18b.

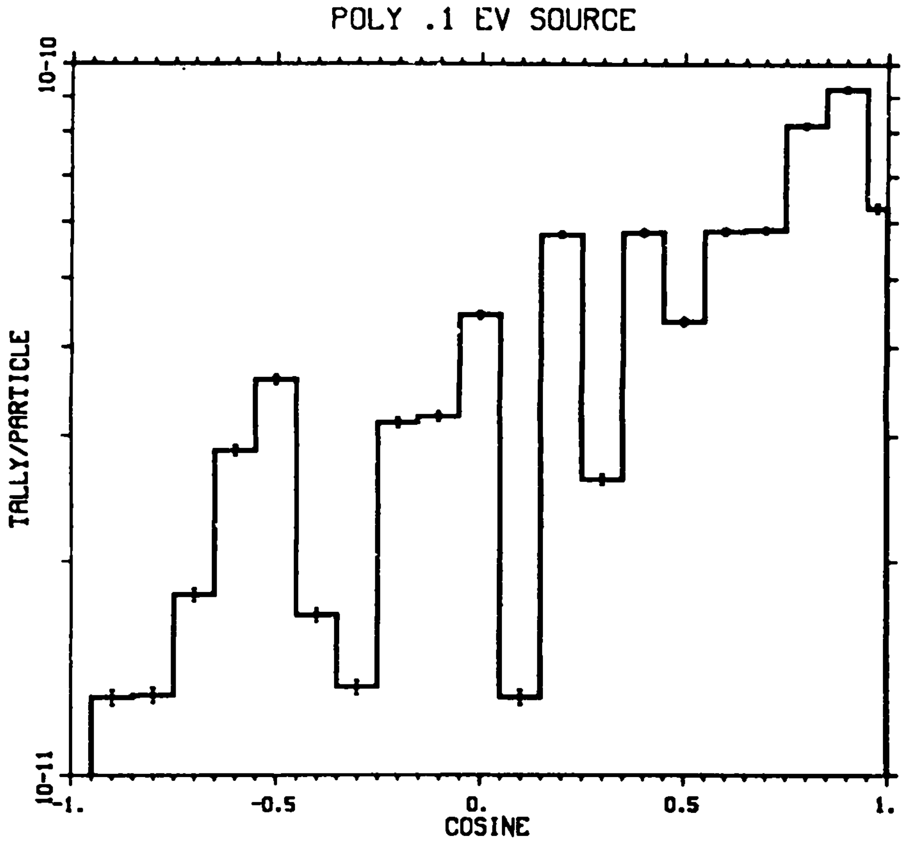

Fig. 19a.

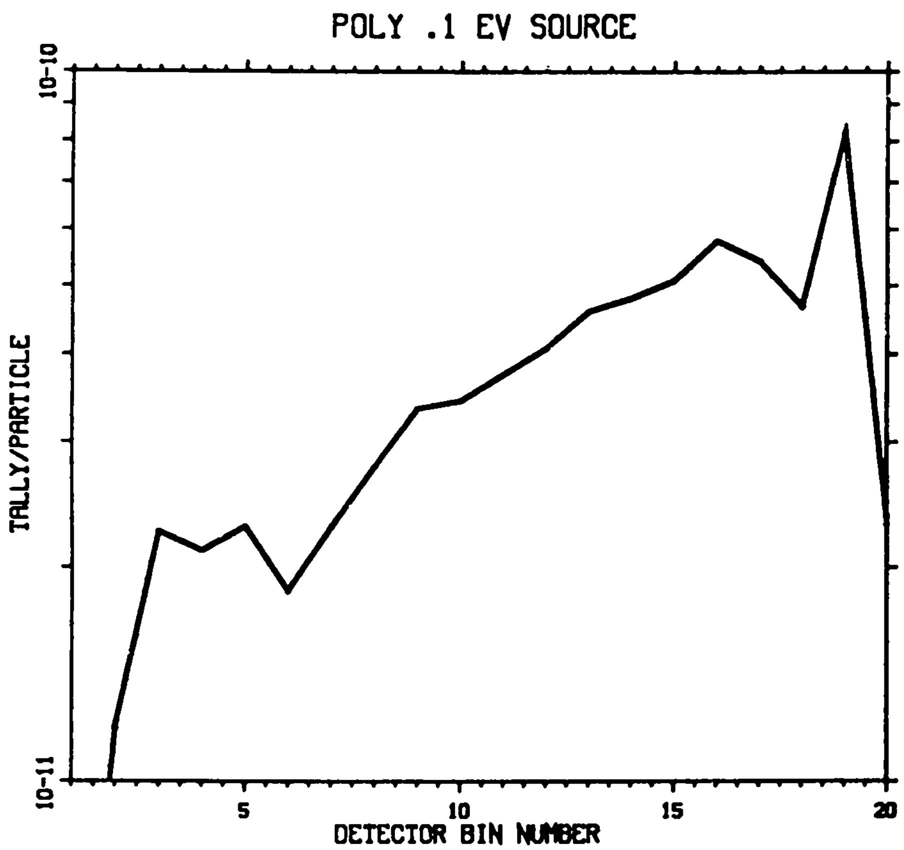

Fig. 19b.

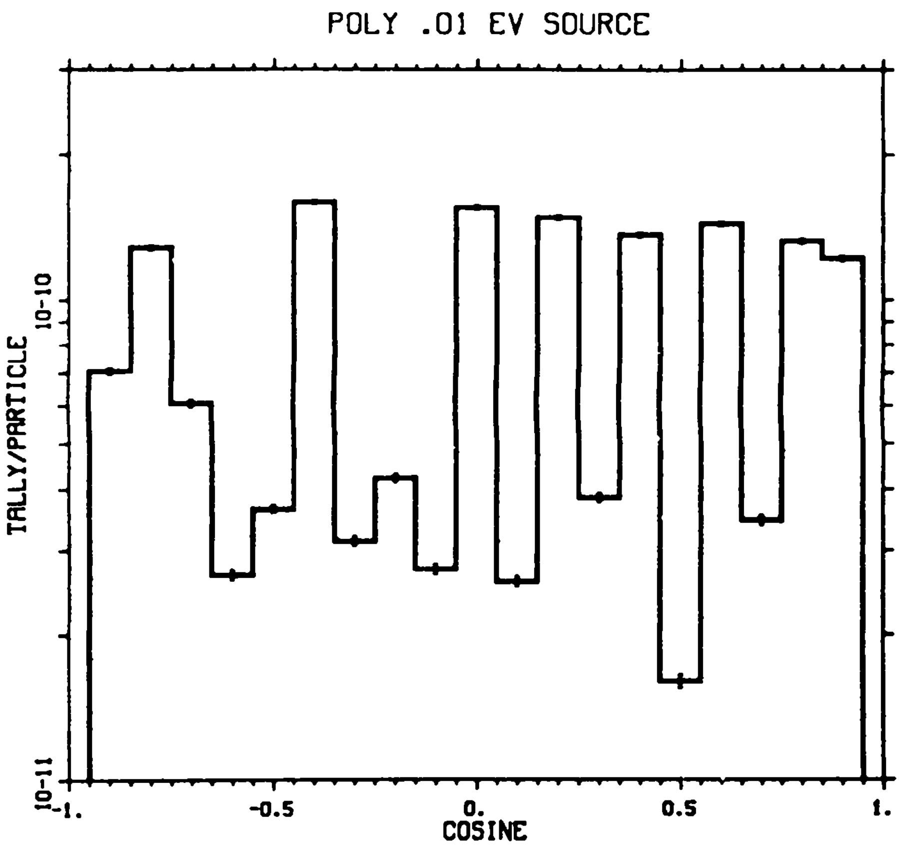

Fig. 20a.

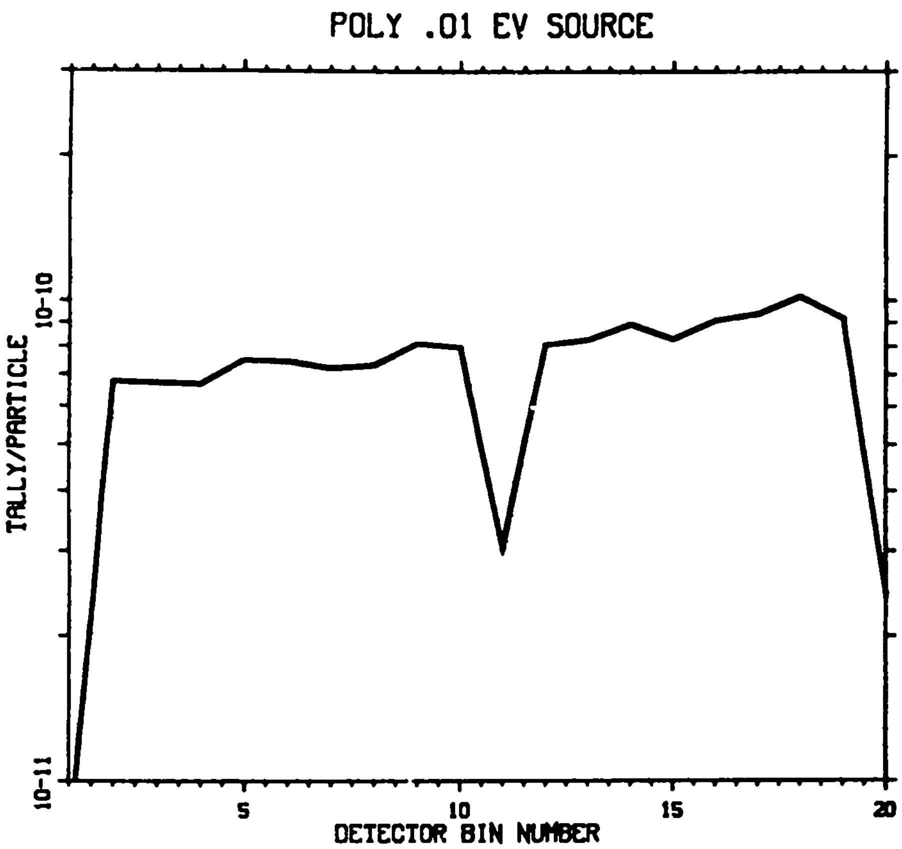

Fig. 20b.

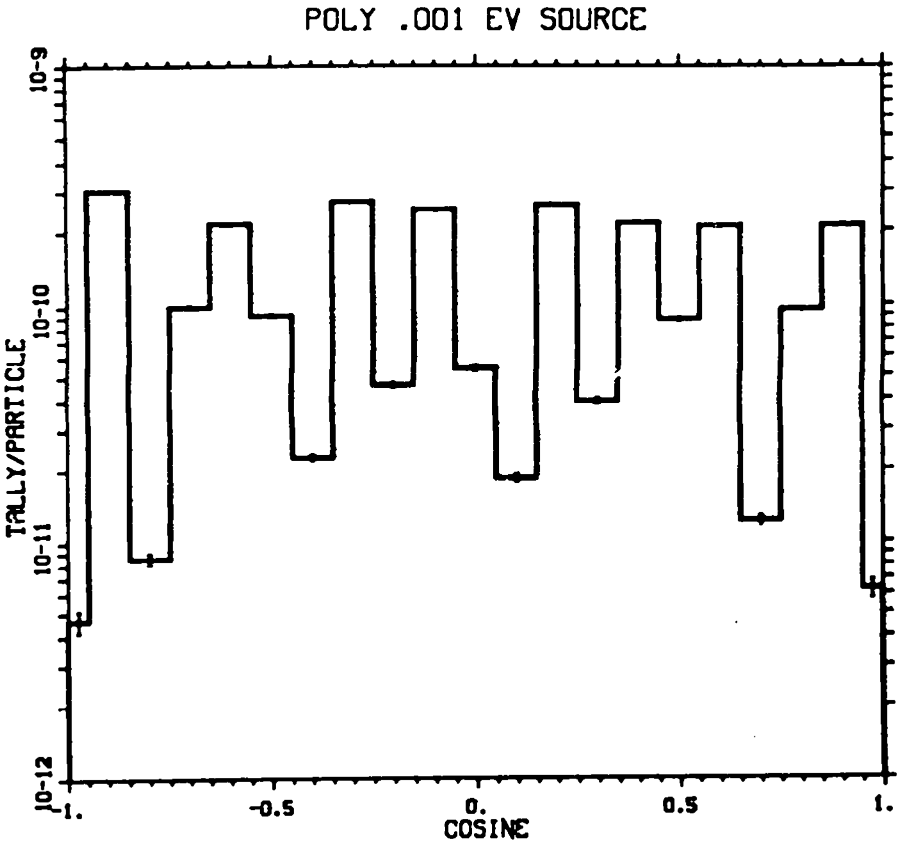

Fig. 21a.

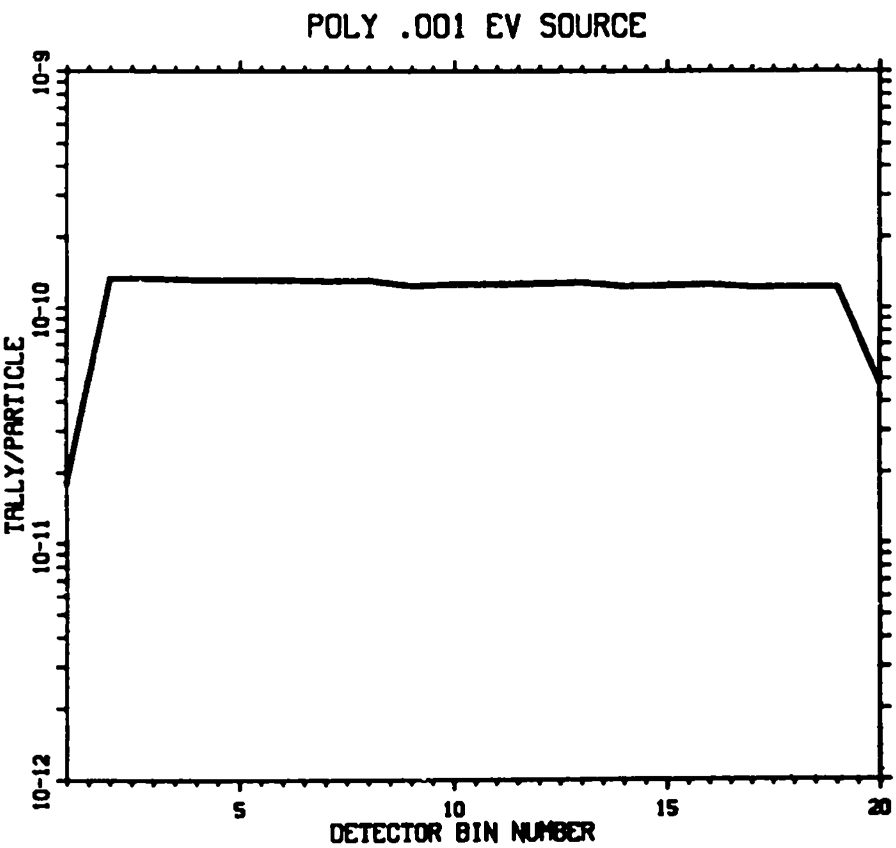

Fig. 21b.

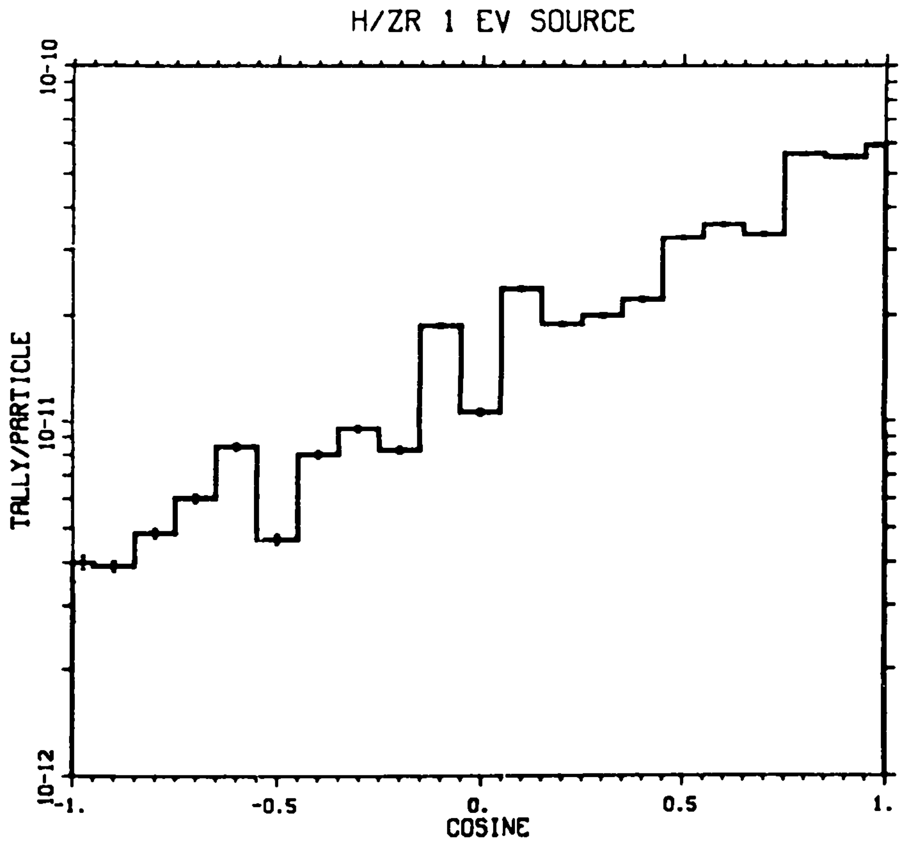

Fig. 22a.

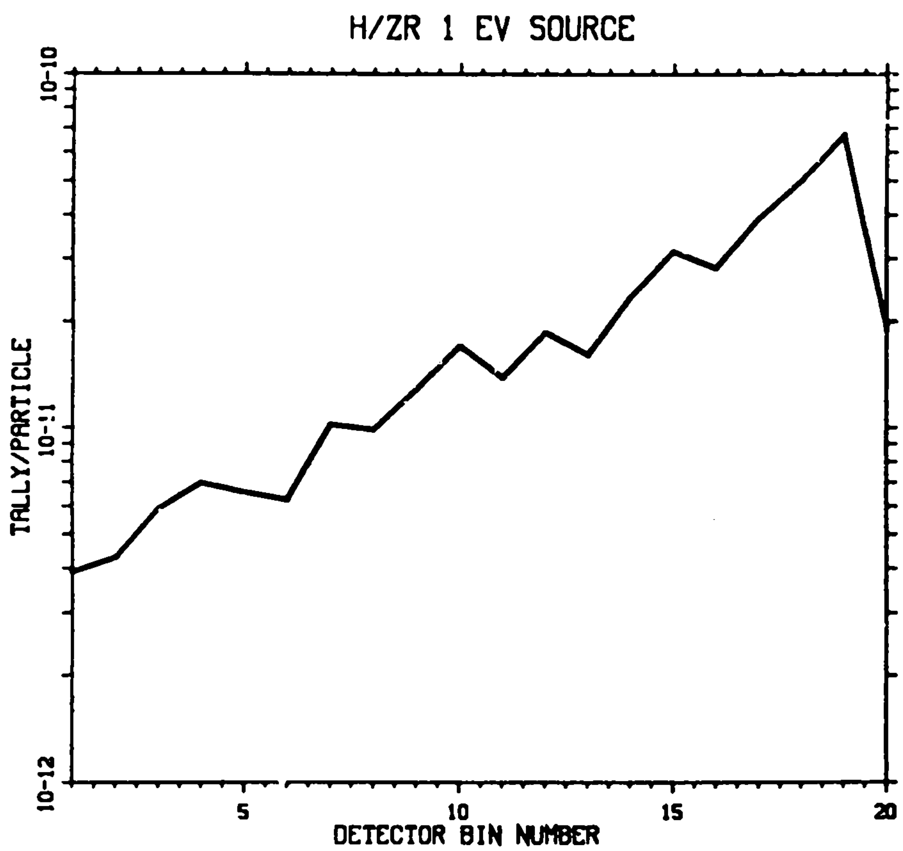

Fig. 22b.

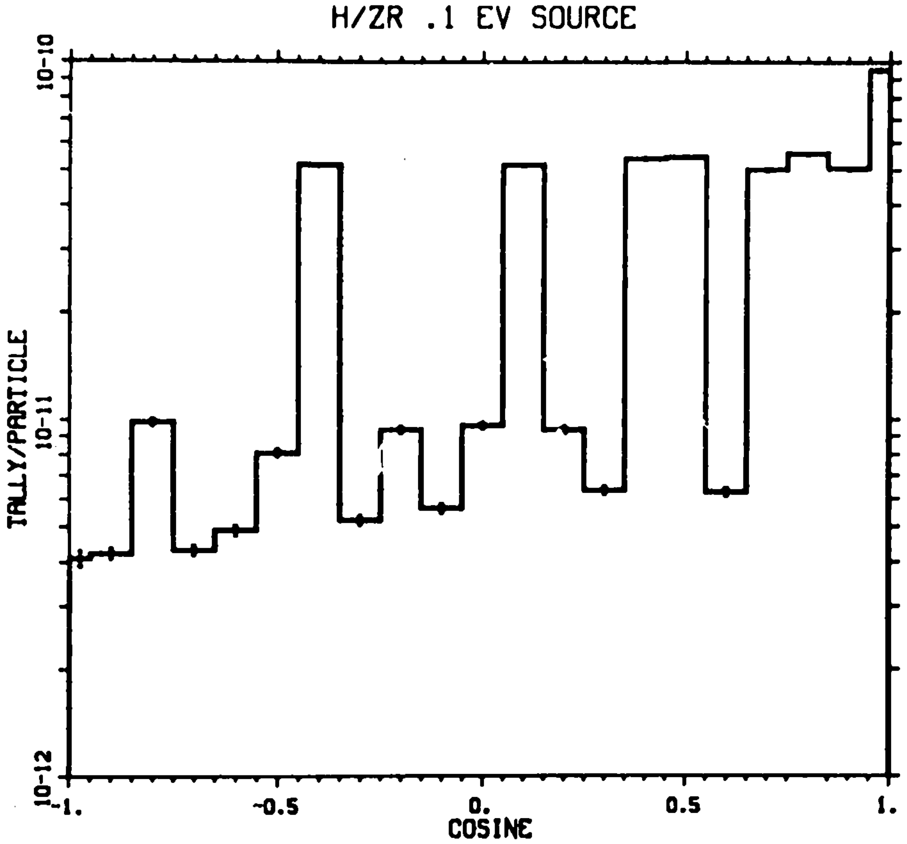

Fig. 23a.

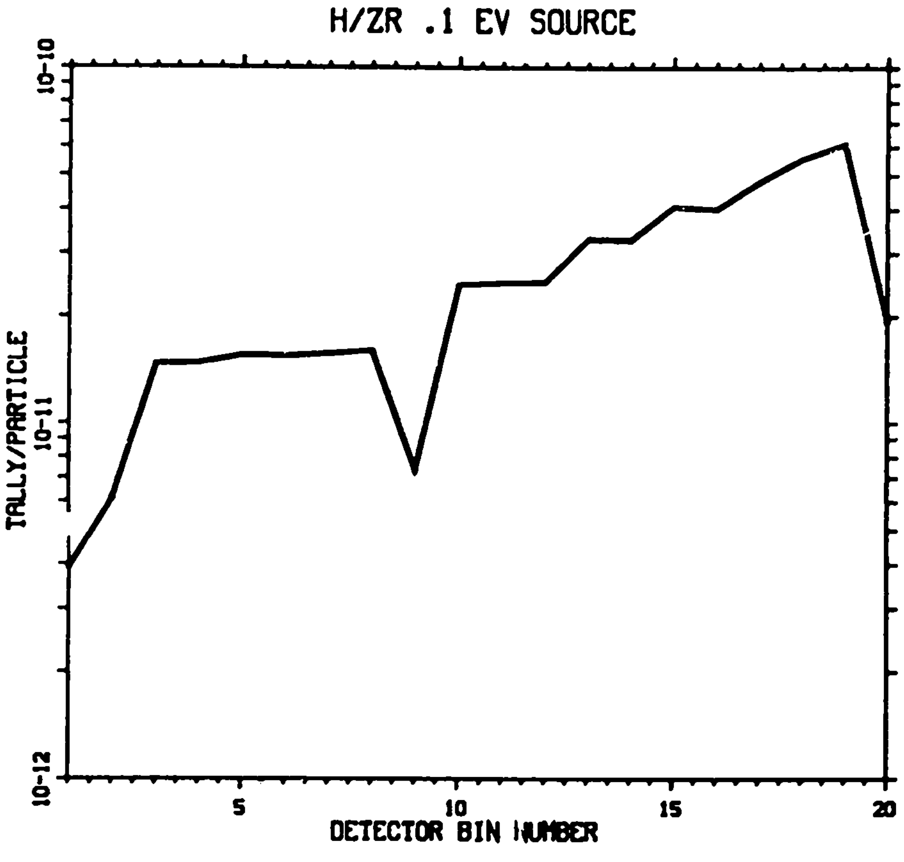

Fig. 23b.

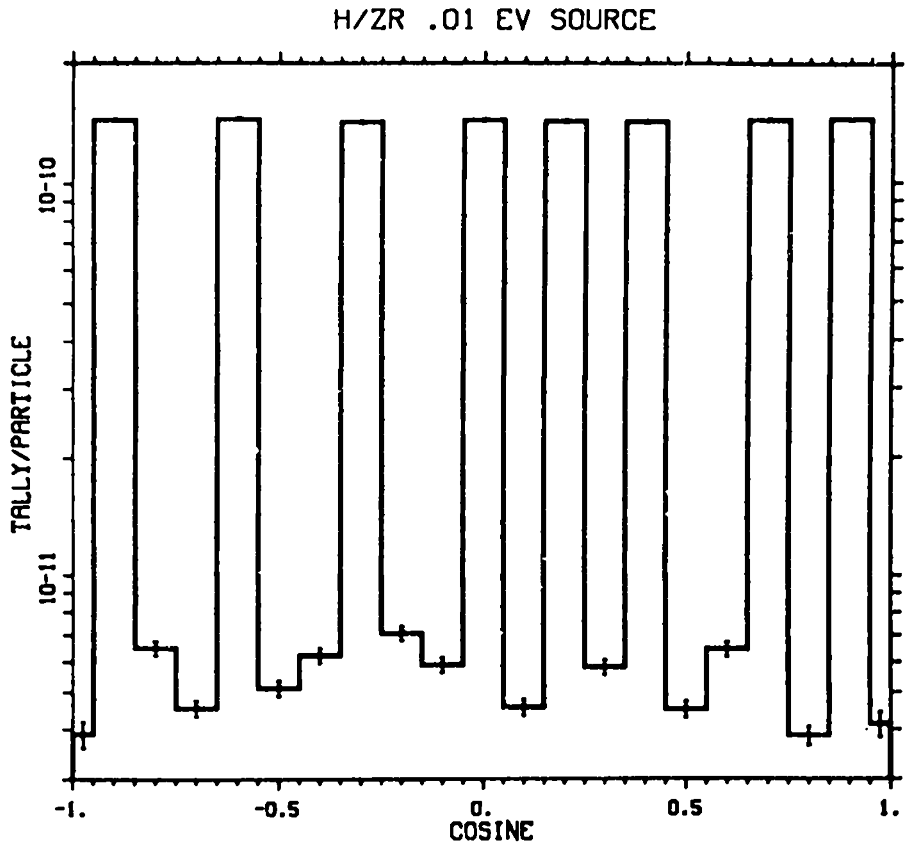

Fig. 24a.

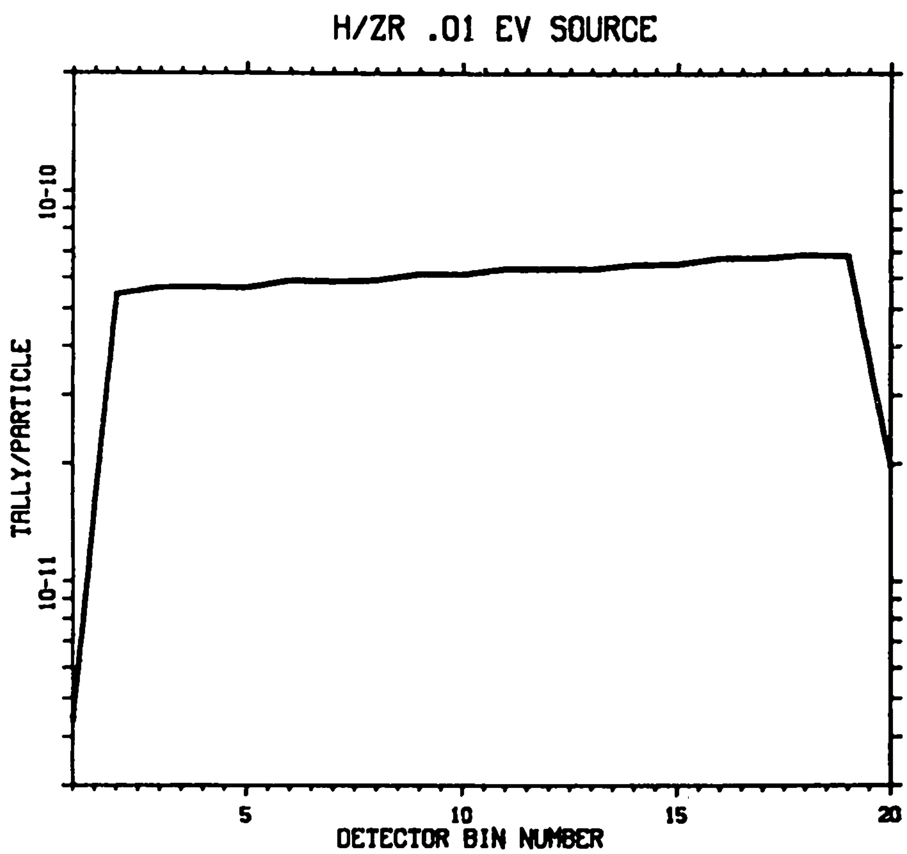

Fig. 24b.

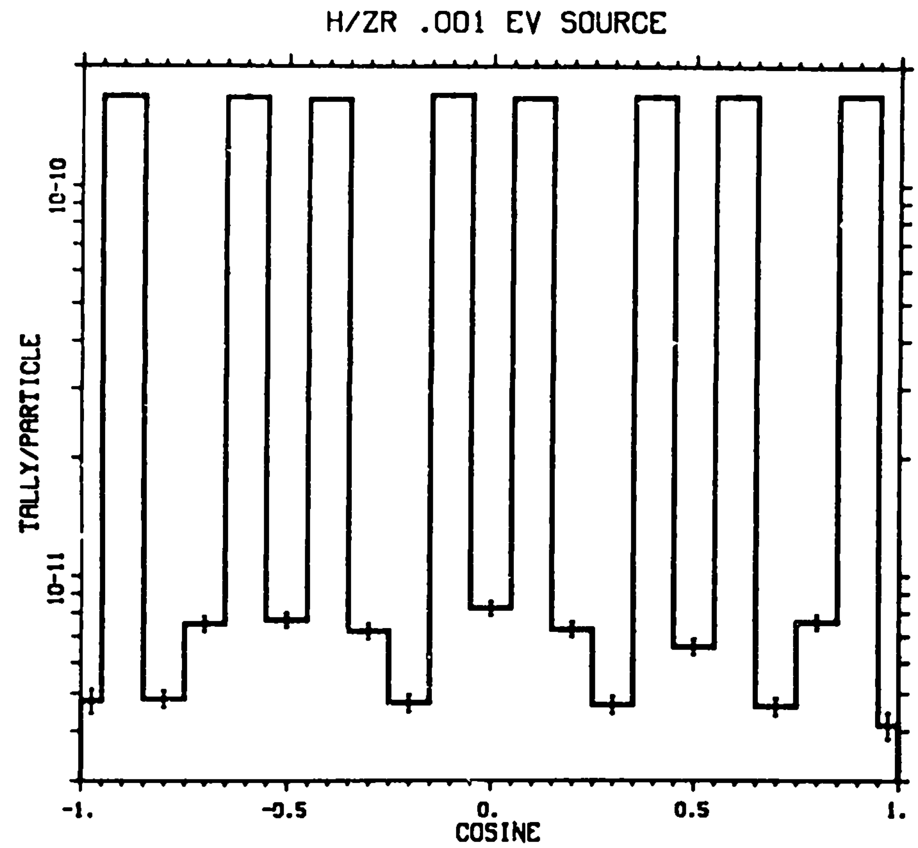

Fig. 25a.

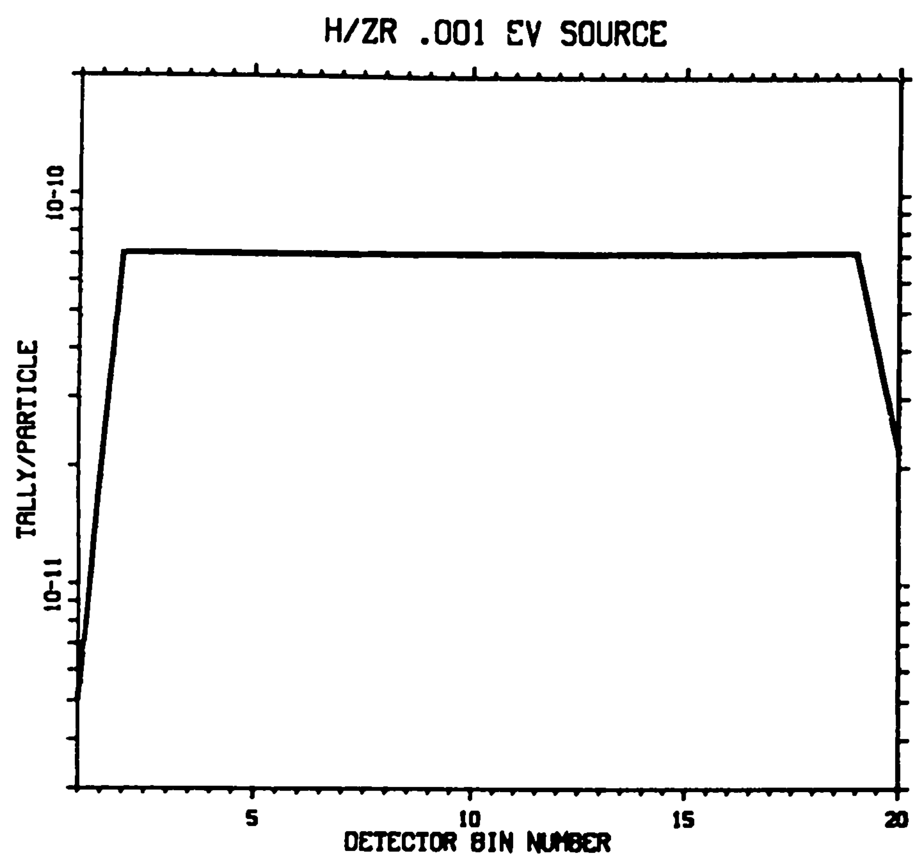

Fig. 25b.

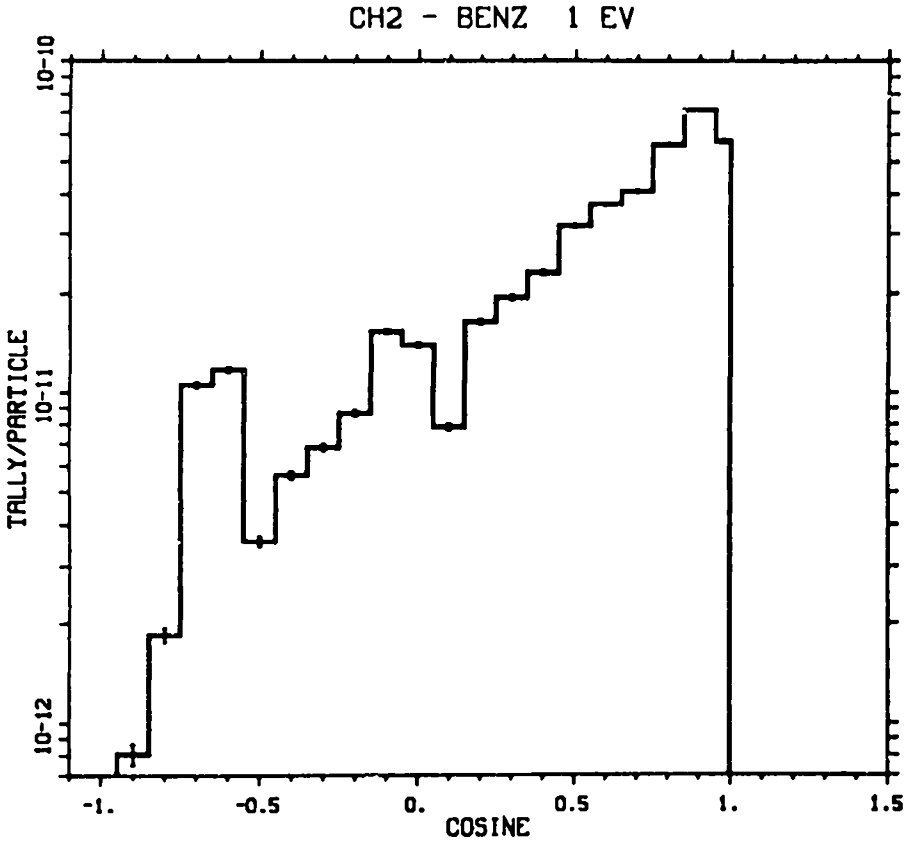

Fig. 26a.

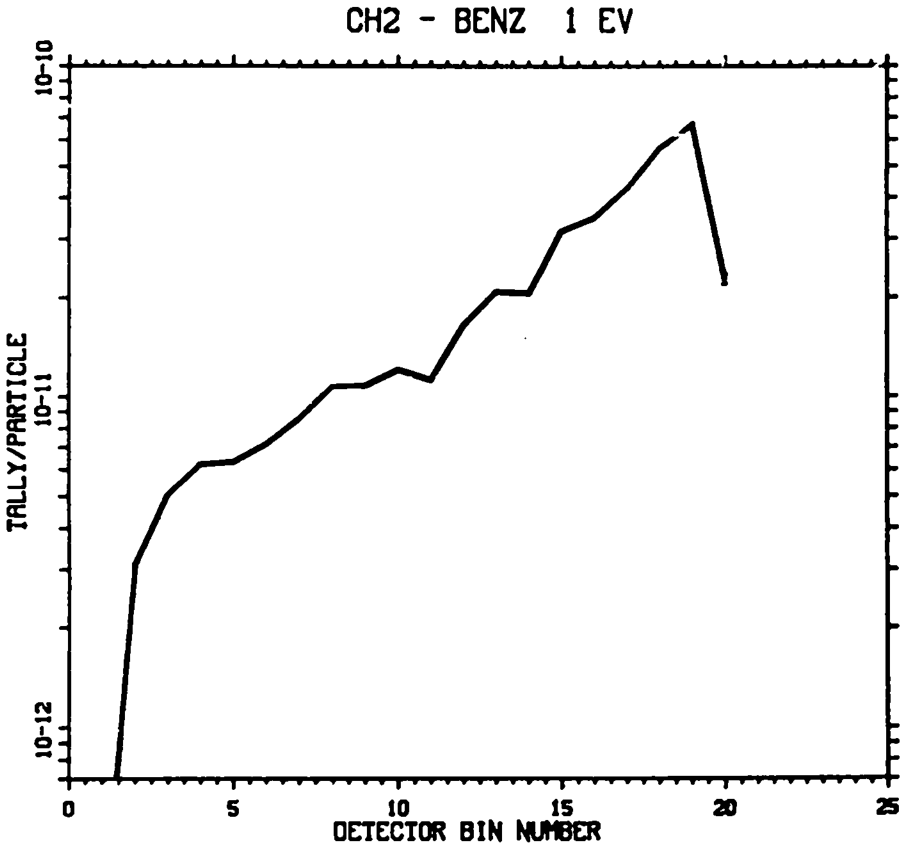

Fig. 26b.

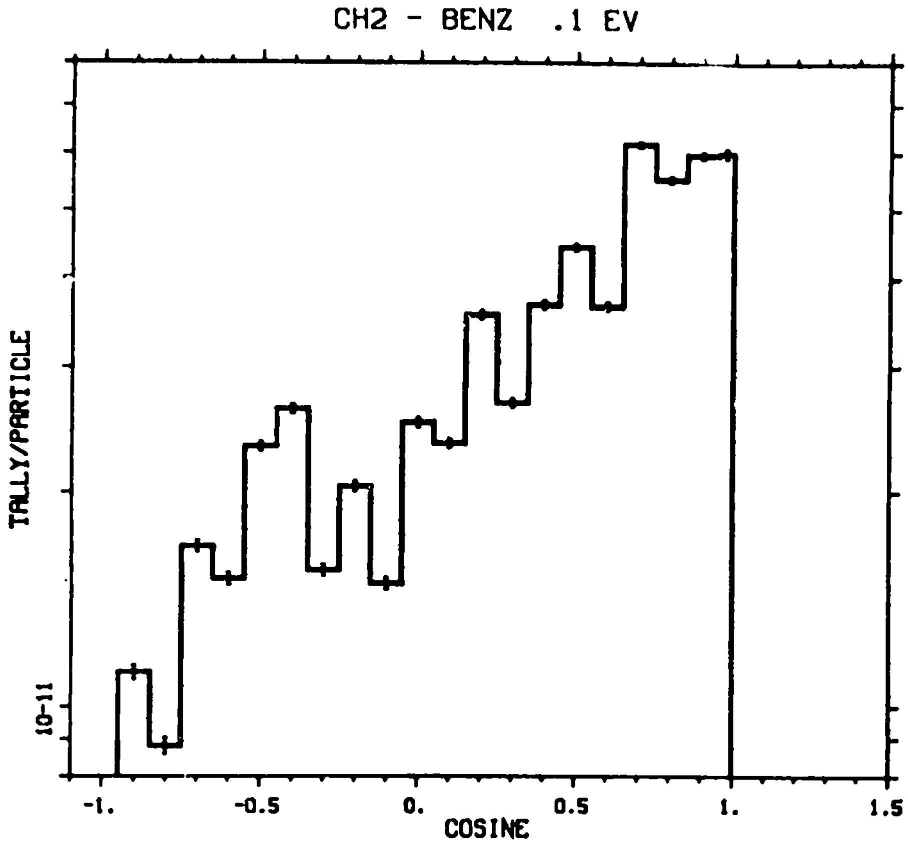

Fig. 27a.

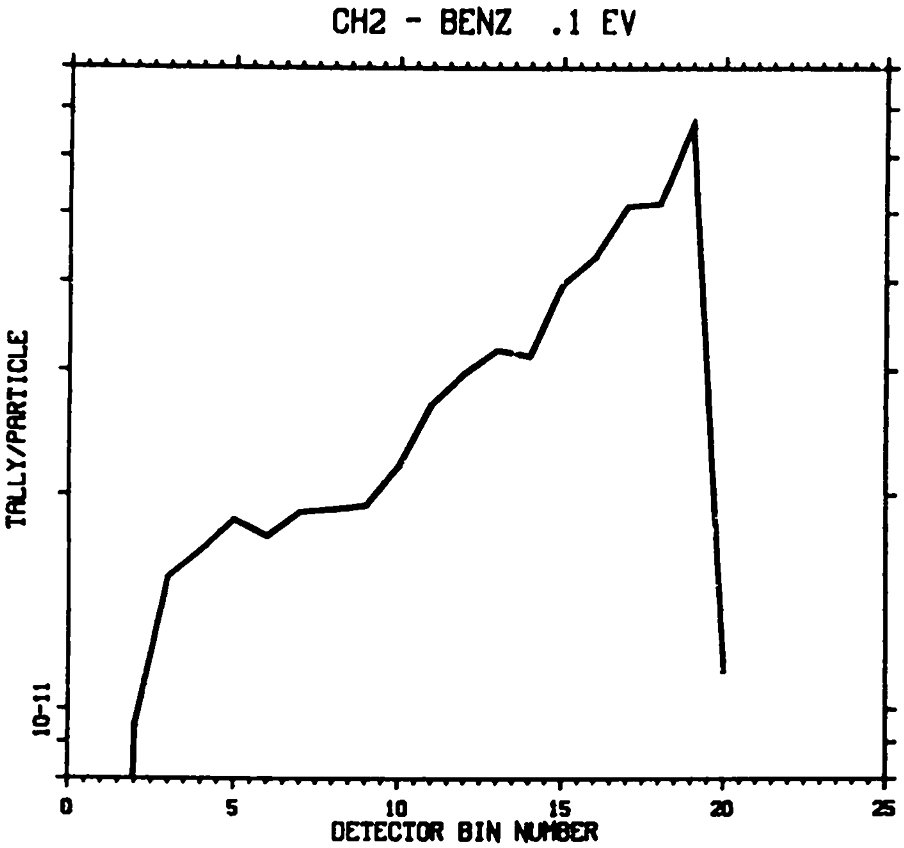

Fig. 27b.

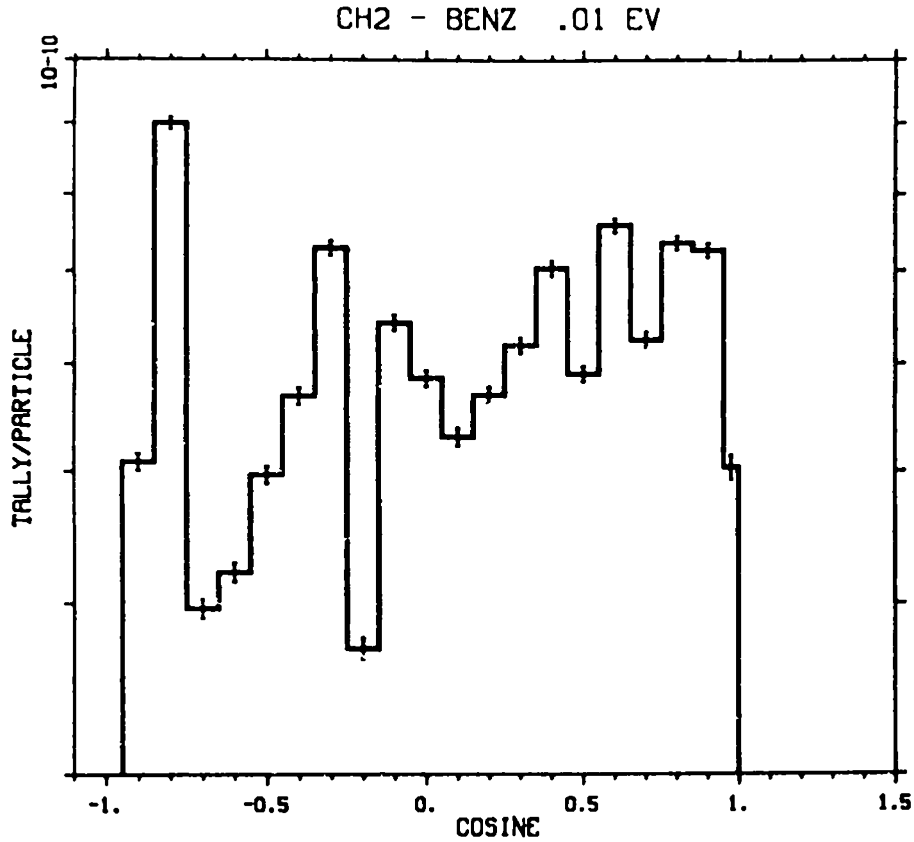

Fig. 28a.

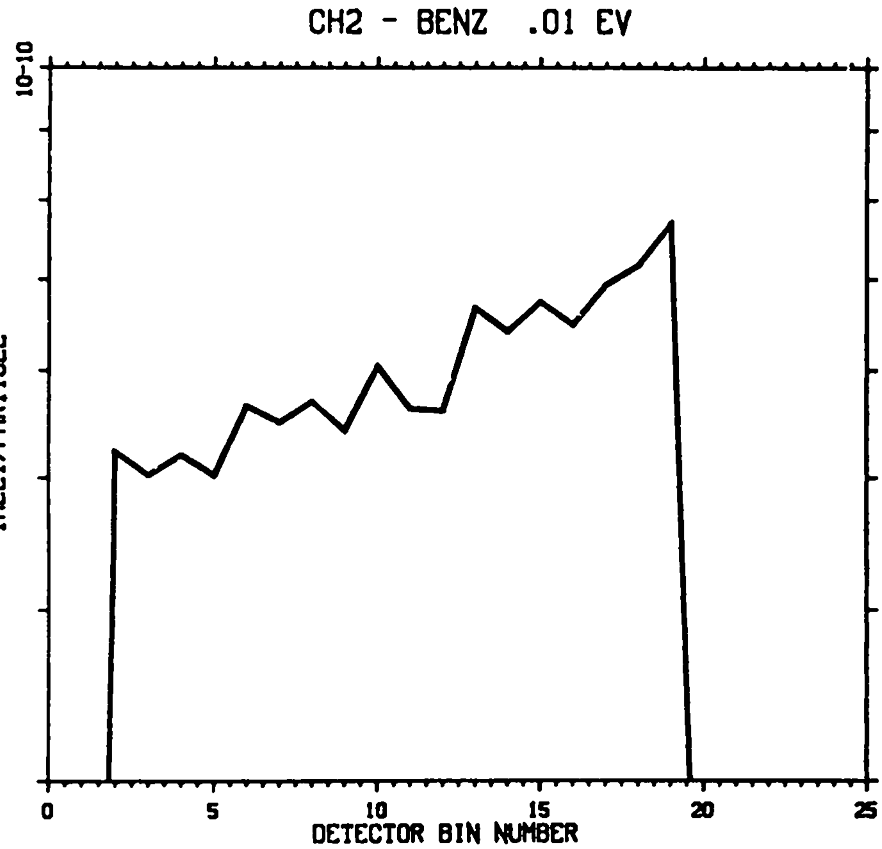

Fig. 28b.

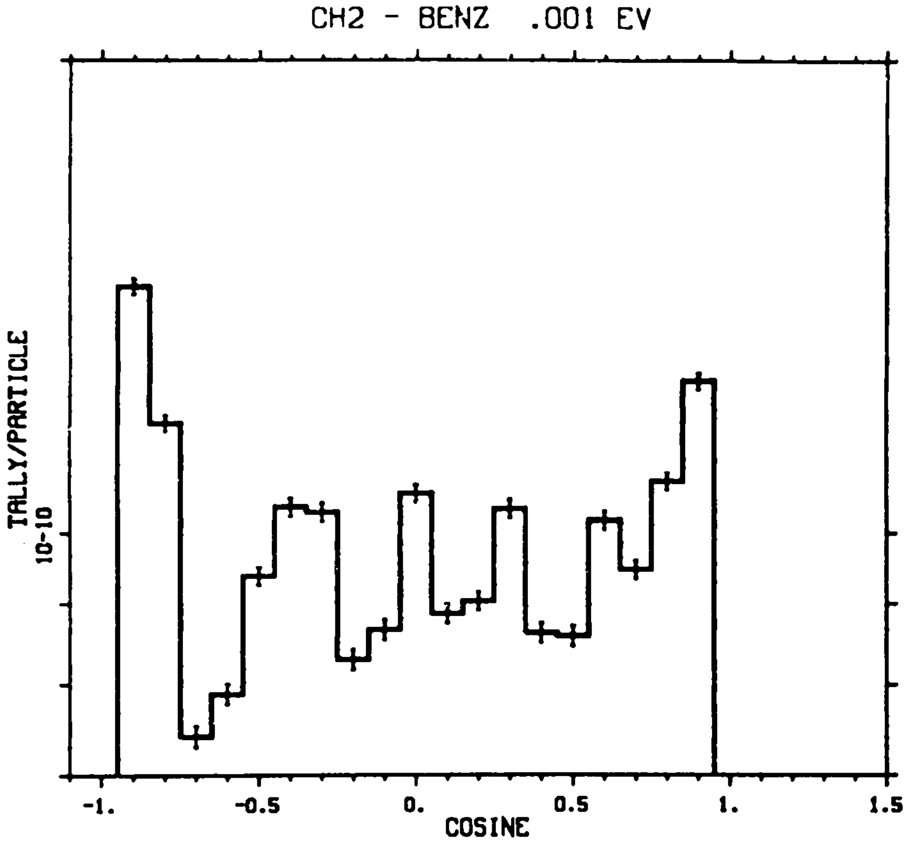

Fig. 29a.

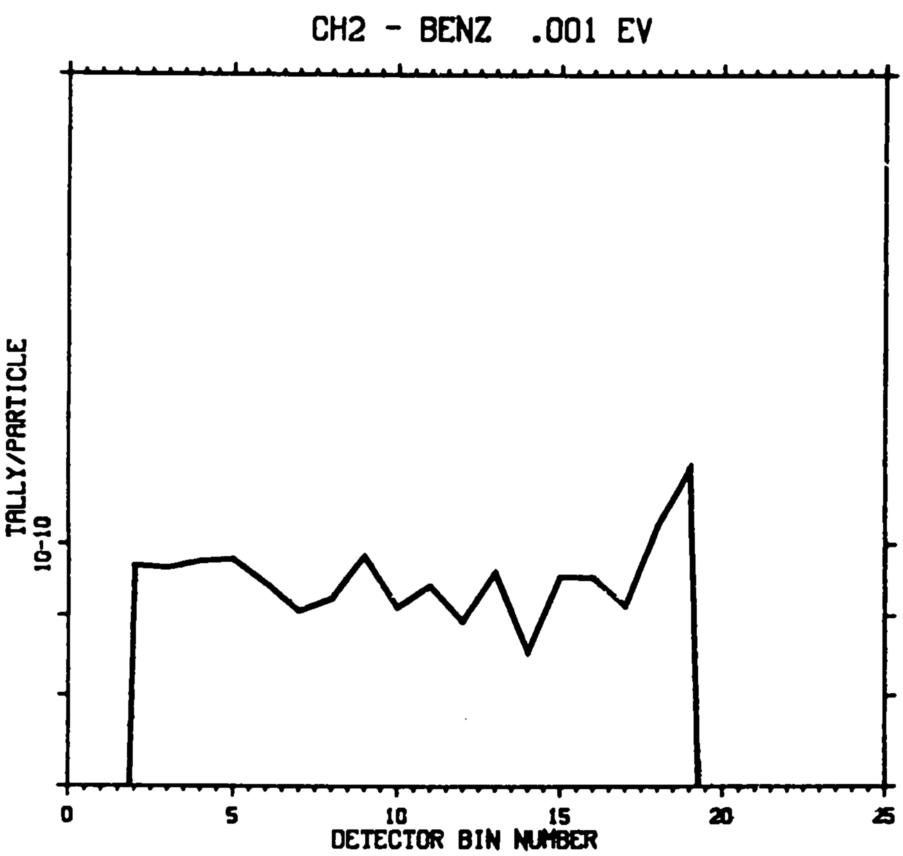

Fig. 29b.

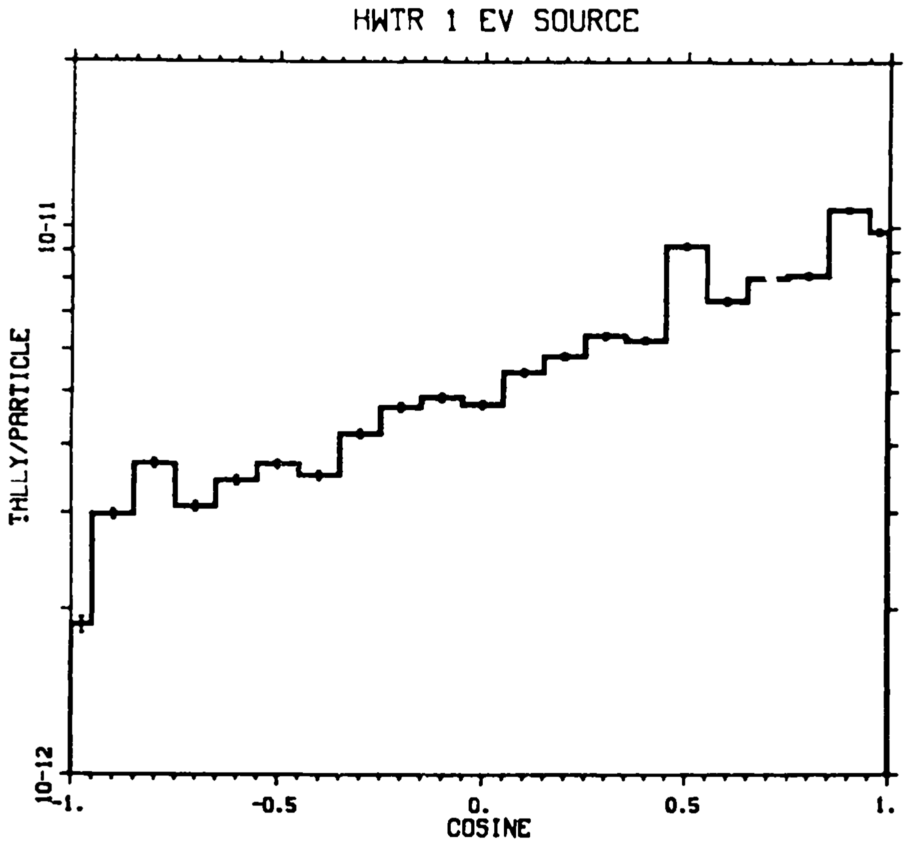

Fig. 30a.

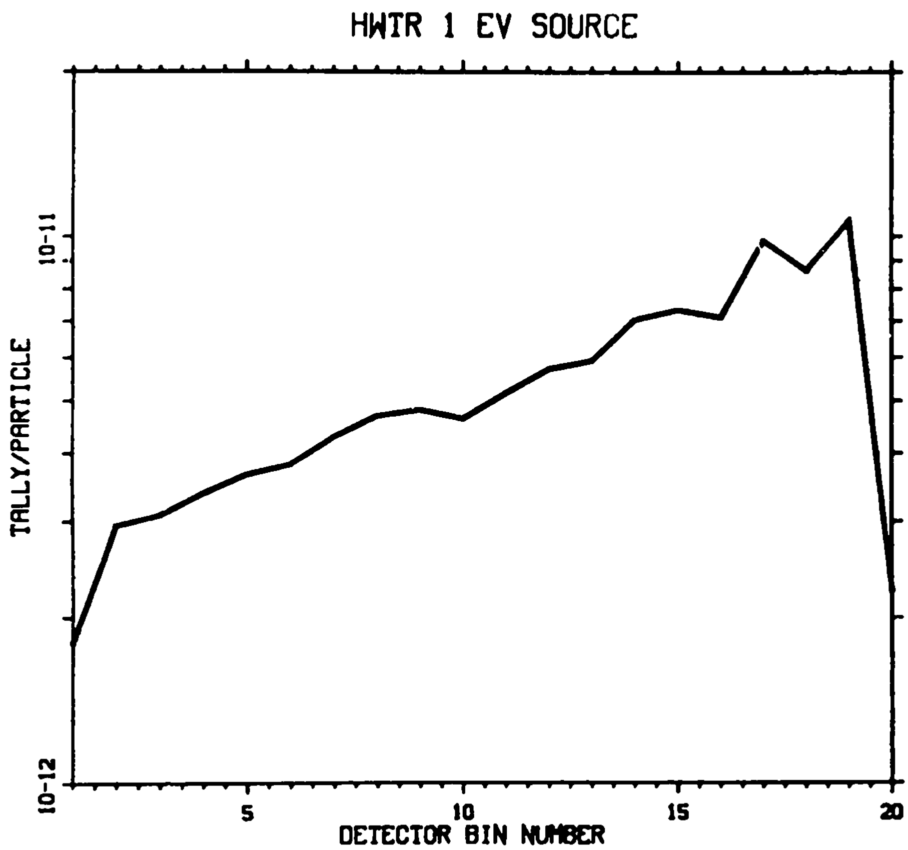

Fig. 30b.

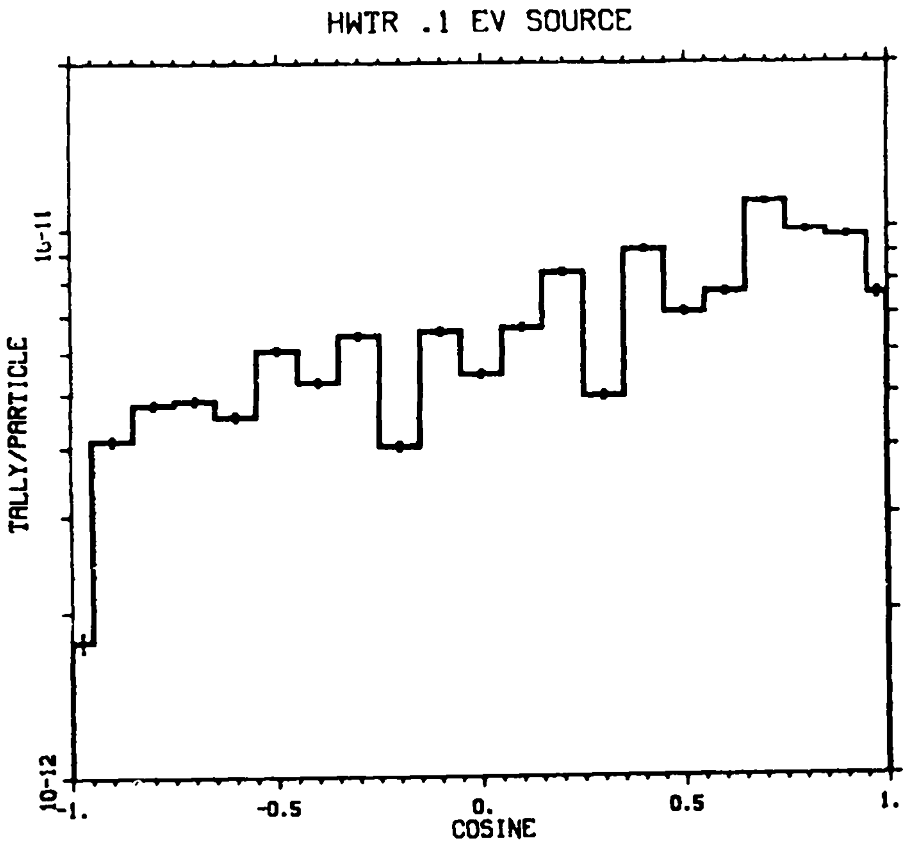

Fig. 31a.

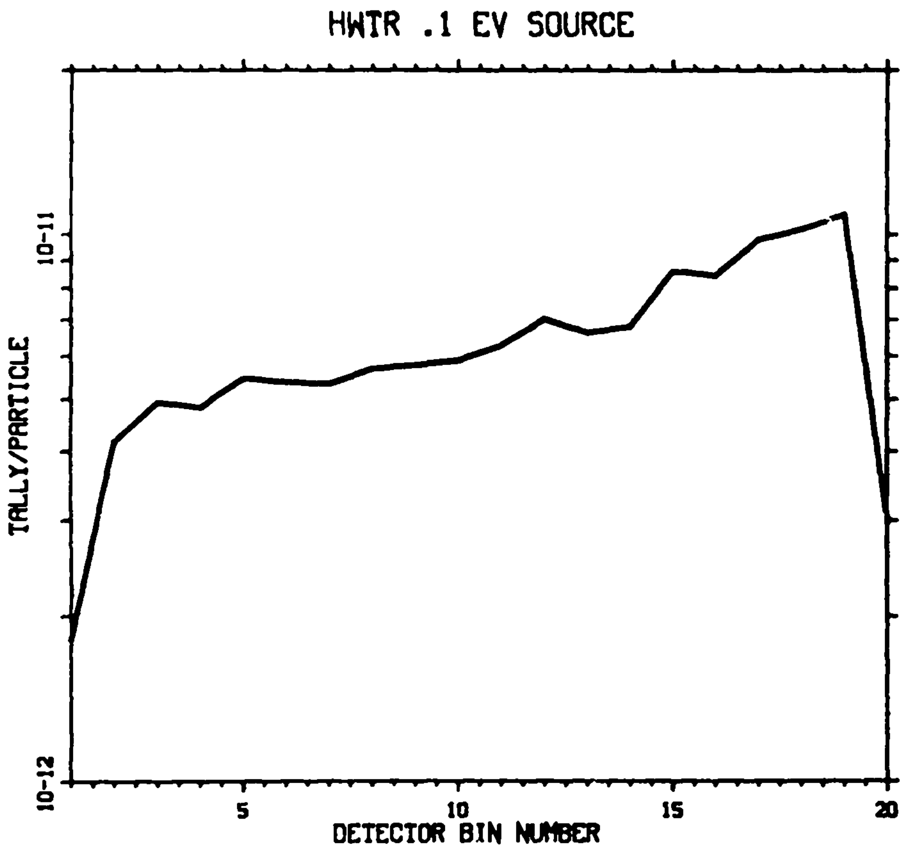

Fig. 31b.

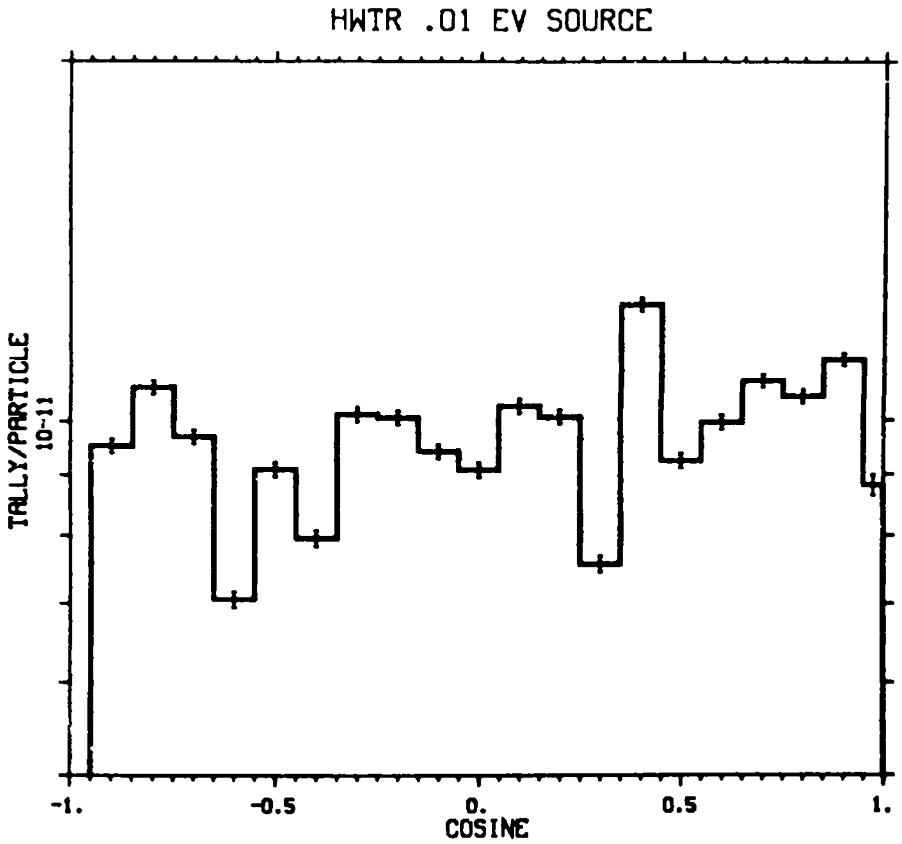

Fig. 32a.

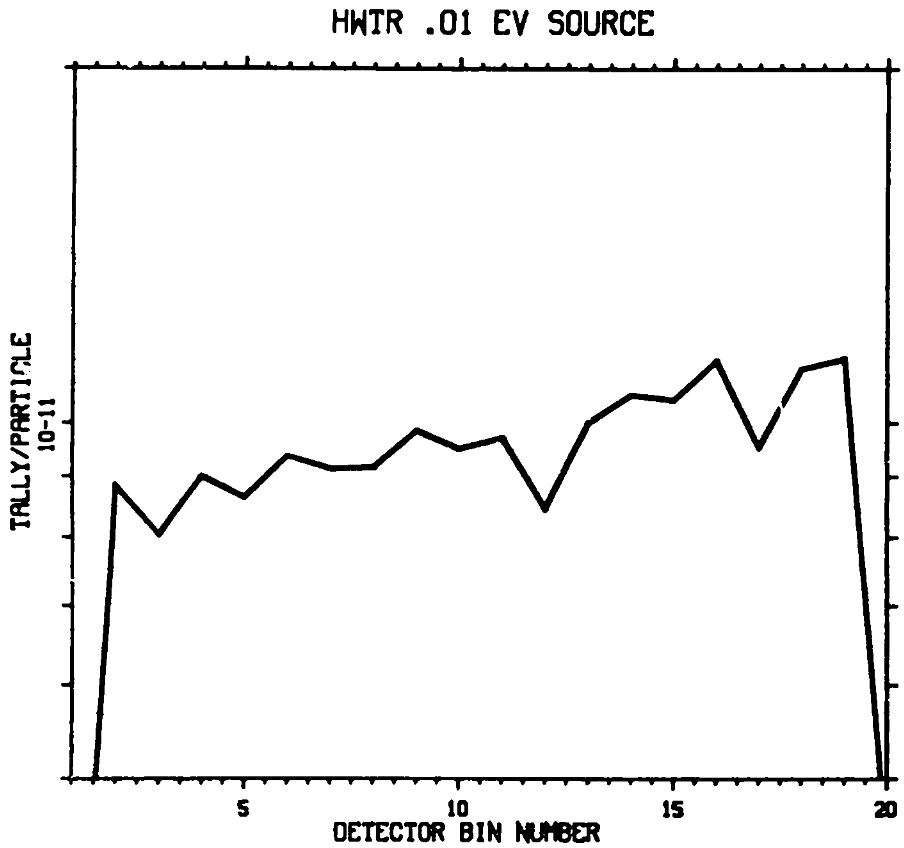

Fig. 32b.

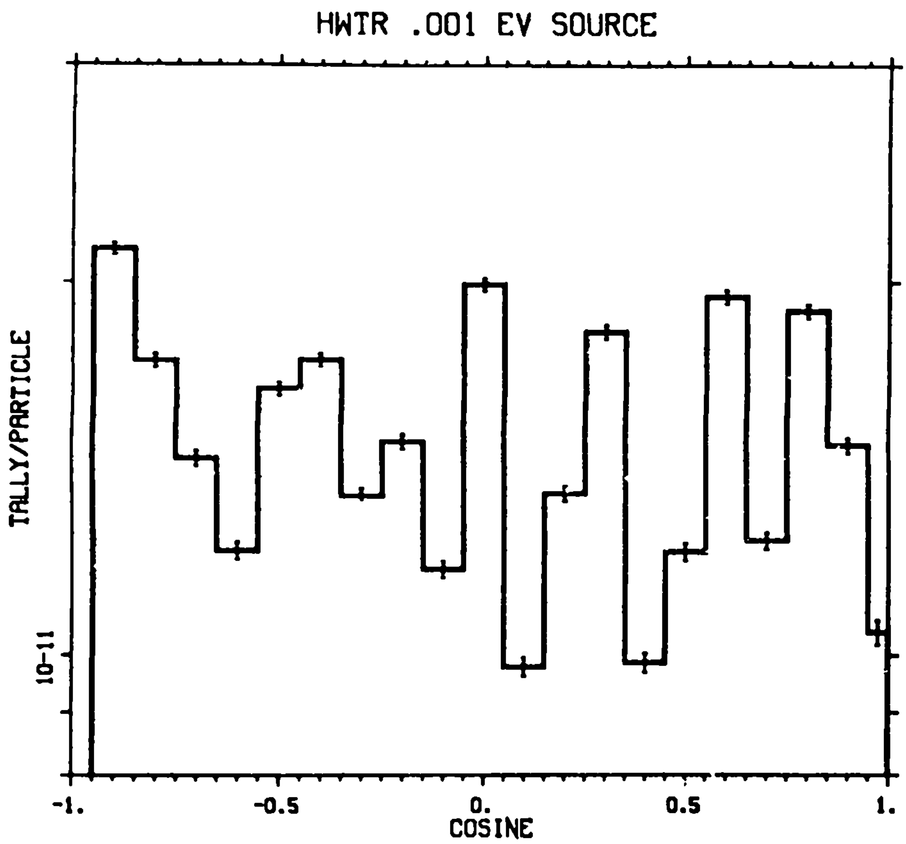

Fig. 33a.

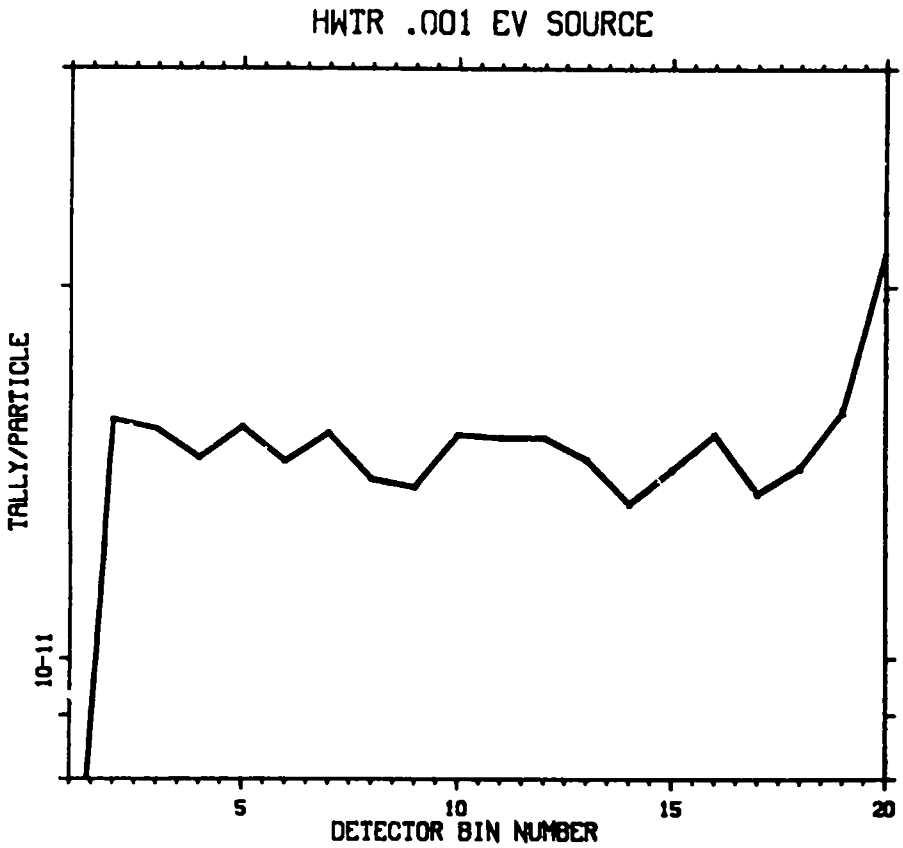

Fig. 33b.

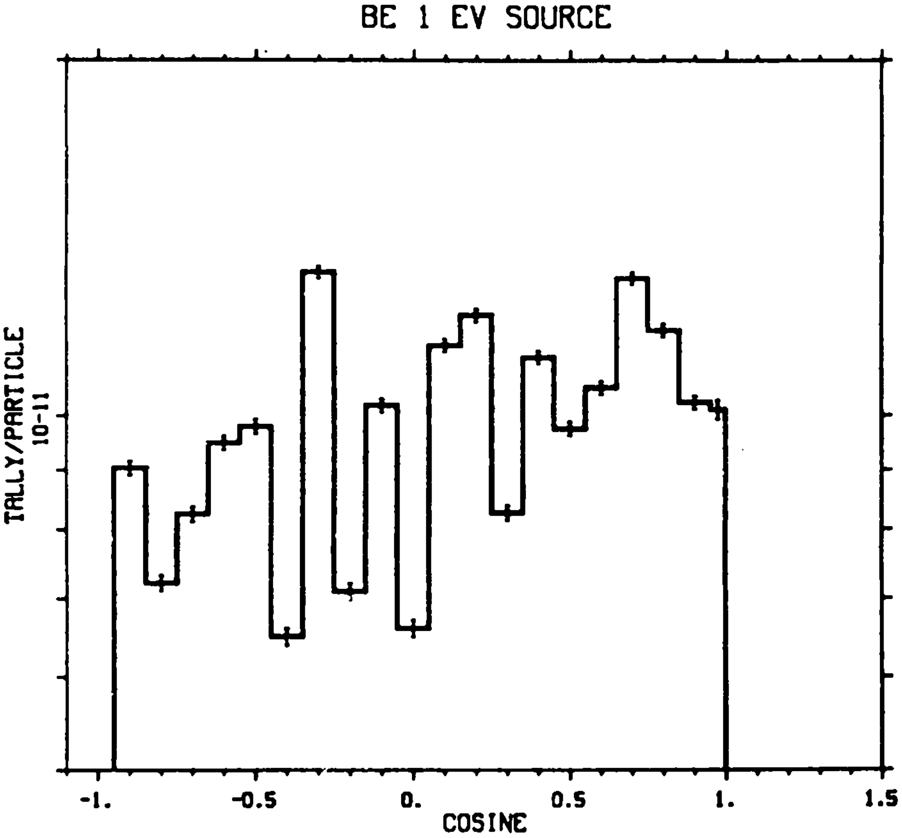

Fig. 34a.

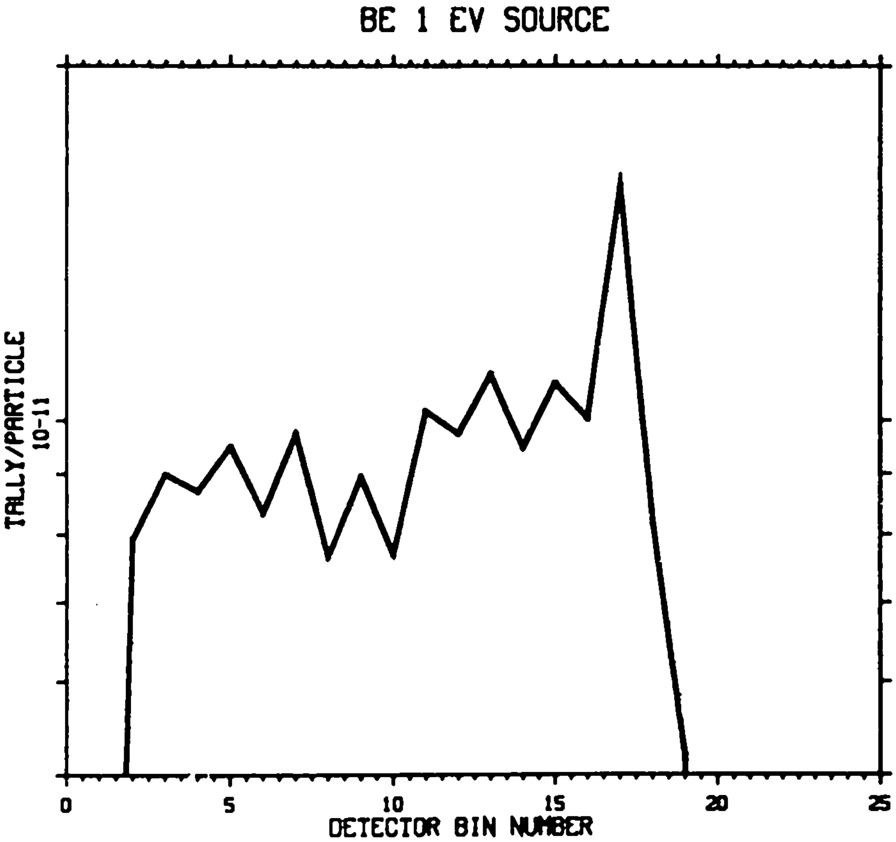

Fig. 34b.

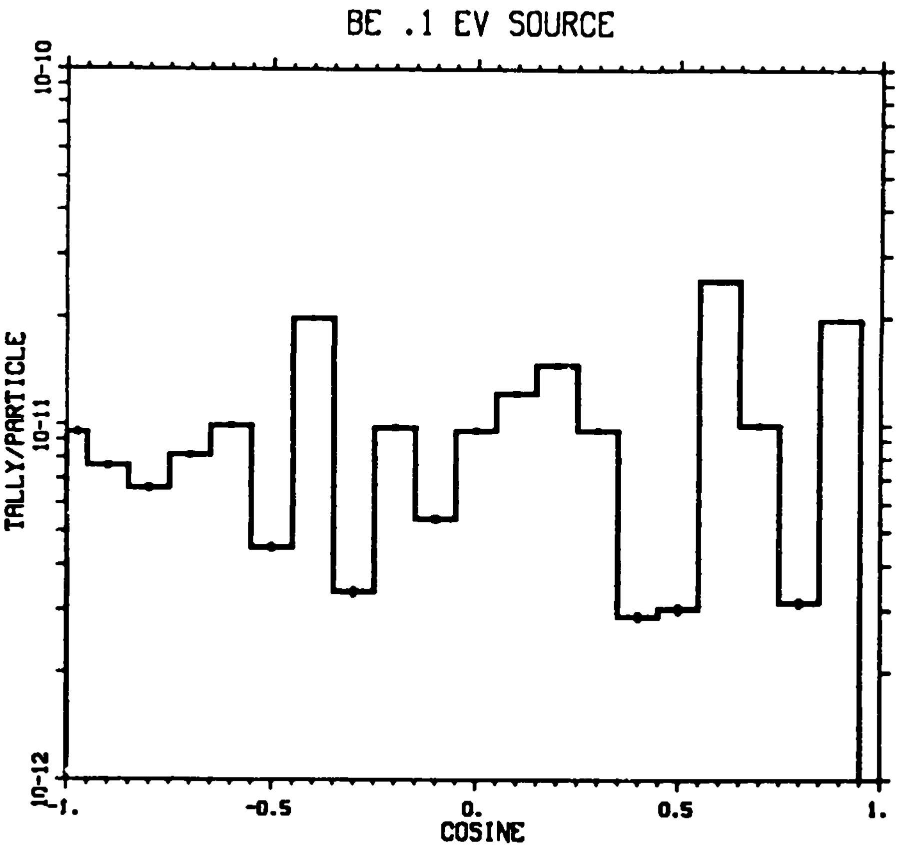

Fig. 35a.

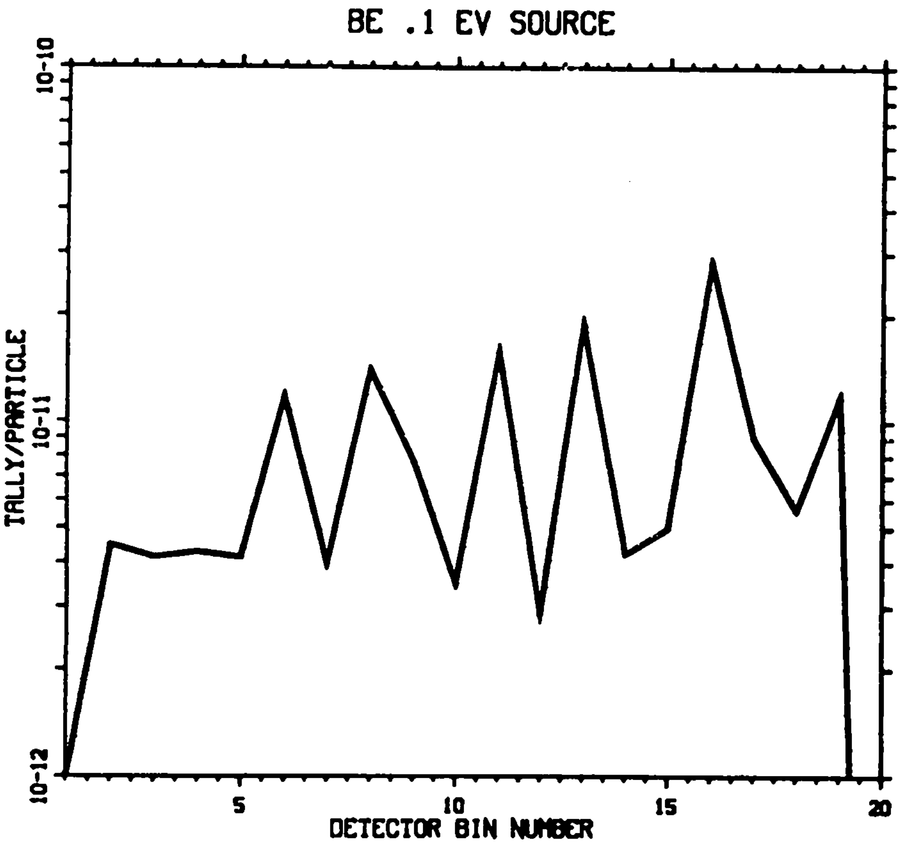

Fig. 35b.

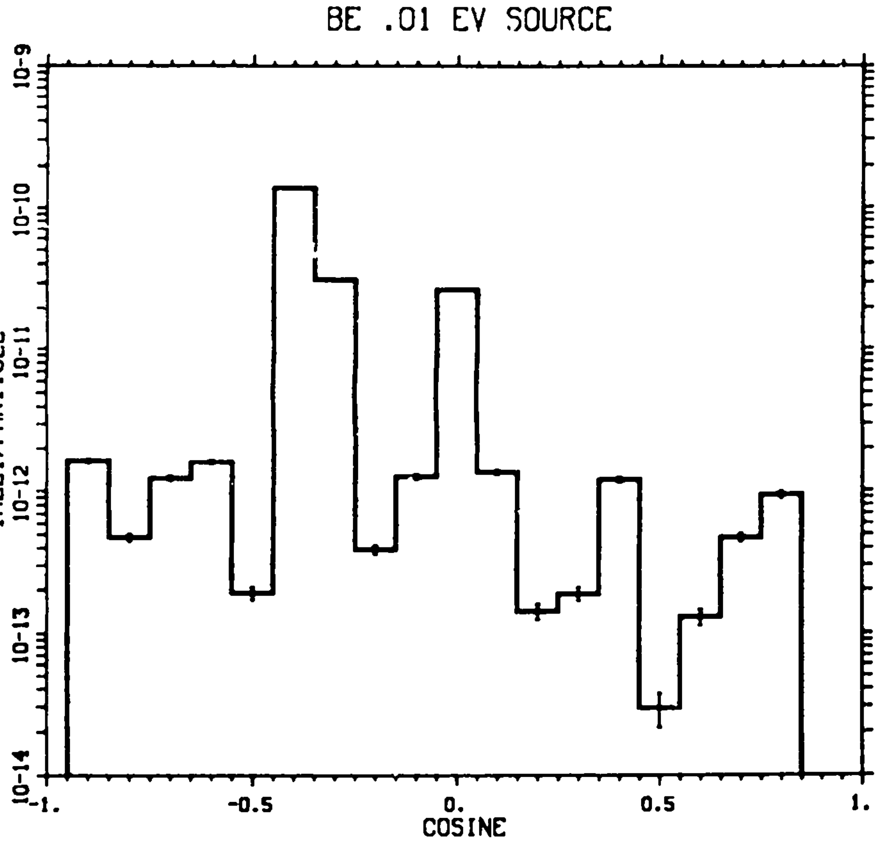

Fig. 36a.

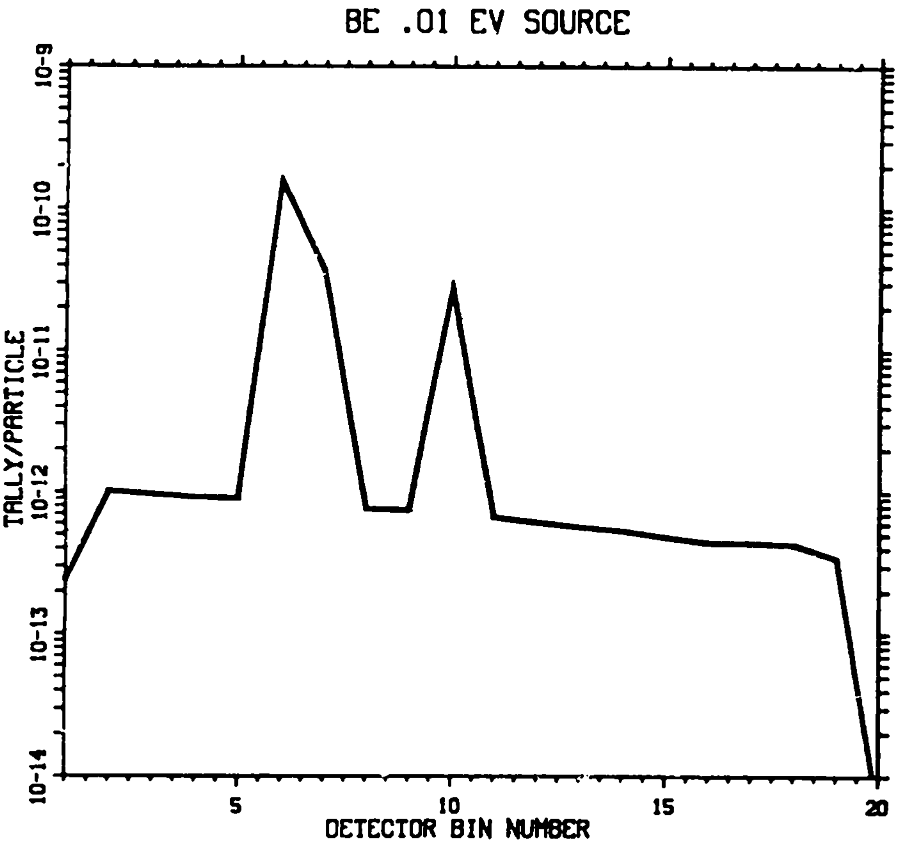

Fig. 36b.

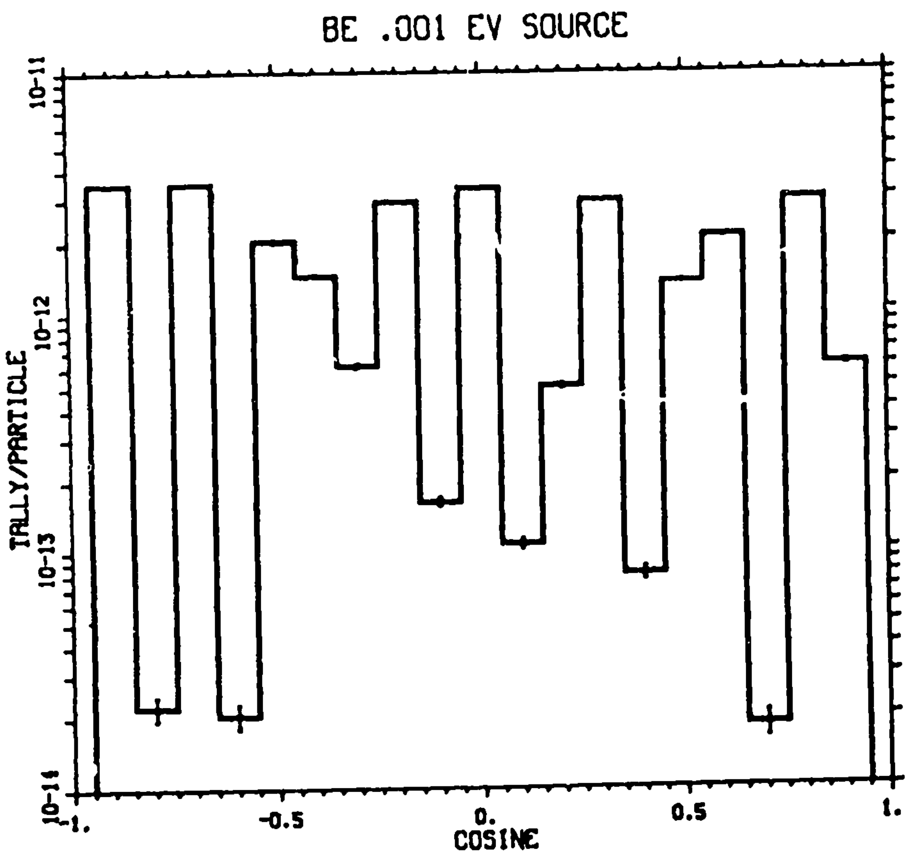

Fig. 37a.

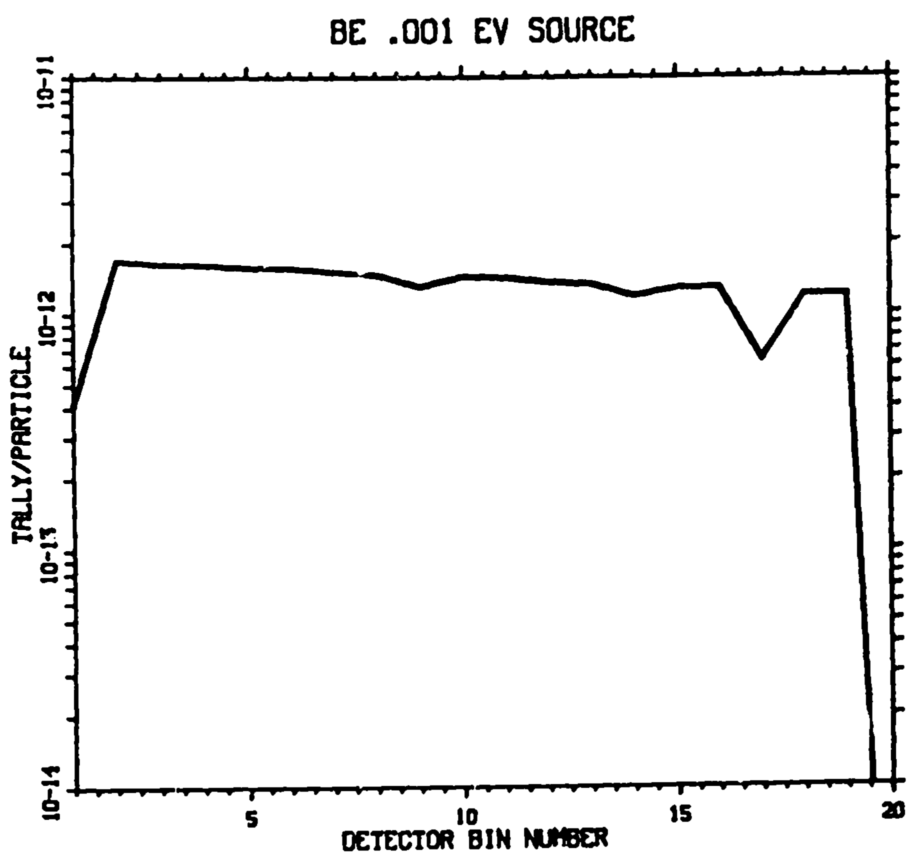

Fig. 37b.

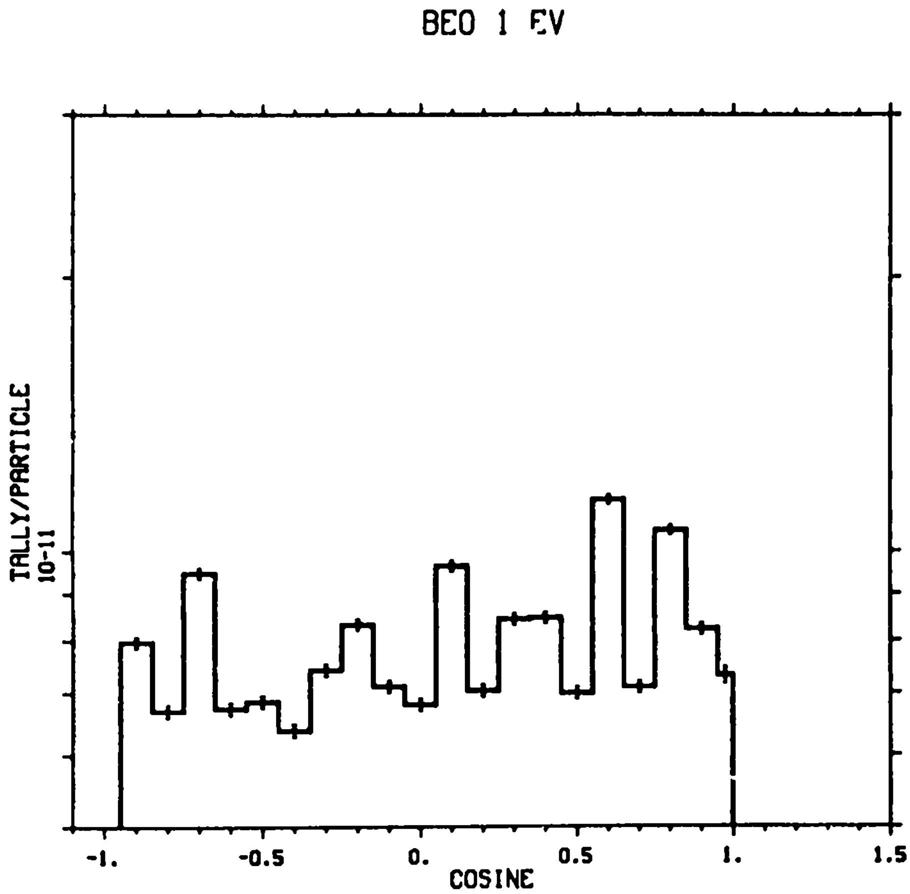

Fig. 38a.

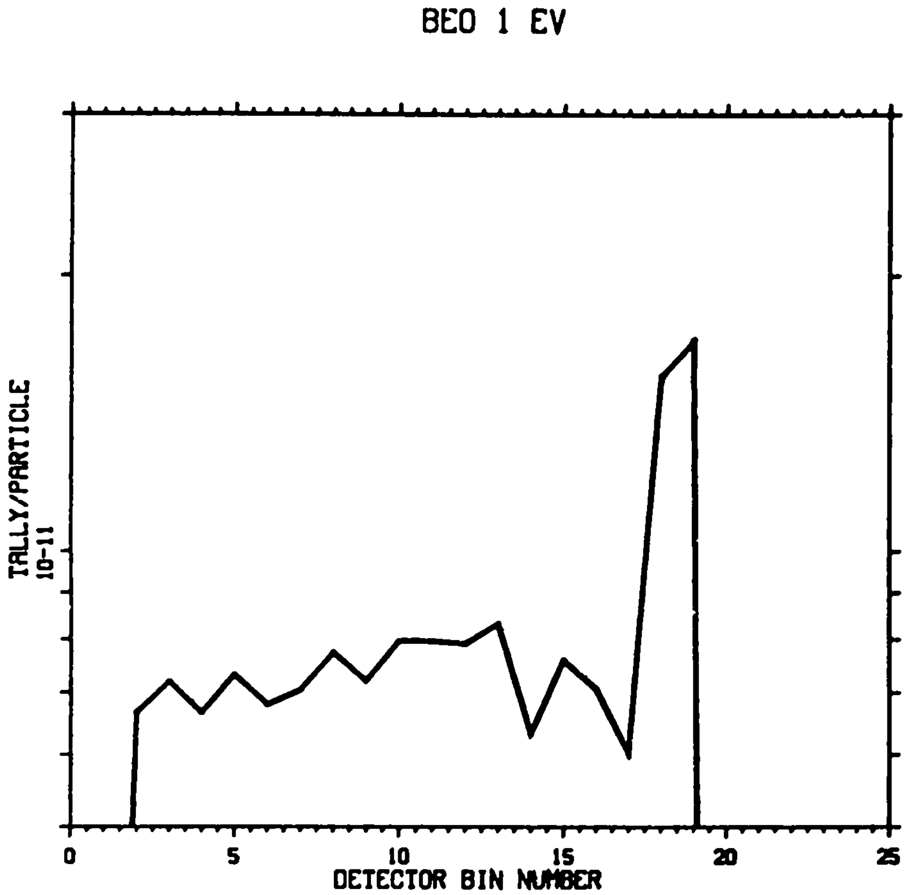

Fig. 38b.

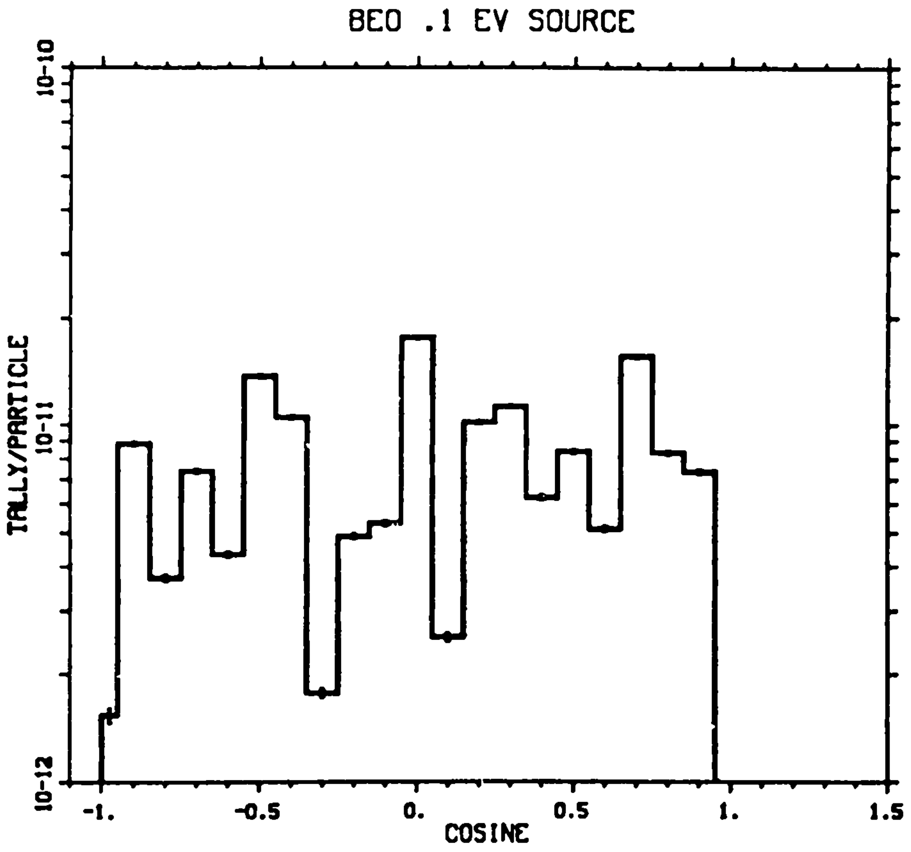

Fig. 39a.

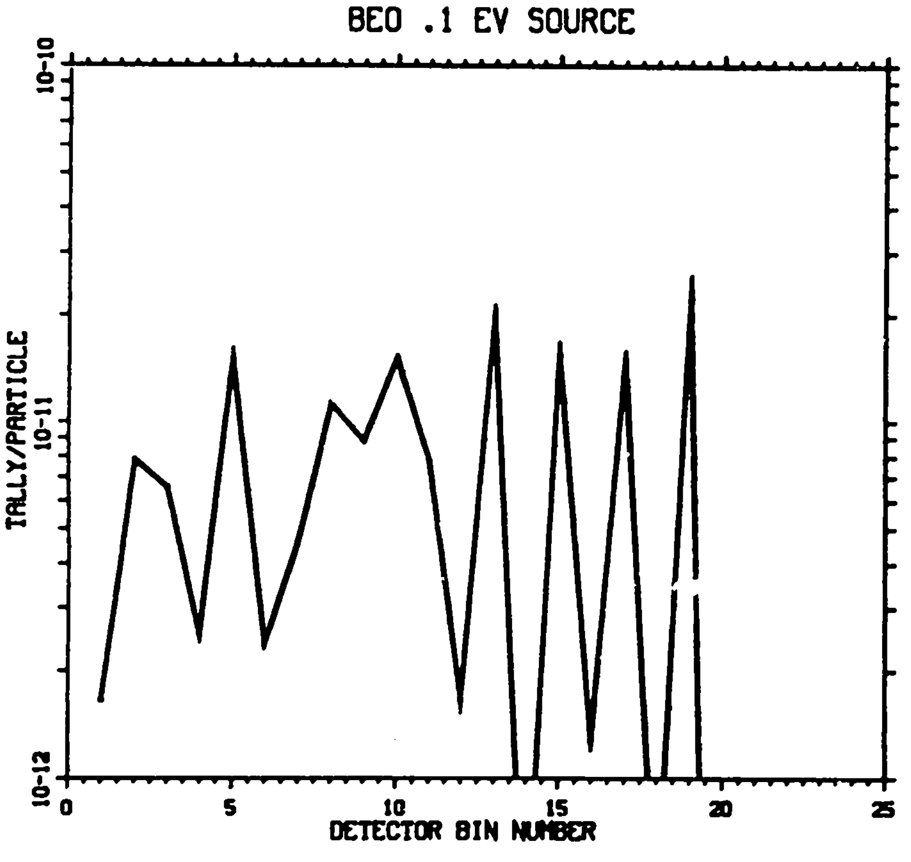

Fig. 39b.

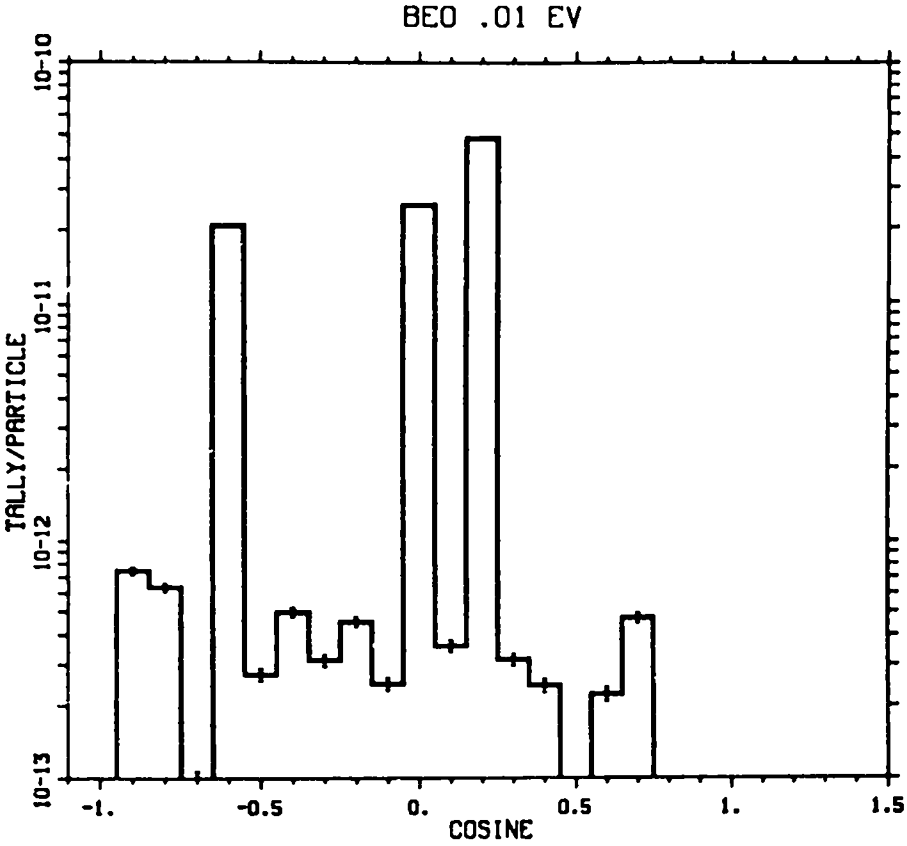

Fig. 40a.

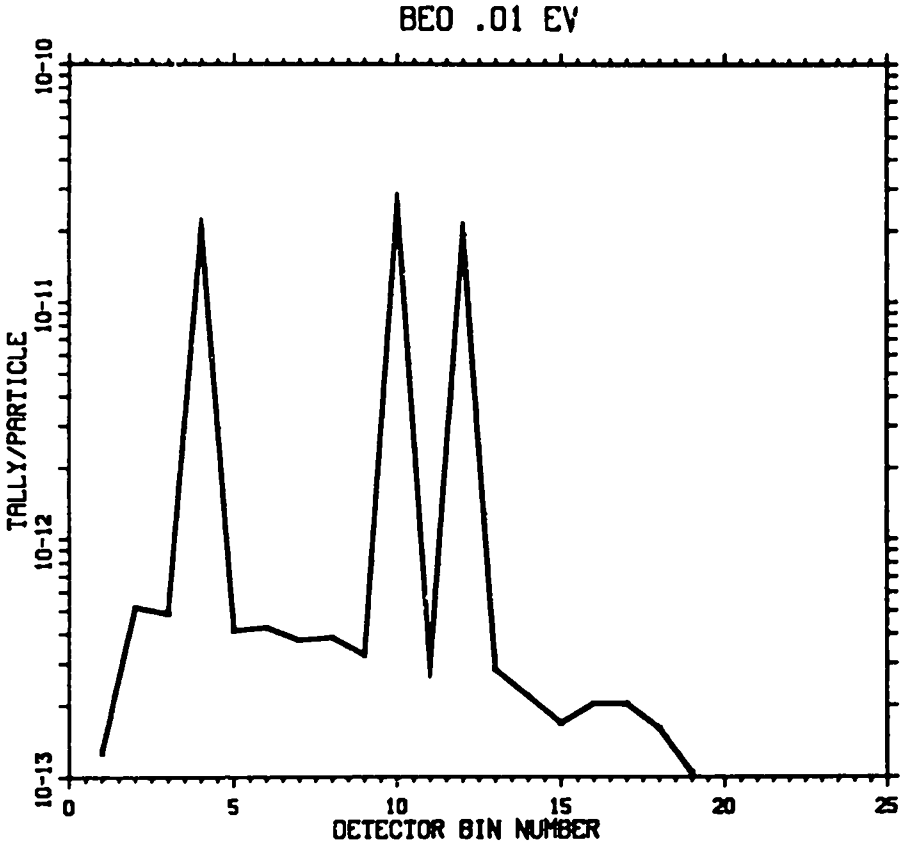

Fig. 40b.

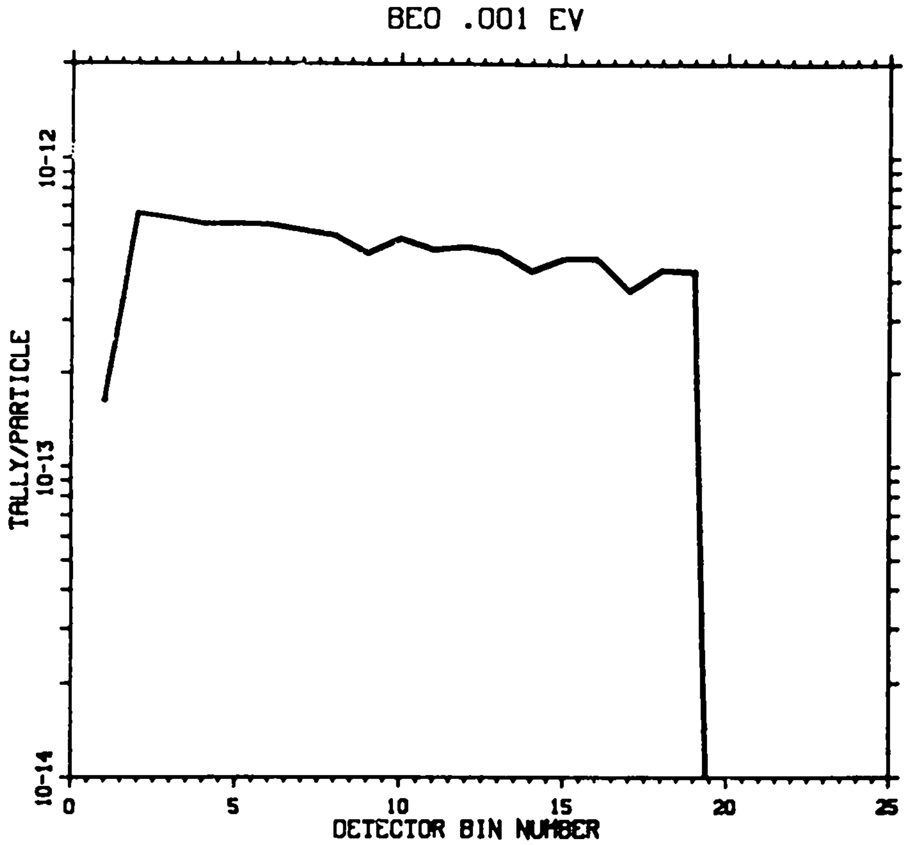

Fig. 41a.

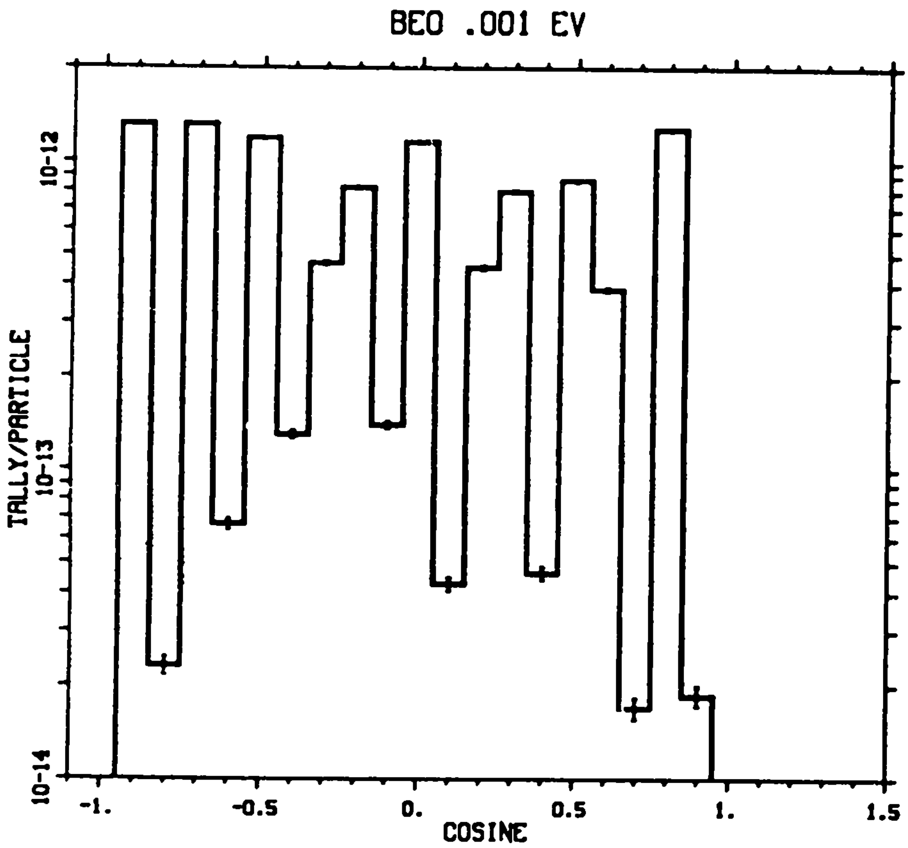

Fig. 41b.

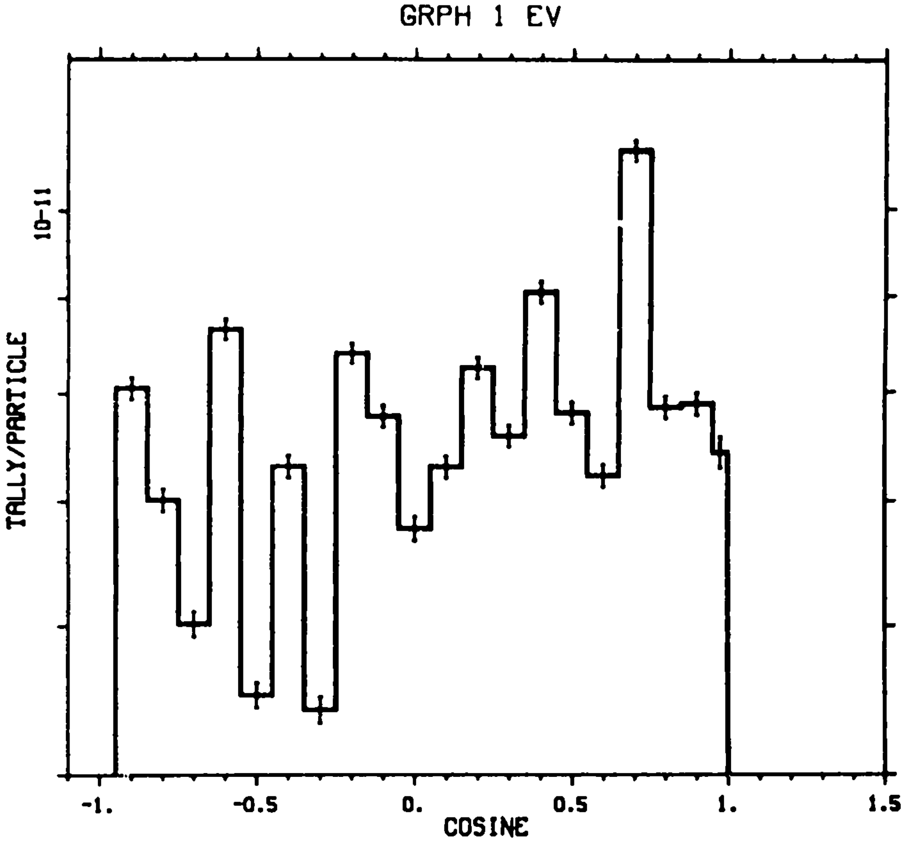

Fig. 42a.

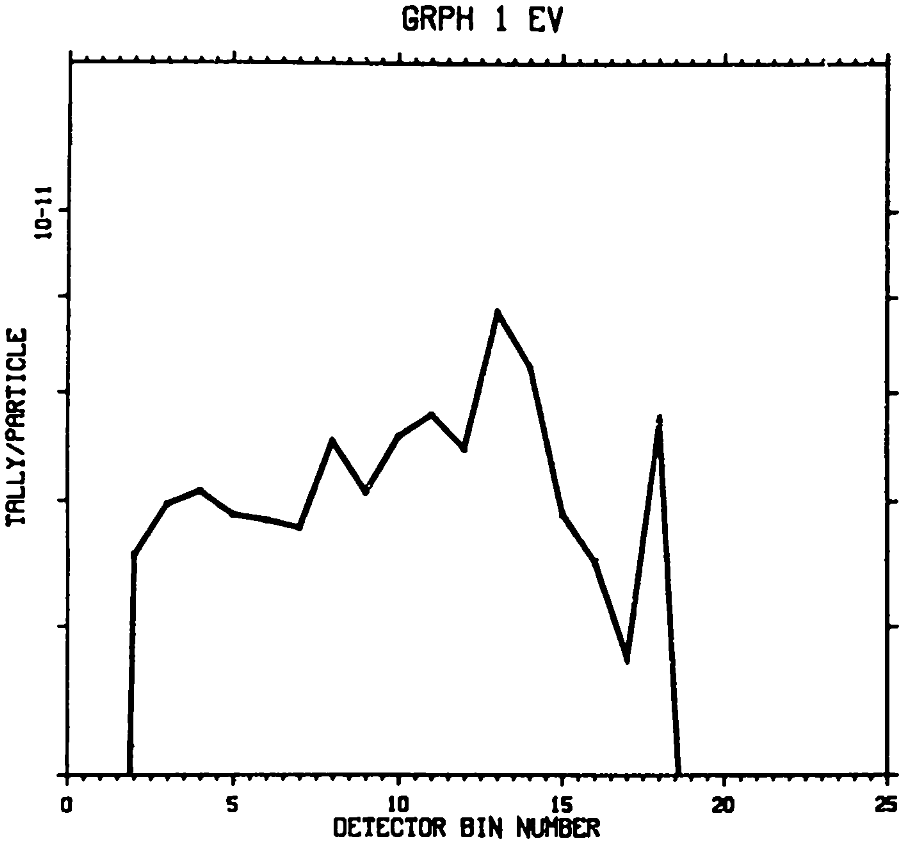

Fig. 42b.

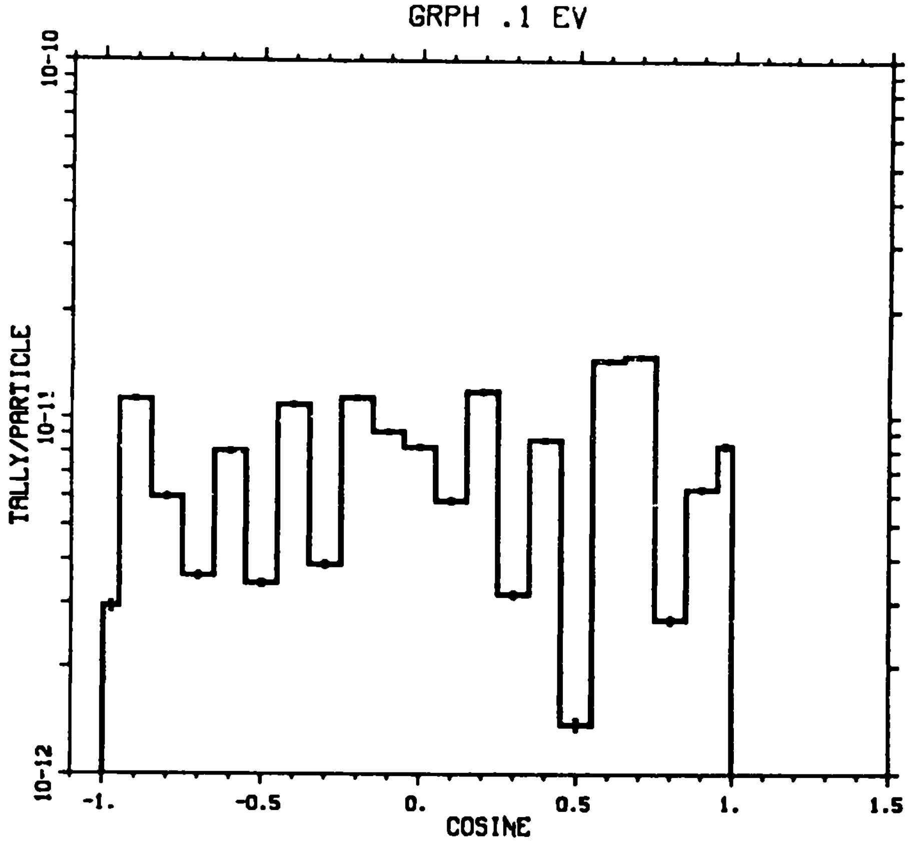

Fig. 43a.

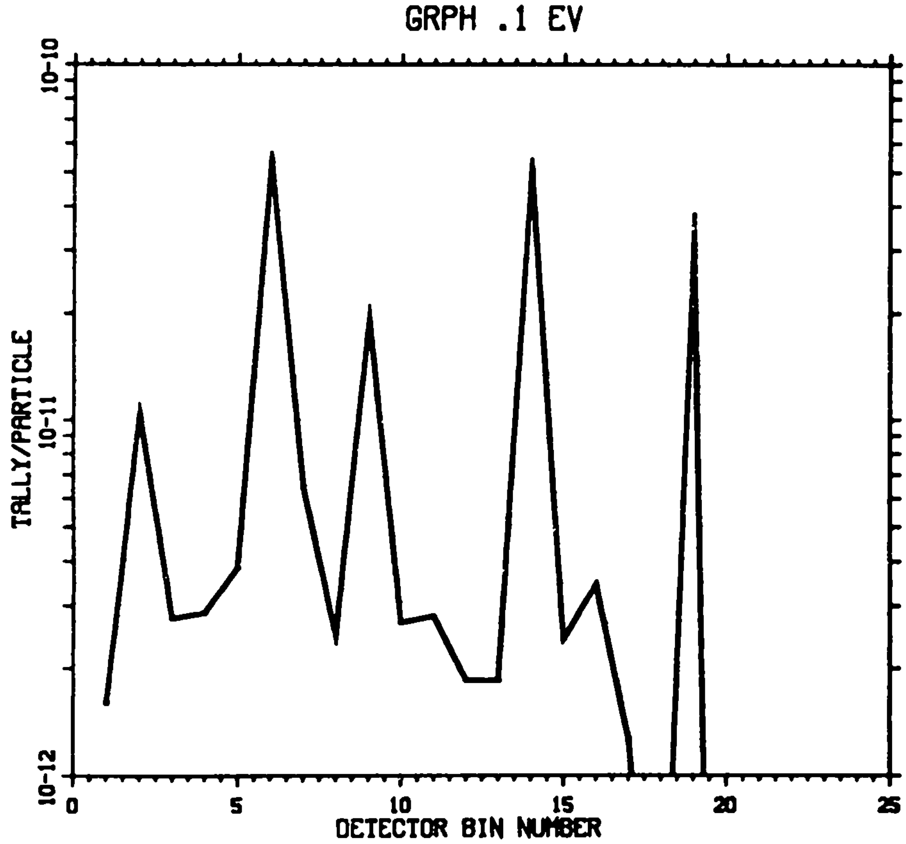

Fig. 43b.

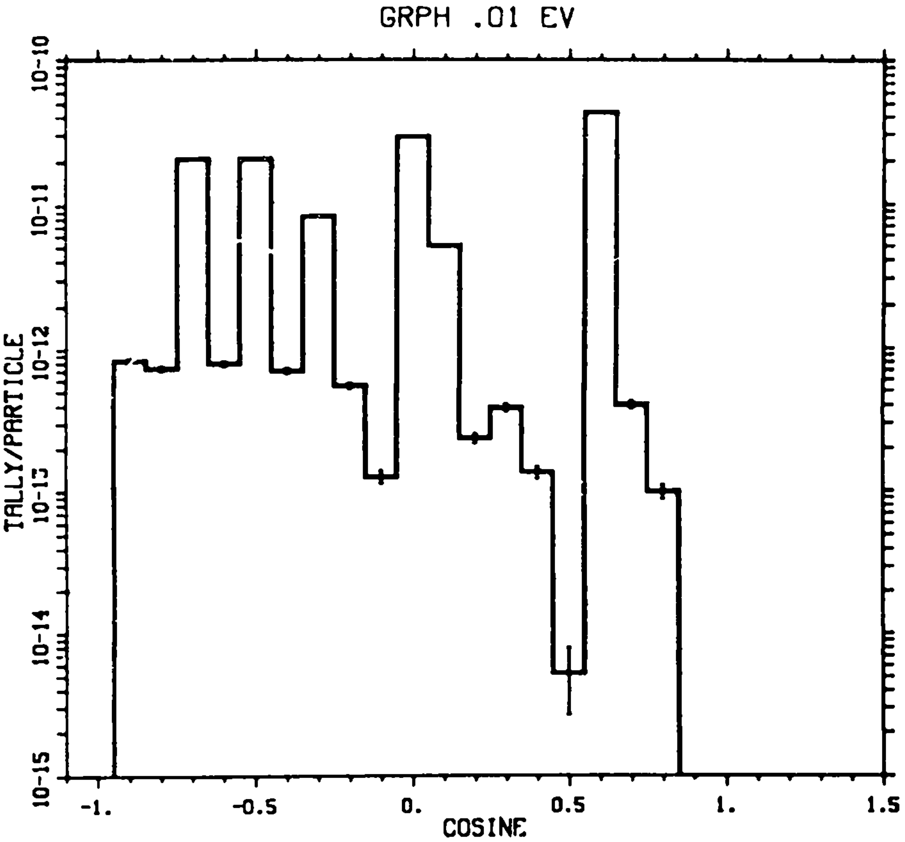

Fig. 44a.

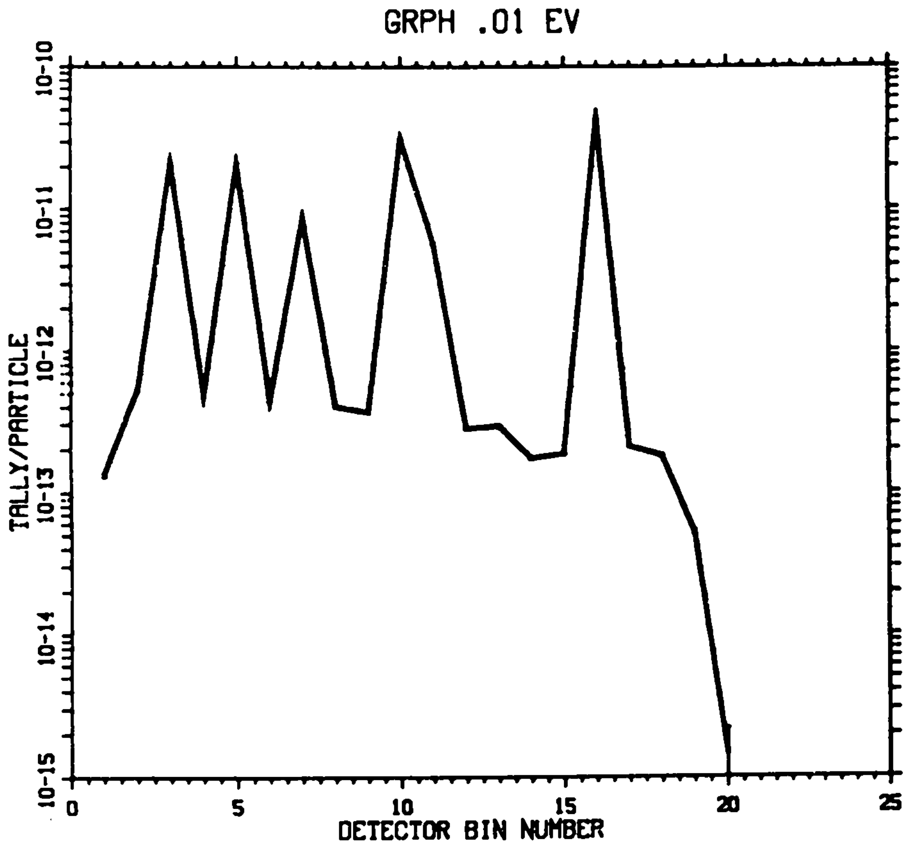

Fig. 44b.

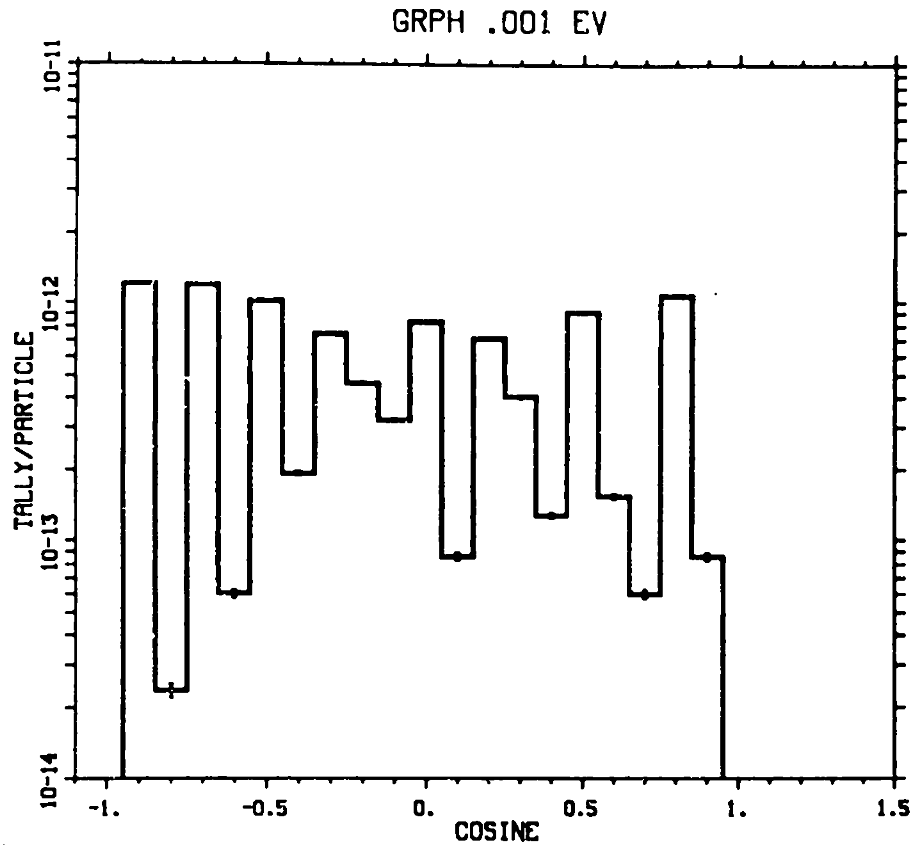

Fig. 45a.

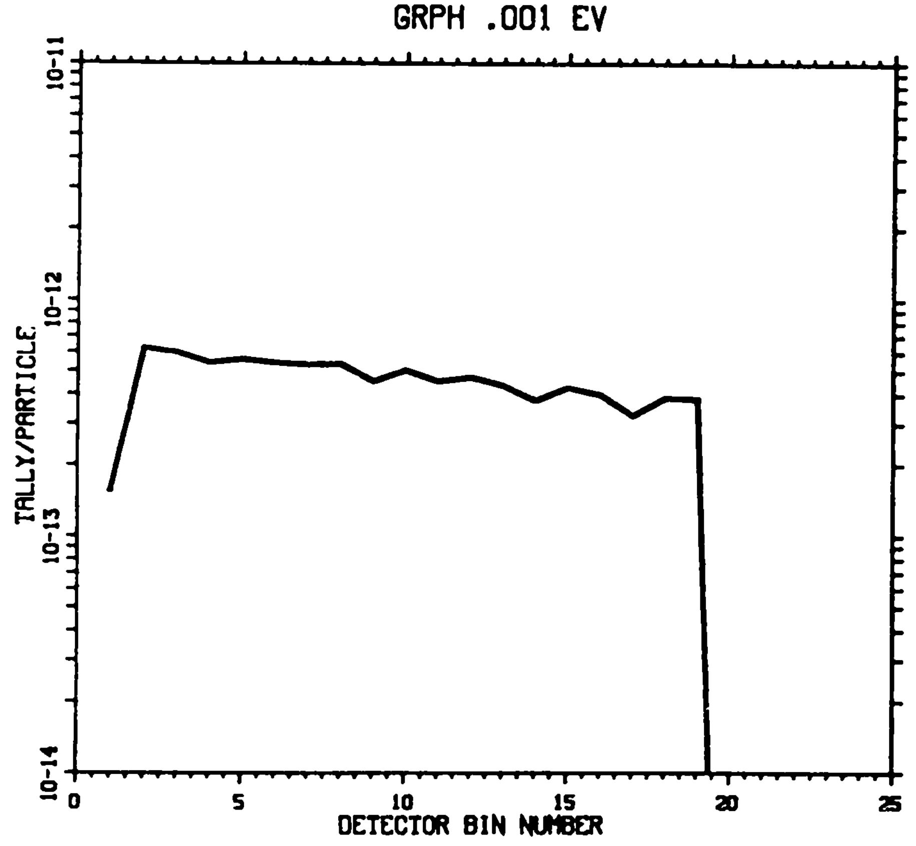

Fig. 45b.

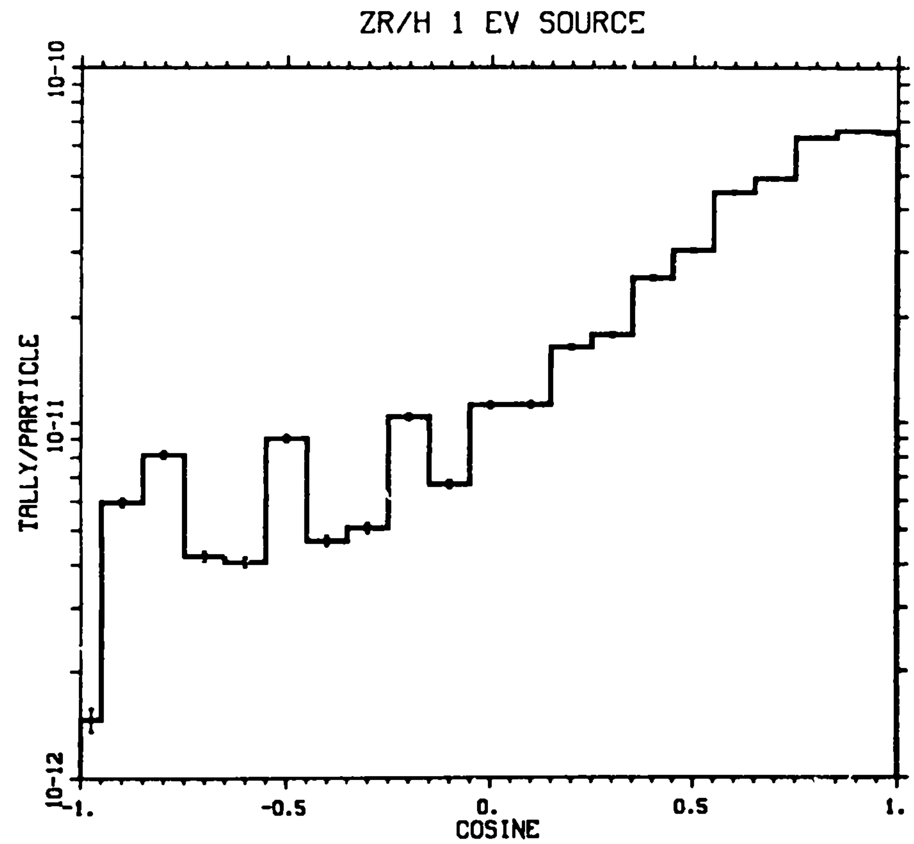

Fig. 46a.

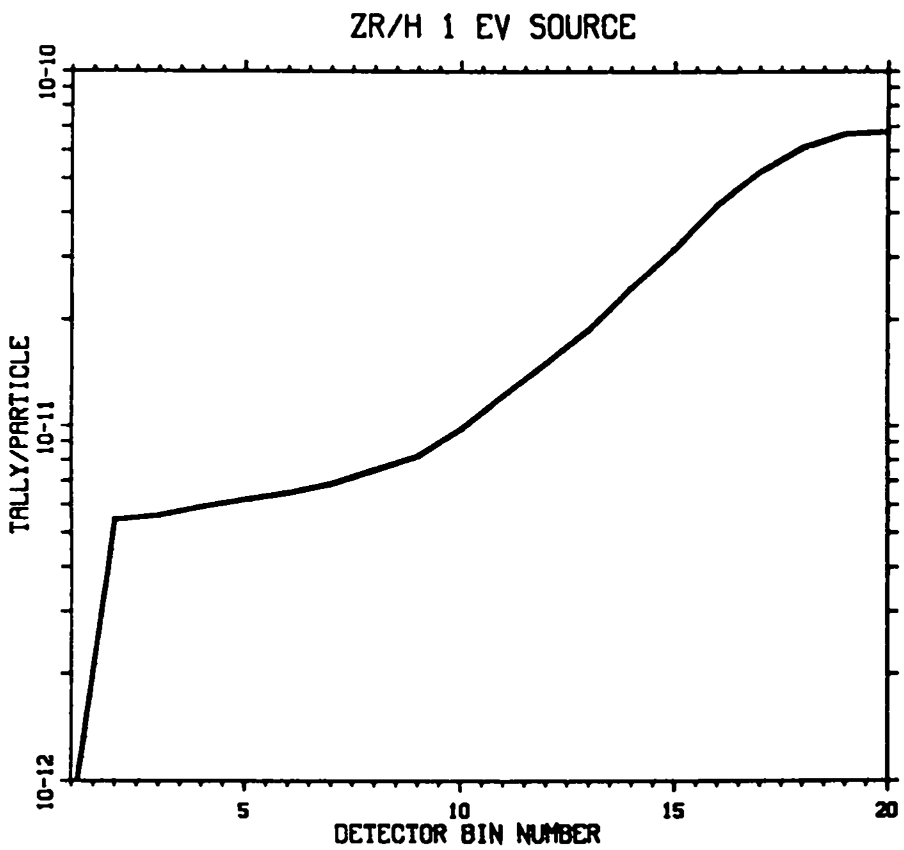

Fig. 46b.

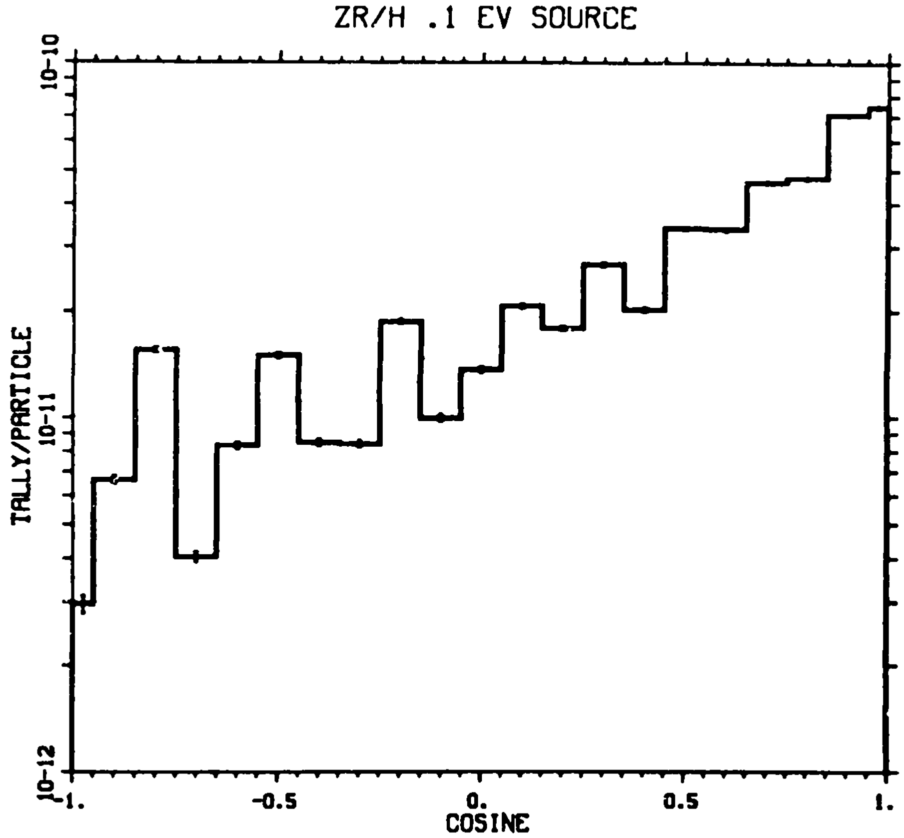

Fig. 47a.

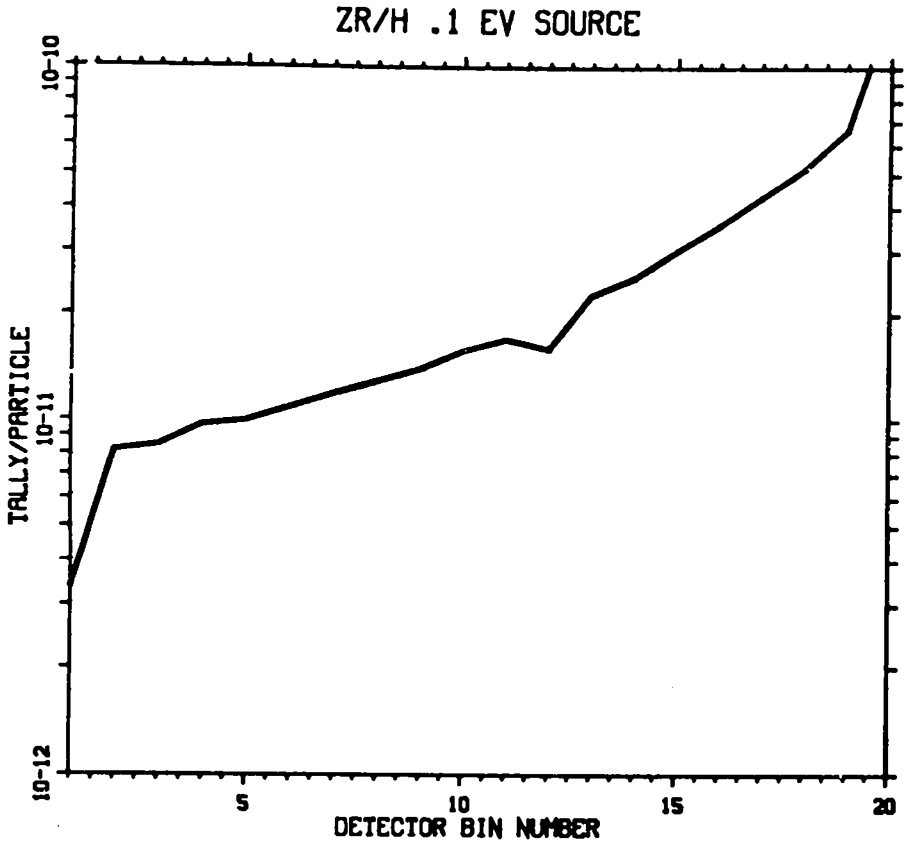

Fig. 47b.

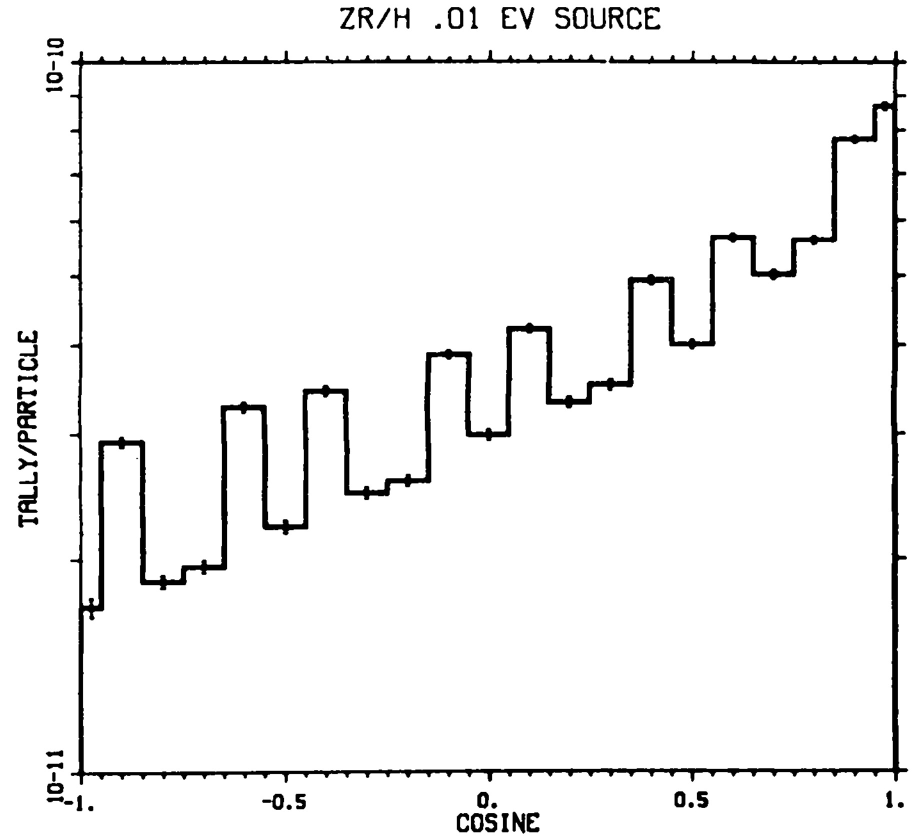

Fig. 48a.

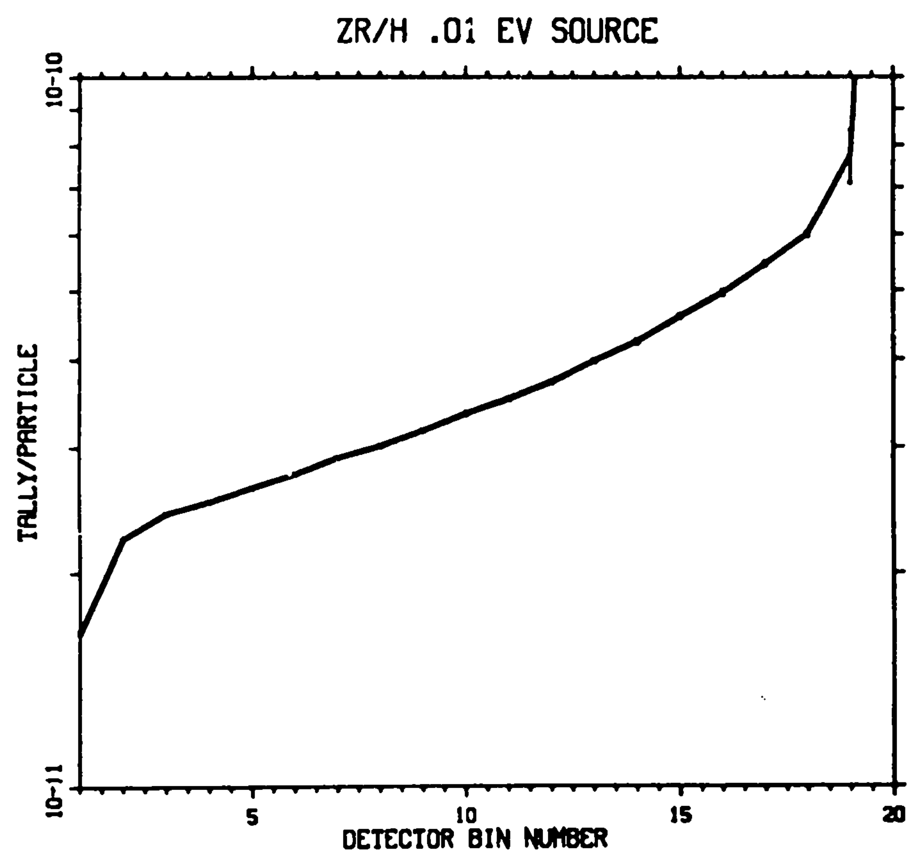

Fig. 48b.

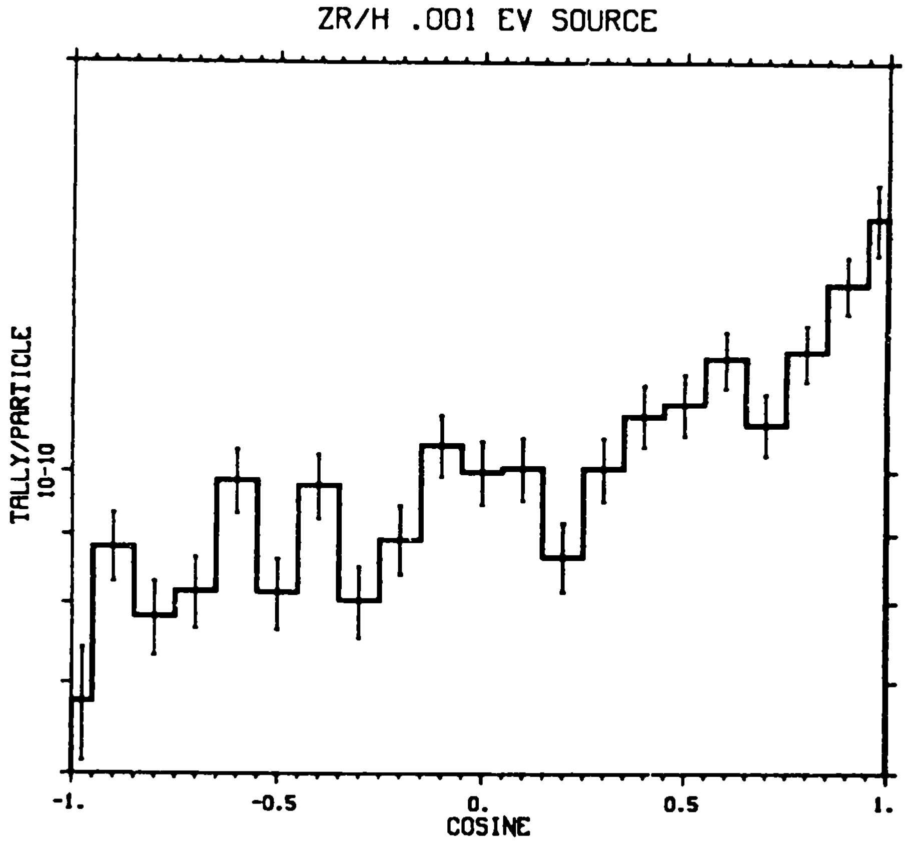

Fig. 49a.

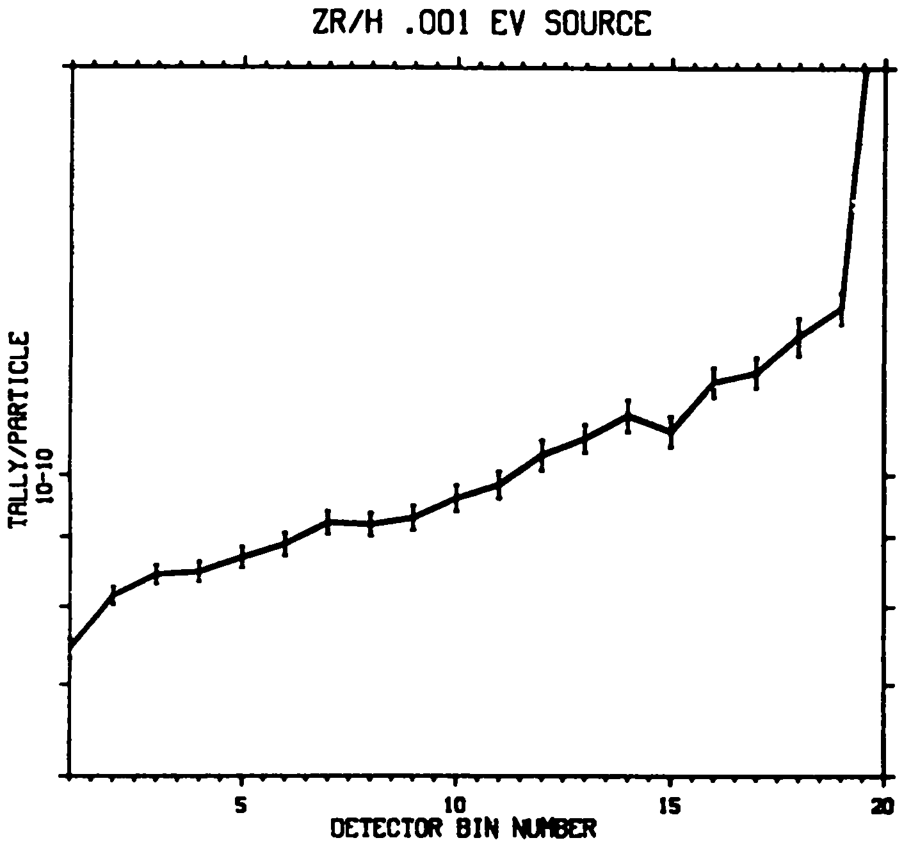

Fig. 49b.

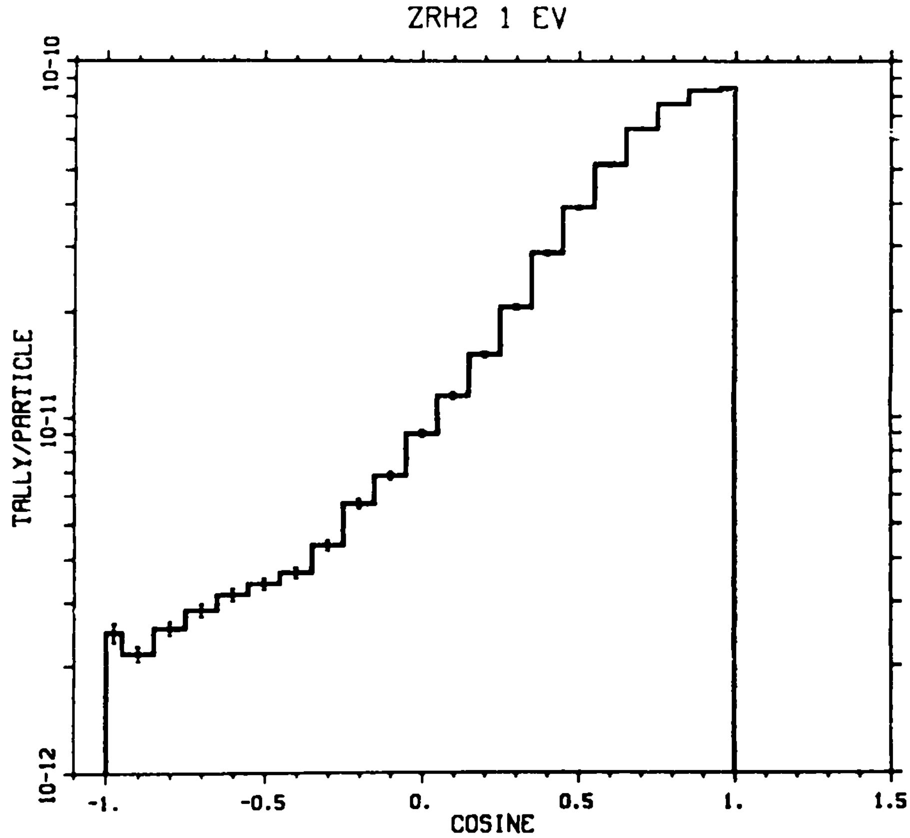

Fig. 50a.

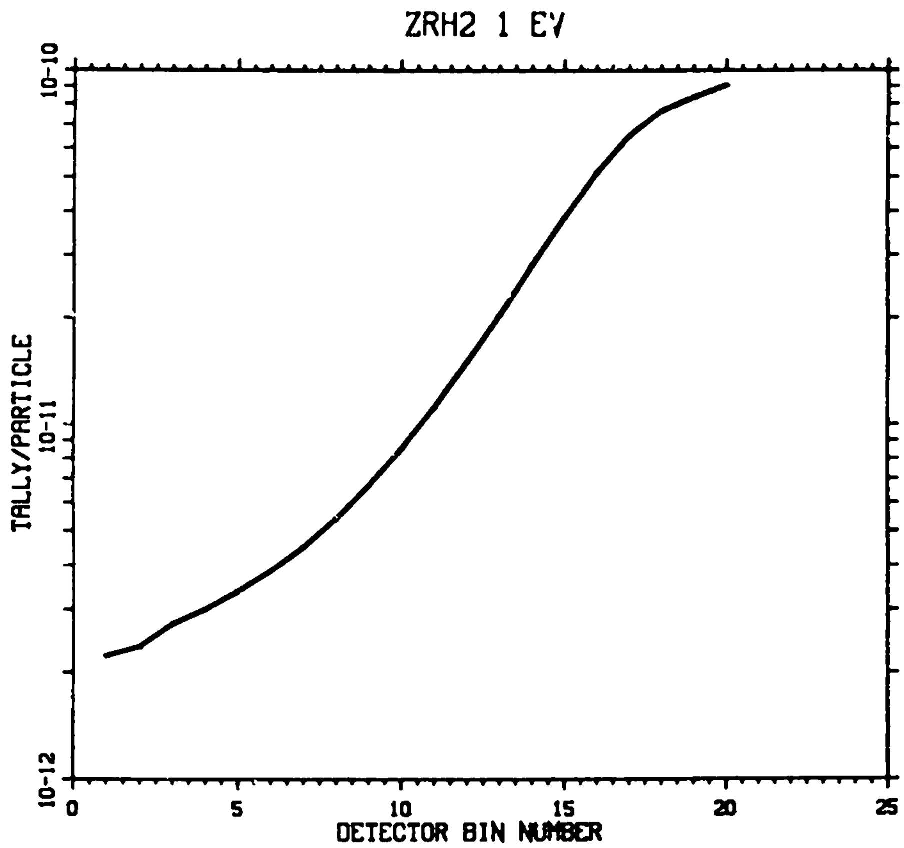

Fig. 50b.

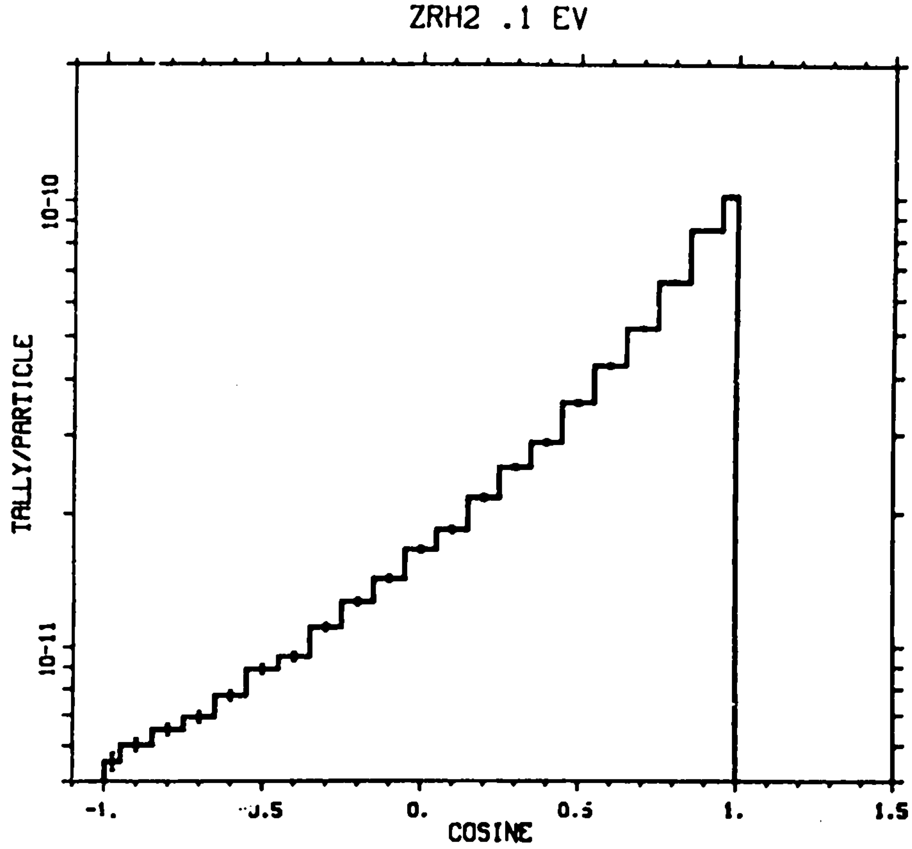

Fig. 51a.

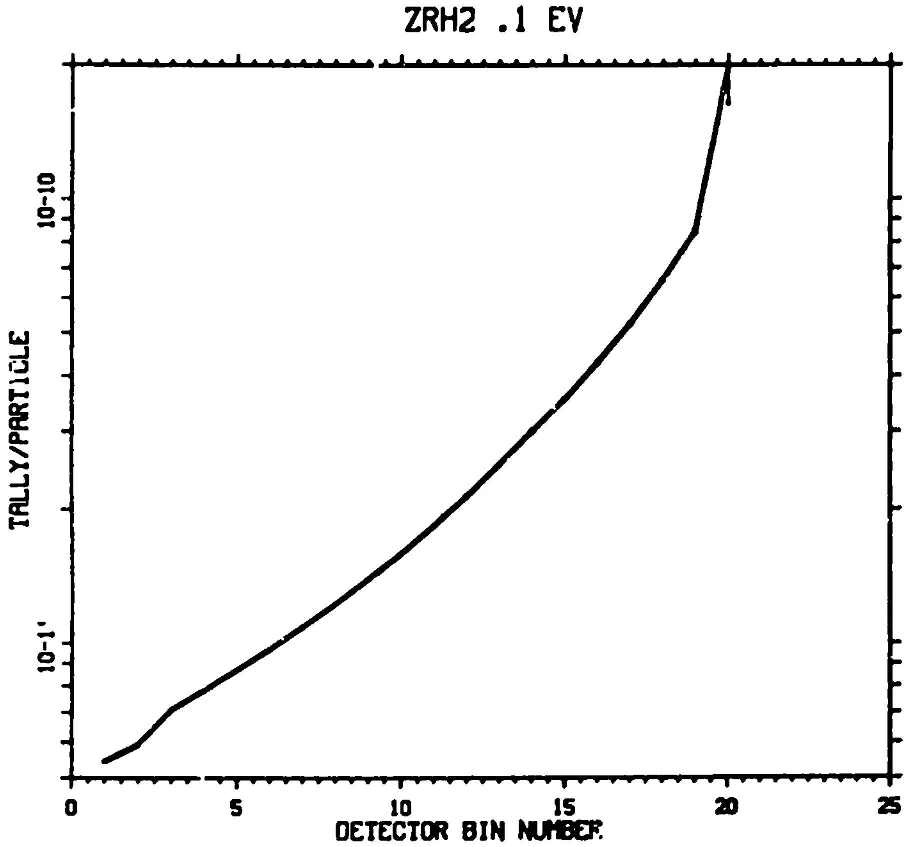

Fig. 51b.

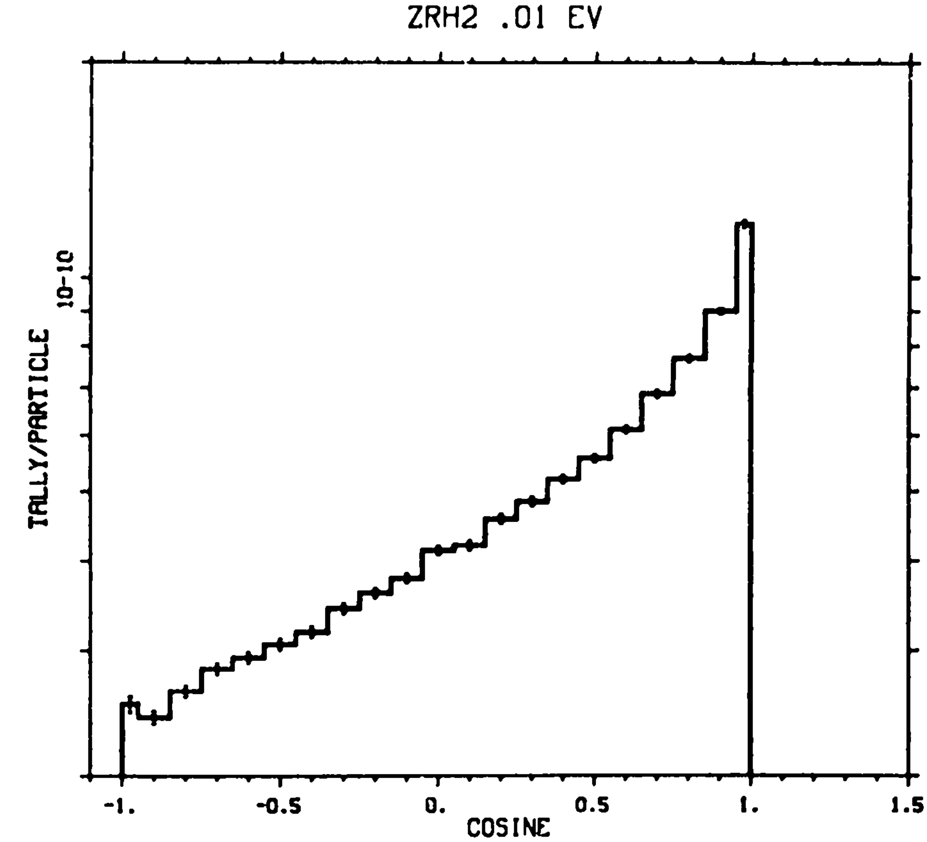

Fig. 52a.

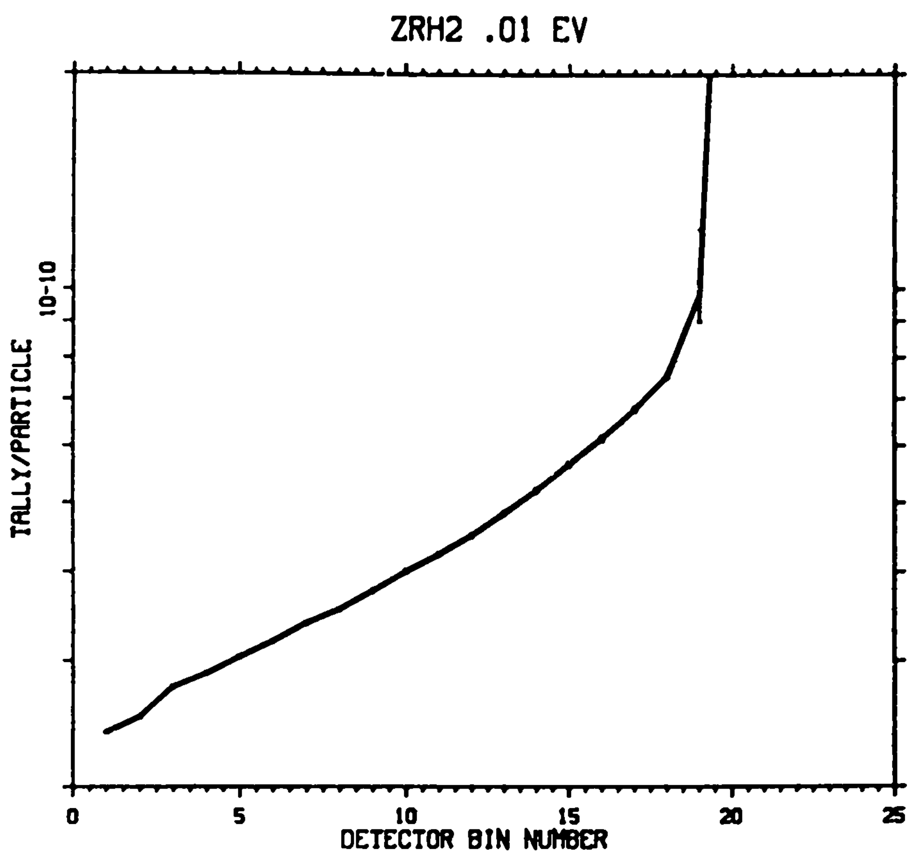

Fig. 52b.

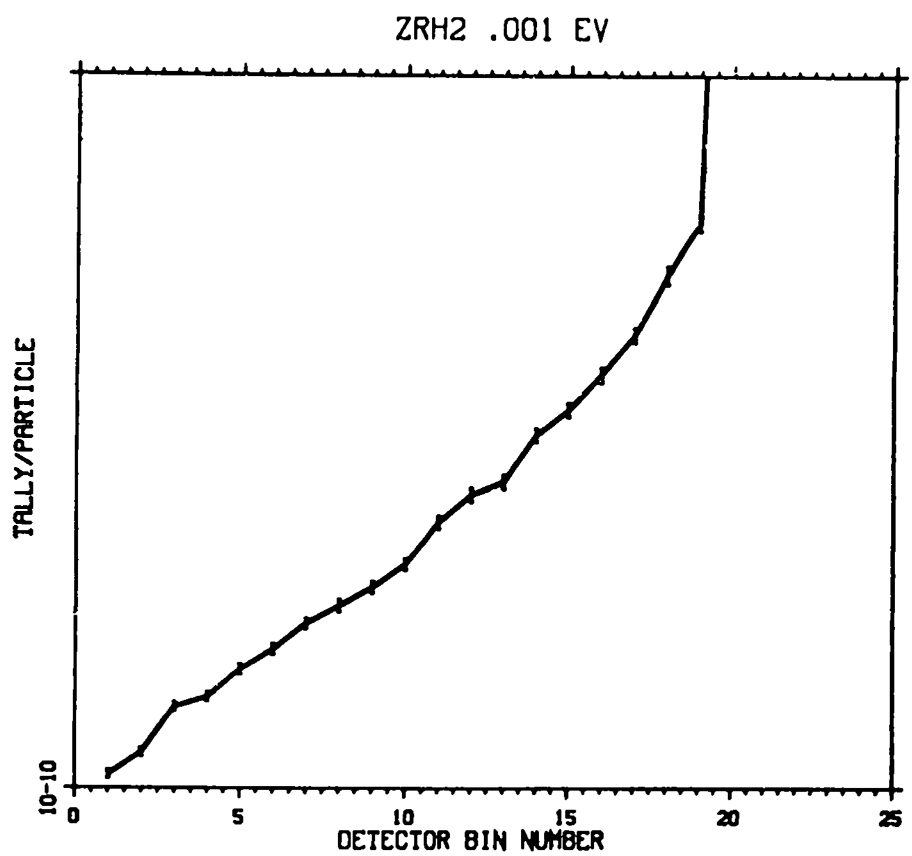

Fig. 53a.

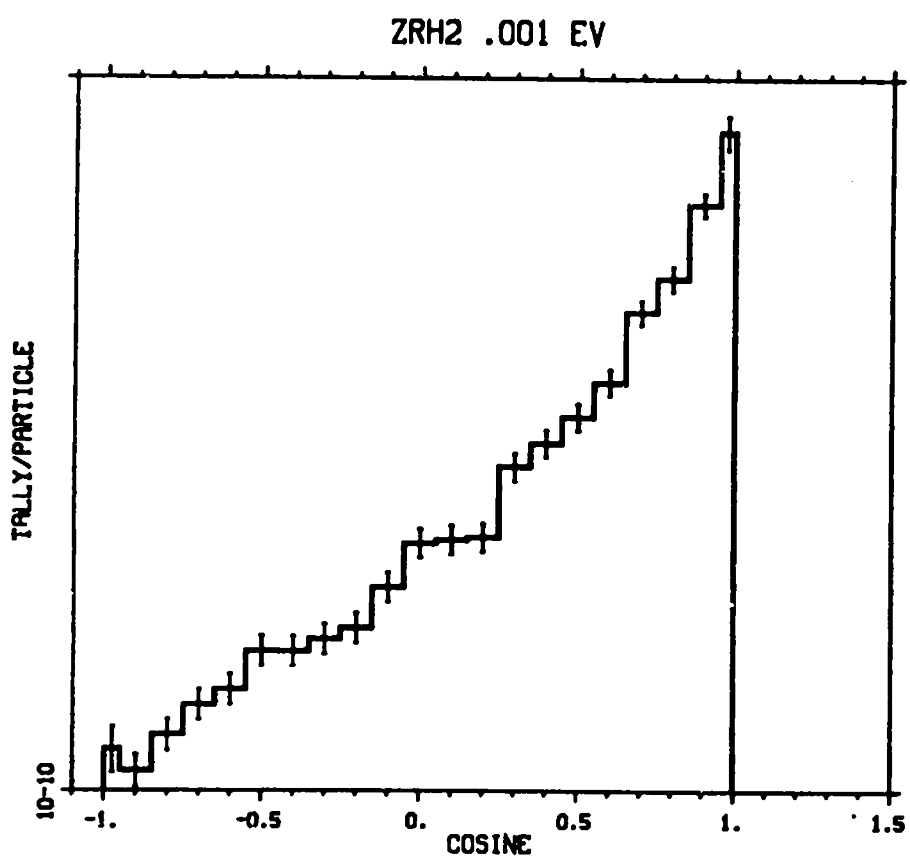

Fig. 53b.

TABLE IV

SINGLE COLLISION PROBLEMS INPUT FILE

```
ZRH2 .1 EV
1       1 0.0001 -1
2       0 1 -2
3       0 2

1       SO .1
2       SO 1000.1

M1      1001 2 8016 1
MT1     ZR/H.01
PHYS:N   100
TMP1   2.584-8  0 0
THTME   1.0E+123
SDEF POS=0 -1 0 VEC=0 1 0 DIR=1 ARA=1 ERG=1.E-7
FCL:N    -1 0 0
FC1     ZRH2 .1 EV
FC5     ZRH2 .1 EV
WWP:N 1.E30 1.E20 1.0001 -1
WWN1:N 1.E-20 0 -1
F1:N  2
C1       -.95 18I .95 .999 1 T
FT1     FRV 0 1 0
C       DIVIDE BY 2.*PI*R**2*DMU
CM1  3.183099E-6 1.591549E-6 18R 3.119437E-6 O.
C          7.959949E-8
C      EG     1.-10 3.16-10 1.-9 3.16-9 1.-8 3.16-8 1.-7 3.16-7 1.-6
C       2.-6 3.-6 4.-6 5.-6 6.-6 7.-6 8.-6 9.-6 9.999-6 1.0001-5 2.-5
NPS     100000
PRDMP  2J 1
PRINT
FQ1  C E
FQ5  F E
F5:N    0 -1000 0 0 ND
        -435.8899 -900 0 0
C       600 -800 0 0
        -714.1428 -700 0 0
        0 -600 800 0
        866.0254 -500 0 0
        916.5151 -400 0 0
        -953.9392 -300 0 0
        0 -200 979.7959 0 ND
        0 -100 994.9874 0
        0 0 1000 0
        994.9874 100 0 0
        979.7959 200 0 0
        0 300 953.9392 0
        916.5151 400 0 0
        0 500 -866.0254 0
        0 600 800 0
        -714.1428 700 0 0
        600 800 0 0
        0 900 435.8899 0
        0 1000 0 0
DD    0
```

degree of angular scattering resolution. But the detector approximation, which represents the discrete lines as histograms that are spread out until they touch each other smooths out the data and provides a better representation of continuous angular distribution functions than the discrete angle treatment used in the random walk.

We recommend that the representation of continuous distribution by discrete angles by the NJOY nuclear data processing code be reconsidered. There is already a mechanism in MCNP for utilizing equiprobable bin data that is continuous. Where the data is truly continuous, that representation should be used.

IV. Summary

Prael's histogram method has been incorporated into MCNP4 to allow detector and DXTRAN estimates from $S(\alpha,\beta)$ thermal collisions. The method has been extensively tested and appears to be working. For calculations where there are many collisions and angular effects are washed out, both the new approximation and the random walk physics are adequate. However, for some problems that are sensitive to the scattering distribution the approximation is actually better than the "exact" random walk because the NJOY processing of the data into discrete lines is a poor representation of the physics.

V. References

1. J. F. Briesmeister, Editor, "MCNP - A General Monte Carlo Code for Neutron and Photon Transport, Version 3A," Los Alamos National Laboratory report, LA-7396-m, Rev. 2, (1986).

2. R. A. Forster, R. C. Little, J. F. Briesmeister, and J. S. Hendricks, "MCNP Capabilities for Nuclear Well Logging Calculations," Proc. IEEE Trans. Nucl. Sci. to be published.

3. L. L. Carter and E. D. Cashwell, "Particle Transport Simulation with the Monte Carlo Method," *ERDA Critical Review Series,* TID-26607 (1975)

4. F. G. Bischoff, M. L. Yeater, and W. E. Moore, "Monte Carlo Evaluation of Multiple Scattering and Resolution Effects in Double- Differential Neutron Scattering Cross Section Measurements," *Nuclear Science and Engineering,* **48**, 266-280 (1972).

5. J. U. Koppel and D. H. Houston, "Reference Manual for ENDF Thermal Neutron Scattering Data," General Atomics report GA-8744, Revised (ENDF-269)(July 1978).

6. D. Garber, editor, "ENDF/B-V," Brookhaven National Laboratory Report BNL-17541 (ENDF-201), National Nuclear Data Center, Brookhaven National Laboratory, Upton, NY (October 1975).

7. T. E. Booth, "A Sample Problem for Variance Reduction in MCNP," Los Alamos National Laboratory report LA-10363-MS, (October 1985)

8. R. E. Macfarlane, D. W. Muir, and R. M. Boicourt, "The NJOY Nuclear Data Processing System, Volume I: User's Manual," Los Alamos National Laboratory report LA-9303-M, Vol. I (ENDF-324) (May 1982).

9. R. E. Macfarlane, D. W. Muir, and R. M. Boicourt, "The NJOY Nuclear Data Processing System, Volume II: The NJOY, RECONR, BROADR, HEATR and THERMR Modules," Los Alamos National Laboratory report LA-9303-M, Vol. II (ENDF-324) (May 1982).